National Library
of Canada

Canadian Theses Service

Ottawa, Canada
K1A 0N4

Bibliothèque nationale
du Canada

Service des thèses canadiennes

NOTICE

The quality of this microform is heavily dependent upon the quality of the original thesis submitted for microfilming. Every effort has been made to ensure the highest quality of reproduction possible.

If pages are missing, contact the university which granted the degree.

Some pages may have indistinct print especially if the original pages were typed with a poor typewriter ribbon or if the university sent us an inferior photocopy.

Reproduction in full or in part of this microform is governed by the Canadian Copyright Act, R.S.C. 1970, c. C-30, and subsequent amendments.

AVIS

La qualité de cette microforme dépend grandement de la qualité de la thèse soumise au microfilmage. Nous avons tout fait pour assurer une qualité supérieure de reproduction.

S'il manque des pages, veuillez communiquer avec l'université qui a conféré le grade.

La qualité d'impression de certaines pages peut laisser a désirer, surtout si les pages originales ont été dactylographiées à l'aide d'un ruban usé ou si l'université nous a fait parvenir une photocopie de qualité inférieure.

La reproduction, même partielle, de cette microforme est soumise à la Loi canadienne sur le droit d'auteur, SRC 1970, c. C-30, et ses amendements subséquents.

NL-339 (r. 88/04) c

Canadä

UNIVERSITY OF ALBERTA

SN 1987A: the greatest supernova since Kepler

BY

Hugh Jones

A thesis
submitted to the Faculty of Graduate Studies and Research in partial fulfillment of the requirements for the degree of Master of Science

in

Astrophysics

Department of Physics

Edmonton, Alberta

Fall, 1990

National Library of Canada
Canadian Theses Service
Ottawa, Canada
K1A 0N4

Bibliothèque nationale du Canada
Service des thèses canadiennes

The author has granted an irrevocable non-exclusive licence allowing the National Library of Canada to reproduce, loan, distribute or sell copies of his/her thesis by any means and in any form or format, making this thesis available to interested persons.

The author retains ownership of the copyright in his/her thesis. Neither the thesis nor substantial extracts from it may be printed or otherwise reproduced without his/her permission.

L'auteur a accordé une licence irrévocable et non exclusive permettant à la Bibliothèque nationale du Canada de reproduire, prêter, distribuer ou vendre des copies de sa thèse de quelque manière et sous quelque forme que ce soit pour mettre des exemplaires de cette thèse à la disposition des personnes intéressées.

L'auteur conserve la propriété du droit d'auteur qui protège sa thèse. Ni la thèse ni des extraits substantiels de celle-ci ne doivent être imprimés ou autrement reproduits sans son autorisation.

ISBN 0-315-65115-6

UNIVERSITY OF ALBERTA

RELEASE FORM

NAME OF AUTHOR: Hugh Richard Arthur Jones

TITLE OF THESIS: SN 1987A: the greatest supernova since Kepler

DEGREE: Master of Science

YEAR THIS DEGREE GRANTED: 1990

Permission is hereby granted to the UNIVERSITY OF ALBERTA LIBRARY to reproduce single copies of this thesis and to lend or sell such copies for private, scholarly or scientific research purposes only.

The author reserves other publication rights, and neither the thesis nor extensive extracts from it may be printed or otherwise reproduced without the author's written permission.

Hugh R. Jones

(Student's signature)

71 Birchanger Lane,
Bishop's Stortford,
Herts,
England.
(Student's permanent address)

Date: 10 June 1990

UNIVERSITY OF ALBERTA

FACULTY OF GRADUATE STUDIES AND RESEARCH

The undersigned certify that they have read, and recommend to the Faculty of Graduate Studies and Research for acceptance, a thesis entitled *SN 1987A: The greatest supernova since Kepler* submitted by Hugh Jones in partial fulfillment of the requirements for the degree of Master of Science in Astrophysics.

Douglas P. Hube
Supervisor

Eric H. Pinnington

David Routledge
External Examiner

Date: 20 June 1995

TO MY PARENTS

ABSTRACT

Supernova 1987A in the large Magellanic Cloud is the brightest supernova to be observed since Kepler's supernova in 1604. In this thesis the first three years of theoretical and observational research on SN 1987A are reviewed with particular emphasis on those aspects of supernovae which were previously unresolved. The detection of the neutrinos produced at core collapse has not only confirmed the basic ideas of Type II supernova causality and energetics (without being able to distinguish prompt from delayed shock ejection), but also heralded the birth of extra-solar neutrino astronomy. The unusual early light curve has turned out to be a natural consequence of core collapse when the star was compact and blue, after passing through a red supergiant phase. Synthesis of 0.075 $M_\odot$ of ^{56}Ni (previously suspected in type II supernovae with exponentially tailed light curves) has been revealed by a similar light curve and by the gamma-rays accompanying the decay of ^{56}Ni to ^{56}Co to ^{56}Fe. A number of puzzles remain. These include the presupernova evolution of the progenitor and the asymmetry of the envelope, though the most intriguing puzzle is the nature of the remnant left by the collapse of the central core.

ACKNOWLEDGEMENTS

I would like to thank my supervisor, Professor Douglas Hube, for letting me do my thesis the way I wanted to, and for clear explanations of confusing things. I would also like to thank my committee, Professor E. Pinnington, Professor D. Routledge, and Professor J. Gray, for their helpful comments and interest in the progress of my thesis.

It is a pleasure to thank Professor Alan Watson of the University of Leeds for exciting his nuclear physics class about the incredible detection of neutrinos from a star 160,000 light years away.

Back at the University of Alberta, I am grateful to my office mates Mark Salik and Alex Nip for not only their helpful comments about supernovae but also their jovial attitude towards physics.

Finally, for their love, support, and tolerance of my late hours, as well as the more tangible conversion of scruffy tables into a readable format, I thank my co-joins, Constance and Kytai.

TABLE OF CONTENTS

I. INTRODUCTION 1

II. THE PROGENITOR 4

II.1 THE EVOLUTION OF Sk -69° 202 5

II.1(i) The last million years 5

II.1(ii) The onset of core collapse 7

II.2 WHY WAS Sk -69° 202 BLUE? 9

II.2(i) Mass loss 12

II.2(ii) Metallicity 13

II.2(iii) Other factors 14

III. THE EXPLOSION 16

III.1 GENERAL COLLAPSE FEATURES 16

III.2 COLLAPSE TO SUBNUCLEAR DENSITIES 18

III.3 SHOCK FORMATION 21

III.4 THE PROMPT SHOCK WAVE 22

III.5 THE DELAYED EXPLOSION MECHANISM 24

IV. THE NEUTRINO BURST 30

IV.1 NEUTRINO DETECTION 31

IV.2 ANALYSIS OF THE NEUTRINO DATA 34

IV.2(i) Neutrinos around 2:52 UT? 35

IV.2(ii) Gravity waves? 36

IV.2(iii) Neutrinos around 7:36 UT? 36

IV.3 THE STANDARD MODEL 39

IV.4 HOW WELL DO OBSERVATIONS FIT THE STANDARD MODEL? 42
    IV.4(i) Events around 2:52 UT 42
    IV.4(ii) Events around 7:36 UT 43
IV.5 BIZARRE POSSIBILITIES 47
    IV.5(i) Phase Transition 48
    IV.5(ii) Fragmentation on collapse 49
    IV.5(iii) Black hole 49
IV.6 NEUTRINO PROPERTIES 50
    IV.6.(i) Neutrino Mass 51
    IV.6(ii) Neutrino lifetime 52
    IV.6(iii) Magnetic moment 53
    IV.6(iv) Neutrino charge 53
    IV.6(v) Neutrino flavours 53
    IV.6(vi) Special relativity 54
    IV.6(vii) The weak equivalence principle 54
    IV.6(viii) Other interactions 55
IV.7 CONCLUSION 55
IV.8 THE FUTURE? 56

V. THE AFTERMATH 58
V.1 EARLY CONSTRAINTS 59
    V.1(i) The ultraviolet flash 61
    V.1(ii) The distance to SN 1987A 62
V.2 TO THE PEAK 63
    V.2(i) Early Spectra 66
V.3 OVER THE HILL 67

V.3(i) Spectral Evolution 69

V.4 MIXING 71

V.4(i) Asymmetry 72

V.4(ii) Clumping 73

V.4(iii) Blowing bubbles 75

V.5 EXPLOSIVE NUCLEOSYNTHESIS 77

V.6 LATER EVOLUTION 79

V.6(i) Dust formation 79

V.6(ii) The evolution of high energy emissions 81

V.6(iii) The end of the line 84

V.7 THE BEAST WITHIN 85

V.7(i) Spin Rate 85

V.7(ii) Luminosity of a pulsar 86

V.7(iii) Black hole? 88

V.7(iv) Neutron star vibration 89

V.7(v) Strange star? 89

V.8 CIRCUMSTELLAR MATERIAL 91

V.8(i) The mystery spot 91

V.8(ii) Echoes 93

V.9 THE INTERSTELLAR MEDIUM TOWARDS SN 1987A 97

VI. THE FUTURE? 99

REFERENCES 102

BIBLIOGRAPHY 115

APPENDICES 124

APPENDIX A - Mass loss and Rotation 124

A.1 Mass Loss 124

A.2 Rotation 124

APPENDIX B - Neutrinos 126

B.1 Core infall 126

B.2 Neutrino trapping density 128

B.3 Core collapse 129

B.4 Neutrinos escape 130

B.5 Detector efficiencies 131

APPENDIX C - Radioactivity 132

C.1 Cobalt 56 decay? 132

C.2 Mass of Cobalt 56 132

LIST OF TABLES

Table 1. Detector properties 31
Table 2. The events ascertained to be from SN 1987A 33
Table 3. Sketch of neutrino's timetable for emission 40
Table 4. Comparison of models for the neutrino burst 45
Table 5. Neutrino properties 51
Table 6. Sample future detector event totals [from the Galactic centre (8.5 kpc)] 57
Table 7. The early chronology of SN 1987A 58
Table 8. The evolution of light echoes 95

LIST OF FIGURES

Figure 1. Expected structure of Sk - 69° 202 at the onset of core collapse 7
Figure 2. Evolutionary track of an evolved star 11
Figure 3. Free energy of collapsing nucleons 17
Figure 4. Formation of an homologous core 19
Figure 5. Entropy during the collapse to nuclear densities 20
Figure 6. Cross section of star when the early shock wave stalls 23
Figure 7. Angular distribution of neutrinos 38
Figure 8. Neutrinos from Kamiokande and IMB 44
Figure 9. Neutron star models 46
Figure 10. The early light curve 63
Figure 11. Spectra recorded during the first few months 66
Figure 12. Optical spectra during the first month 67
Figure 13. The bolometric light curve until day 250 68
Figure 14. The spectrum from SN 1987A in April 1988 70
Figure 15. The development of instabilities in an expanding supernova envelope 74
Figure 16. An un-mixed model of the supernova's ejecta 76
Figure 17. A mixed model of the supernova's ejecta 76
Figure 18. The composition of the ejecta before explosive nucleosynthesis 77
Figure 19. The composition of the ejecta after explosive nucleosynthesis 77
Figure 20. The bolometric light curve from day 100 to day 750 79
Figure 21. Dust formation in the ejecta 80
Figure 22. The X-ray light curve 82
Figure 23. The gamma-ray light curve 83
Figure 24. Gamma-ray line profile at 847 keV on day 613 83
Figure 25. The bolometric light curve since day 500 84

Figure 26. Schematic diagram of the expected medium around SN 1987A 93
Figure 27. The circumstellar medium as of December 1989 95
Figure 28. A spectrum obtained from the outer light echo 96
Figure 29. The expected input from radioactive energy 99
Figure 30. Kamiokande efficiency 131
Figure 31. IMB efficiency 131
Figure 32. Mount Blanc efficiency 131
Figure 33. Baskan efficiency 131

I. INTRODUCTION

Supernovae have been objects of great mystery and reverence since Ancient times. The annals of the Benedictine monastery of St. Gallen in Switzerland record the following entry[1] for the year 1006. "A new star of unusual size appeared, glittering in aspect, and dazzling the eyes, causing alarm... It was seen likewise for three months in the inmost limits of the South, beyond all the constellations which are seen in the sky".

The supernova of 1006 was the brightest in recorded history, one of very few explosions to have occurred close enough to our Sun to be visible to the naked eye. Fewer than a half-dozen naked eye supernovae have been recorded since that time, and recent research in the field has largely had to make do with an examination of ancient records, along with analyses of the faint light from supernova explosions in galaxies beyond our Milky Way. Until 1987 not one nearby supernova had been caught *in extremis* by the tools of 20th century astrophysics.

Contrast SN 1987A with its counterpart nearly a thousand years earlier. In 1006, the supernova was a blaze in the sky, a portent, a sign from the heavens. In 1987 the supernova, considerably farther away, was bright only to astronomers; to the untrained eye it appeared as just one of the many featureless specks in the dark night sky. Yet in its own fashion, SN 1987A was as much a public event as the supernova in 1006. It was accorded the front cover of *Time*[2] magazine.

From the light curves and spectra supernovae must be classified into at least two different types. Those that show strong hydrogen emission are called type II supernovae and those where hydrogen is absent are classified as type I. The standard interpretation is that the progenitors of type I events are low mass stars with no or very little hydrogen, presumably white dwarf or helium stars. Type II supernovae, on the other hand, are believed to arise from massive stars ($M>8M_\odot$) with extended hydrogen envelopes.

If this interpretation is correct then type II supernovae should ultimately get their energy from the increase in gravitational binding of a collapsing stellar core, and they should be related to the formation of compact objects such as neutron stars or, possibly, black holes. Moreover, if the progenitors are indeed quite massive, type II supernovae will eject large amounts of matter that has undergone nuclear processing and is enriched in heavy elements. This had led to the suggestion that supernovae are the main sites of galactic nucleosynthesis. The expanding shock waves created in supernova explosions are thought to be the place where cosmic rays are accelerated, they may induce star formation in dense interstellar clouds and supernovae may even be used as cosmic distance indicators. Given these far reaching implications a thorough understanding of type II supernovae is vital to astrophysics.

On 23rd February, 1987, a supernova explosion was observed in the Large Magellanic Cloud, a satellite of our Galaxy at a distance of 50±7 kpc [3]. Its position coincided with that of a blue supergiant, Sanduleak (Sk) -69° 202 [4]. Despite the approach to disaster, the progenitor had showed no sign of variation on the 579 plates taken since 1879 when it was first observed[5].

The next chapter will concentrate on how Sk -69° 202 evolved to become a supernova. Study of the progenitor star has been a double-edged sword. It has confirmed that massive stars do become unstable and explode. However, it is the first occasion upon which astronomers have seen the explosion of a *blue* supergiant star. This quandary will be given detailed consideration.

Chapter III (or §III) is devoted to an investigation of the explosive mechanism. Although SN 1987A provided astronomers with verification of the energy released by a supernova explosion, it has only fuelled further questions as to the exact quantitative details of the explosion. To date there is no definitive solution.

SN 1987A was the first object other than our Sun from which astronomers have detected neutrinos. The detection of neutrinos allowed astronomers the chance to view the core of Sk -69° 202. Chapter IV probes the implications of the 30 neutrinos detected around the time of outburst of the supernova. These neutrinos promise to open up a new window on the stars.

In the 3 years since its detection, the 'light' of SN 1987A has been detected by instruments on the ground, below the ground, in space and from balloons, airplanes, and rockets. It has been observed from all continents. In chapter V, I give a chronological investigation of the diverse information that astronomers have gained from these observations of the ashes of Sk -69° 202.

In the concluding chapter, I shall consider what can be expected from SN 1987A over the coming years.

Where possible I have tried to give both a chronological and physical interpretation of observations whilst emphasizing the main event: the test of stellar evolution represented by the observations. The author is privileged to have studied the first naked-eye supernova since SN 1604 was recorded by Johannes Kepler.

II. THE PROGENITOR

Because of detailed stellar surveys, the appearance of SN 1987A in the Large Magellanic Cloud could be identified with its progenitor star. So for the first time astronomers have observations of a star as it proceeded from its final nuclear burning phases, through detonation, to its new status, that of an evolving supernova remnant.

Identification of the progenitor was initially confused by the presence of two close companion stars appearing as a composite image. As the supernova dimmed, it was soon determined, to within[6] 0.05 arc sec, that Sk -69° 202 was the precursor of SN 1987A.

From the nature of its progenitor, light curve (§V), and presence of hydrogen lines in its spectrum (§V), SN 1987A can be classified as a type II supernova. Its precursor's spectral classification (B3) and luminosity class (Ia) indicated[7] that its main sequence mass was in the range 16-22 $M_\odot$. That it was a massive star came as no surprise. It is believed from both observation and theory that only stars more massive than 12 $M_\odot$ can give rise to type II supernovae[8]. Less massive stars cannot attain the core temperatures necessary to initiate the more advanced stages of nuclear burning required to produce an unstable iron core. Iron corresponds to the peak in the nuclear binding energy curve beyond which point nuclear fusion reactions are endothermic. The star thus loses the source of radiation pressure necessary to support the star against gravity. The subsequent core implosion and rebound produces a supernova explosion.

A large body of theory describing the evolution of massive stars and the production of supernovae was in place prior to SN 1987A. I shall give the prevailing scenario for the evolution (§II.I) and then discuss why Sk -69° 202 was so unusual (§II.2).

II.1 THE EVOLUTION OF Sk -69° 202

Sk -69° 202 was one of a few dozen OB stars in NGC 2044[9] born around ten million years ago. It was formed with close to 20 $M_\odot$ and for 90% of its life was a blue dwarf star powered by the fusion of hydrogen to form helium.

II.1(i) The last million years[10]

As hydrogen finishes fusing into helium in the innermost 30% of the star, the central regions begin a gradual contraction. Over about 5×10^4 years, the core is compressed, from a density (ρ_c) of about 5 g/cm^3 to 1.1×10^3 g/cm^3 and so heats up from approximately 4×10^7 K to 1.9×10^8 K. The higher core temperature (T_c) and pressure ignites helium fusion. At the same time the outer layers of the star respond to the additional radiation from the core by expanding from a radius of about 6 $R_\odot$ to 500 $R_\odot$[11]. The star is now a red supergiant.

Helium burning lasts approximately one million years and synthesizes a carbon-oxygen core of about 4 $M_\odot$. As the helium at fusion temperature becomes exhausted, the process of core contraction begins anew. A slight decrease in the luminosity of the core leaves the star unable to support its red giant envelope. The resultant contraction makes it once again blue. This transition, which will be discussed in section 2 of this chapter, is a source of great controversy.

Once this contraction increases T_c to about 7×10^8 K (ρ_c=1.5×10^3 g/cm^3), carbon synthesis is initiated. This creates neon, magnesium and sodium, and provides the power source for about a thousand years. From this time on, the evolution of the star becomes very rapid:

(a) The fusion of heavy elements with increasingly large electrical charges (and correspondingly large Coulomb repulsion barriers) requires increasingly extreme temperatures. At the same time, the specific energy per gram available from nucleosynthesis decreases with heavier fuels. The lifetimes of advanced nuclear burning stages are consequently very short.

(b) At temperatures above 5×10^8 K weak interactions become increasingly efficient. Copious high energy photons in the plasma produce neutrino-antineutrino pairs $(\upsilon\bar{\upsilon})$,

$$\gamma <\!\!\longrightarrow e^+ + e^- <\!\!\longrightarrow \upsilon + \bar{\upsilon}, \qquad \text{(II.1)}$$

which above 7×10^8 K radiate more efficiently than photons. The neutrino emission rate is very temperature sensitive, and thus the burning of heavier fuels powers the star for an ever decreasing period.

Beyond carbon ignition, the evolution of the inner few solar masses proceeds so rapidly that there is no time for the outer envelope to adjust (the radiative equilibrium timescale governing the envelope is 2×10^4 years[12]). The star remains a blue supergiant of about 50 $R_\odot$ and it is this configuration which explodes[13]. However the core continues to evolve. After carbon fusion, it shrinks, heats up, and undergoes a brief period of nuclear readjustment, in which neon converts to (more) oxygen and magnesium. Following this, oxygen fuses, chiefly generating silicon and sulphur. It lasts about a year at a temperature of 2.1×10^9 K (1.6×10^7 g/cm^3). By this phase, the $\upsilon\bar{\upsilon}$ pair losses are prodigious - amounting to 10^5 times the photon luminosity[14].

The most abundant nuclei in the centre are now isotopes of silicon and sulphur, chiefly ^{28}Si, ^{30}Si, ^{32}S and ^{34}S. Instead of direct fusion, nuclear processes are initiated when photons strip protons, neutrons and alpha-particles from the nuclei present - known as photodisintegration. So the nucleons rearrange themselves to nuclei with the highest binding energy, namely the iron group. Since ^{28}Si is the most resistant of these nuclei to disintegration, the duration (1-3 days[14]) of the quasi-equilibrium process $2(^{28}\text{Si}) \dashrightarrow {}^{56}\text{Ni}$ is set by the temperature and rate of disintegration of the ^{28}Si in the core[15].

When this 'silicon burning', at $T_c \sim 3.5\times10^9$ K ($\rho_c = 5\times10^7$ g/cm^3), is completed in the inner core ($\sim 1.4\ M_\odot$), the configuration of Sk -69° 202 is as shown in Fig. 1[16]. No more energy can be derived from nuclear rearrangements and so the iron group core becomes dynamically unstable. The 10 million year war against gravity has come to the final battle. In order to support itself, the core again shrinks, and heats up.

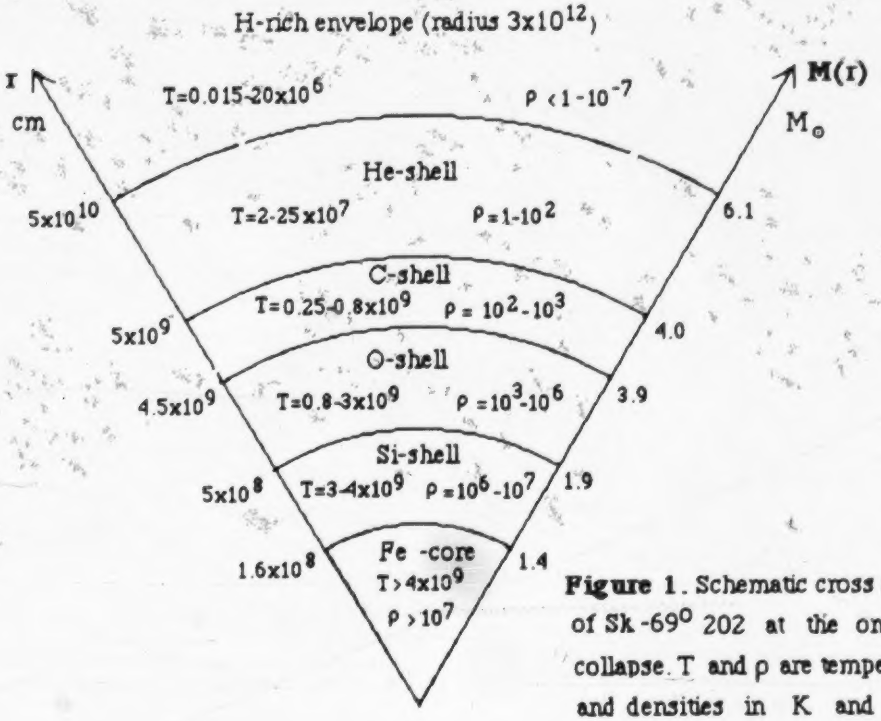

Figure 1. Schematic cross section of Sk -69° 202 at the onset of collapse. T and ρ are temperatures and densities in K and g/cm^3 respectively.

II.1(ii) The onset of core collapse

Two processes accelerate the contraction[17]:

(a) Electron capture,

$$e^- + p <\text{--}> n + \nu_e.$$

$$e^- + A(Z,N) <\text{--}> A(Z\text{-}1,N+1) + \nu_e. \qquad \text{(II.2)}$$

The rates for electron captures on free protons can be computed exactly but electron captures on nuclei are more problematic. Fortunately, various equations of state (EOS) predict a sufficiently high proton concentration that captures on nuclei may be neglected.

(b) Photodisintegration of iron group nuclei, typically,

$$^{56}\mathrm{Fe} \longleftrightarrow 13\,{}^{4}\mathrm{He}_2 + 4n. \qquad \text{(II.3)}$$

This process, which begins during the silicon burning stage, proceeds with increasing efficiency as the temperature increases. It is staged on iron group nuclei and demands a great deal of energy (E= -124 MeV)[18].

The outcome of the collapse is determined by the pressure. Pressure is governed by two factors: the number of particles in the system and their average energy. There are several competing processes.

In the core both nuclei and electrons contribute to the pressure but the electron component is much higher. Consequently, a high rate of electron capture (a), drastically reduces pressure. On the other hand, photodisintegration (b), increases the number of nuclear particles, thereby raising their pressure contribution; however, this dissociation reduces the average energy of the system. The energy for this process comes from the electrons and further decreases their pressure. This loss in electron pressure is more important than the gain in nuclear pressure[19]. As a result, the core now collapses very rapidly.

It has been shown[6] that stars in the mass range from 8-12 $M_\odot$ terminate their nuclear burning with an oxygen-neon or neon-silicon core. This stable core is supported by degenerate electron pressure. However, more massive stars such as Sk -69° 202 form an iron group core of mass range 1.3-2.2 $M_\odot$. The exact value depends upon the main sequence parameters, e.g. main sequence mass, metallicity, etc.

Chandrasekhar showed that there is a limit to the amount of gravitational pressure that can be resisted by degenerate electron pressure[20]. Equilibrium, and thus a stable core, is only possible if the core mass is less than a critical value. This is denoted by the Chandrasekhar mass, M_{CH}. If the mass of the core at zero temperature is greater than

$$M_{CH} = 5.76 Y_e^2 M_\odot, \qquad \text{(II.4)}$$

where the electron concentration is given by $Y_e = n_e/\rho N_A$, where n_e is the average number of electrons per nucleon and N_A is Avogadro's constant, then the core must collapse. The composition of Sk -69° 202's pre-supernova core has been investigated in detail[21,19,22,23,24,25,26]. In these calculations Y_e varies from 0.32 to 0.45, at the onset of collapse. Temperature dependent profiles from such stellar model computations give the progenitor's M_{CH} to be in the range 0.7-0.9 $M_\odot$.

Further discussion of the sequence of events following the destabilisation of the Chandrasekhar mass core is given in §II. For now I wish to investigate why Sk -69° 202 was so unusual.

II.2 WHY WAS Sk -69° 202 BLUE?

Theory developed to explain the light curves of hundreds of distant supernovae indicates that type II's originate from massive red supergiant ancestors. Although Sk -69° 202 was massive, the surprise came from its colour. It was blue not red.

There is general agreement that Sk -69° 202 became a blue supergiant only just prior to exploding. The evidence is as follows.

Observations with the International Ultraviolet Explorer (IUE) have, from 24 May 1987 onwards, shown multiply ionised narrow lines of C, N, and O; since December 1987, these results have been verified by a number of ground based optical telescopes. The detections indicate the presence of highly processed material in a dense, low velocity circumstellar shell.

(a) Spectroscopic analyses[27,28] indicate electron densities of 1-3x10^4 cm^{-3}. Although this is greater than expected for the wind shed by the precursor star, in either its blue supergiant or preceding red supergiant phase[29], the density can be attributed to the shock region where the blue and red supergiant winds interact.

(b) A nebular analysis[26] of the line strengths reveals a large nitrogen overabundance: N/C=37±16 and N/O=12±6, relative to solar values[30]. Such a strong nitrogen enhancement is consistent with CNO-processed material being mixed into outermost regions which are subsequently lost to the stellar wind. This is consistent with the large scale mixing expected during a convective red supergiant phase.

(c) The frequently observed OIII and NII emission lines yield velocities of 10-20 km/s which is indicative of a red supergiant wind (10-30 km/s)[31] rather than blue supergiant wind (500-700 km/s)[32].

(d) The extent of the emitting region has been determined by a number of observers[33,31] to be an oval nebula approximately centred on the supernova with radii of 1.3±0.5 arcsec E-W and 0.9±0.5 arcsec N-S, at a fiducial distance of 50 kpc this corresponds to radii of about 0.7-1.0 light years.

Taken all together, these data imply the narrow emission lines arise from the inner part of the red supergiant wind that has been swept up by the fast wind of the blue supergiant phase. Since the shock interface between the red and blue supergiant winds is expected to expand at about 50 km/s, the time elapsed since Sk -69° 202 was a red supergiant can be estimated as less than 7000 years. So, the blue supergiant phase must have been the consequence of changes in the stellar interior that accompanied the termination of helium burning: helium burning takes (of order) 6×10^5-1×10^6 years and all subsequent phases take less than about 10^3 years.

Evidence for the blue nature of the progenitor also comes from the rapid rise of the light curve following the detection of neutrinos (§V.1); from the subsequent light curve to maximum luminosity (§V.2); and from the early spectra [§V.1(i)].

Careful scrutiny has revealed that other type II progenitors were also blue, e.g., SN 1984E[34] and SN 1990H[35], but the question still remains: why was SN 1987A's progenitor blue?

Theoretical models of Sk -69° 202's evolution until it exploded have been derived[12, 36,37]. All models are initially blue, then proceed through a red phase, before finally reverting back to the blue in time to explode (e.g. Fig. 2). Model calculations depend very sensitively on composition, mass loss, choice of criteria for convection, handling of discontinuities, etc. Which path is followed by a particular real star will be a delicate function of its properties: composition, magnetic field structure and so forth. So the simultaneous presence of coeval Wolf-Rayet stars, red, and blue supergiants in the 30 Doradus region of the LMC where SN 1987A exploded is not surprising.

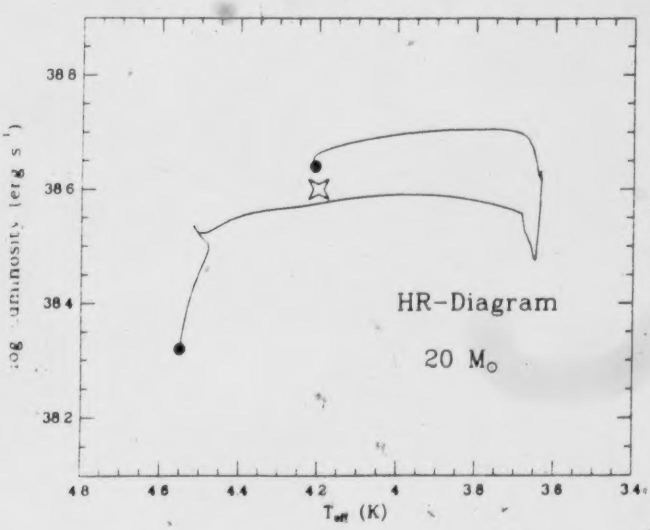

Figure 2. Evolutionary track of a 20 $M_\odot$ which completes its evolution with a temperature and luminosity very similar to that of Sk -69° 202 (shown as the four pointed star). The model[12] becomes a blue supergiant 20,000 yr before explosion, has a metal abundance one-quarter solar, and convection according to the Ledoux criteria.

Computer simulations of Sk -69° 202 have yielded similar case histories[12,36,37]. until the evolution to red supergiant. At this point the models diverge. There appear to be two basic processes which in some combination allow the evolution of the star to the blue supergiant stage.

(i) The star lost mass [§A.1], decreasing its gravitational potential, thereby making it more compact and shifting it into the blue phase.

(ii) The lower metallicity compared to our own Galaxy changed the evolution to allow it to explode with a smaller radius than one might expect.

II.2(i) Mass loss

Well before SN1987A, it was noticed that a massive star which had lost most of its hydrogen envelope during helium burning, would evolve back toward the blue on the Hertzsprung-Russell diagram, exploding as a blue supergiant or, in the extreme limit of complete hydrogen loss, a Wolf-Rayet star[38]. A star with no hydrogen envelope is more compact; so too, is one with a little hydrogen. The last few solar masses of envelope contain a high helium abundance and hence have an average atomic weight much greater than material in the outer envelope (primarily hydrogen). Such stars assume a smaller radius. So perhaps mass loss might have allowed Sk -69° 202 to become a blue supergiant (§A.1).

However, there are problems with using a large mass loss as the sole explanation for the compact nature of the progenitor. Firstly, 20 $M_{\odot}$ is rather light for a star to lose nearly all af its envelope: there is evidence that the bulk of the Wolf-Rayet stars in the LMC originate from progenitors heavier than 40 $M_{\odot}$ [39]. Secondly, the radius and luminosity of Sk -69° 202 were such that the most recent numerical models allow only two (very distinct) scenarios[40,41] - either it underwent little mass loss (a few solar masses at most), or it lost almost its entire hydrogen envelope. Intermediate values of envelope mass yield red supergiant progenitors. Neither of these arguments is convincing. The strong evidence against a large amount of mass loss has appeared as the supernova has evolved.

A number of observations have convinced astronomers that Sk -69° 202 exploded with a substantial hydrogen envelope in place. These include the slow rise of the optical light curve to maximum (85 days, see §V.2), the lack of early gamma-rays and X-rays from radioactive decay [150 days, see §V.6(ii)], and the late appearance of the slowest moving hydrogen (25-40 days, see §V.2). Had the hydrogen envelope been a few solar masses or less, the early light curve would have quickly evolved to a brighter supernova; X-rays and gamma-rays would have appeared much sooner and peaked at least a factor 10 greater[42] ; and the slowest moving hydrogen (indicating the base of the hydrogen envelope) would have been uncovered after less than a week with a substantially higher velocity. Integrations of the density and velocity from the spectra are consistent with that of a 10 $M_{\odot}$ rather than a few $M_{\odot}$ hydrogen envelope. Although Sk -69° 202 did undergo at least one episode of mass loss[43] (§II.2), a substantial (certainly more than 7 $M_{\odot}$ [5], probably 9-11 $M_{\odot}$ [44]) envelope mass remained at the time of explosion and so other causes for making the progenitor a blue star need to be investigated.

II.2(ii) Metallicity

Evolutionary models of massive stars have been well studied for solar metallicities, but the value for the Large Magellanic Cloud (LMC) is smaller by a factor 2-4 (e.g.[45]). Recent models all indicate that a reduced metallicity leads to a decreased radius in pre-supernova stars. This is not as straightforward as simply altering the opacity[46] - thus making an envelope containing metallic elements more prone to extension (energy is radiated away more slowly because of the opaque nature of the envelope). In addition, decreased metallicity reduces the rate at which nuclear energy is released at a given temperature during hydrogen burning by the CNO cycle[47]. This leads to a more centrally concentrated core with a greater gravitational potential at its boundary, producing a smaller, bluer star.

Spectral analyses[29] of Sk -69° 202 and the early spectra from SN 1987A [§V.2(i)] give strong evidence for a metallicity lower than solar by a factor 3-4. Several different stellar modelling groups have extended evolutionary calculations to include metallicity. The models of Saio et al[36]. change from the blue to the red during helium burning and spend less than one tenth of their helium-burning lifetimes as a red supergiants (RSG's). Although these models are in accordance with the number ratios between blue and red supergiants in the local region - in the 30 Dor region of the LMC there are ~200 BSG's and 12 RSG's[47,48] - they do not comply with observations of circum-supernova material (§II.2). On the other hand, the models of Woosley and collaborators[12,37] spend almost their entire helium burning phase as red supergiants, evolving back to blue in the last 4×10^4 years. Although the latter is in better accord with observation, it must be noted that such models use artificial tuning for convection parameters and take no account of rotation [§II.2(iii)].

The ways in which metallicity influences the evolution are complex and not fully researched. But it should be noted that the low frequency of bright type II supernovae in irregular (low metallicity) galaxies[49], suggests the low metallicity of Sk -69° 202 is vital in obtaining a blue supergiant progenitor.

II.2(iii) Other factors

The strength of the circumstellar nitrogen lines (§II.2) and many subsequent observations of the ejecta (§V.4) suggest that heavily processed material was ejected from a previous red supergiant phase. They indicate that the star had a convective envelope that mixed-up matter formed in the core of the star. In attempting to model convection a number of mixing criteria can be used, e.g. Ledoux, Schwarzschild, etc.[50]. However, only by employing shallow composition gradients in the envelope that arise from restricted convection in the semi-convective layers, are models able to result in blue to red to blue evolution[51]. However, this limited mixing of the stellar material gives ratios of N/C and N/O at least a factor of three smaller than those inferred from observation[29]. This suggests that a full evolutionary model for Sk -69° 202 will have to incorporate convective overshooting[51] - not as yet incorporated in models.

Rotation also plays a role in stellar evolution and is expected to decrease post main sequence luminosity, increase rates of mass loss (§A.1), and promote mixing (§A.2).

Indeed observations of the envelope of SN 1987A indicate an asymmetric shape [§V.4(i)]. In addition to altering the evolution of the progenitor, rotation will lead to a non-axisymmetric collapse. Such a collapse could in principle be distinguished by its effect on the flux of neutrinos and gravity waves from SN 1987A. However, the inconsistencies of these detections are insufficient to constrain the infant theoretical models for evolution of differentially rotating stars[52].

Understanding the issue of the blue progenitor is of great importance in determining the frequency of SN 1987A-like events. Statistical samples are strongly biased against faint supernovae. At maximum luminosity, SN1987A had M_V=−16.2, corresponding to a factor ~13 fainter[53] than a 'typical' type II supernova. Thus, if supernovae such as SN1987A were as frequent as typical supernovae per unit cosmic volume, they would be detected only $13^{-3/2} \sim 0.02$ times as often in a magnitude limited sample. If metallicity is indeed important then this factor will be further reduced since within the local group (to the Milky Way) the population of metal-poor galaxies is low[54]. The answer to this can come only from a better understanding of what makes the presupernova choose between blue and red solutions.

In conclusion it seems that a combination of factors caused the presupernova star to be blue, with low metallicity playing an important, but only partial role.

III. THE EXPLOSION

On the night of February 23 1987, the outcome of the rapid collapse of the central regions of Sk -69^o 202 was visible for all those viewing the 30 Doradus region of the LMC. However, the processes which allowed the progenitor to transmute from an unstable blue supergiant to a supernova explosion are less clear. I shall elucidate general collapse characteristics until nuclear densities and then argue how Sk -69^o 202 may have become SN 1987A: how did rapid implosion become rapid explosion?

III.1 GENERAL COLLAPSE FEATURES

The explosion of Sk -69^o 202 is understood to arise from the collapse of the central iron core to nuclear densities. The subsequent core bounce produces a shock wave of sufficient energy to eject the outer layers of the star and cause it to become a supernova.

The salient feature allowing the core to collapse to very high densities is the low entropy involved. Sk -69^o 202 is subject to the convective stability criterion: entropy must be either constant or increase radially outward from the core. Throughout its evolution the core of Sk -69^o 202 can be pictured as digging itself into an 'entropy hole'.

The entropy, S, is given by $S = \ln W$, where W is the available number of states. By the start of carbon burning, the radiation of photons reduces the entropy, measured in units of k (Boltzmann's constant), to approximately 3 (from an initial value at stellar coalescence of 15)[19] . However, from this time on, the entropy evolution is determined by the far more bountiful neutrino losses. Following silicon burning, these are 10^5 times the losses from photons[11].

By the onset of core infall, nucleon entropy is less than 1.5 per particle. Given this low entropy, nucleons remain bound in nuclei: drip-neutrons carry an entropy of 5 to 10 per particle[19]. Electrons, the major source of core pressure, are already highly degenerate

(S~1). Altogether, there is an astoundingly high order in the system. This order persists throughout the collapse. Thus, the partial disintegration of nuclei into alpha particles (II.2) before the onset of collapse is reversed at higher densities as the alpha particles go back into nuclei.

For 100 years before collapse, the progenitor's entropy losses are dominated by neutrino emission. However, once collapse densities reach 10^{11} g/cm^3 (see §B.2), matter becomes opaque to neutrinos: the diffusion time for neutrinos (of all types) is of the order of 0.1-10 s and thus much longer than collapse times, about 10^{-3} s. Consequently neutrinos are trapped.

By the time trapping density is reached, the efficacy of neutrino-electron scattering (the dominant neutrino interaction) equilibrates the neutrino energy distribution. In addition, weak interaction rates are sufficiently fast that matter is essentially in equilibrium and thus little entropy is generated (Fig. 5). As a result, the nature of the implosion is, to a good approximation, adiabatic.

Computations indicate that, for collapse densities 10^{11}-10^{14} g/cm^3, nucleons associate in large globules, see Fig. 3. The formation of such very heavy excited nuclear states, having large heat capacities, led to a 'relatively' cool (10^{10} K) imploding core.

Figure 3. Free energy of a Wigner-Seitz cell versus mass number for $T=2.5$ MeV, $\rho=6\times10^{11}$ g/cm^3, and $Y_e=0.3$. The configuration with about 560 nucleons has the lowest free energy and is therefore, the most stable one [55].

Calculations imply that the thermal pressure of hot nucleons is small and, consequently, the collapse pressure is dominated by contributions from degenerate relativistic electrons. At initial collapse densities, 10^{10}-10^{11} g/cm^3, the equation of state can be taken as that of non-interacting Boltzmann particles. However, this approximation breaks down at higher densities when nucleon-nucleon and nucleon-nucleus interactions become important. Nuclei can no longer be treated as point particles. Thus, the Boltzmann gas equation has to be replaced by a microscopic model accounting for the Fermi pressure of degenerate nucleons.

Contemporary calculations utilize a series of hydrodynamic codes to simulate the high density equation of state. Nuclear interactions are modelled in a variety of ways: the temperature dependent Hartree-Fock (e.g.[56]); the Fermi gas model (e.g.[26]); and the liquid-drop heavy-nucleus with neutron-drip description (e.g.[23]). These simulations give generally concurrent results. However, nucleon-nucleon forces are only weakly constrained by experimental data (±50%, see review[23]). Thus, models lose reliability with increasing density. As will be seen later (Fig. 9), the outcomes of numerical simulations of collapse are very sensitive to the properties of the equation of state above nuclear densities.

III.2 COLLAPSE TO SUBNUCLEAR DENSITIES

Once the Chandrasekhar mass core is destabilised by electron capture and photodisintegration [§II.1(i)], it collapses until the density of the star exceeds that of an atomic nucleus. In 1 second, the configuration, about the size of the Moon, collapses to one with a radius of about 20 km. The velocity during the collapse reaches about 70,000 km/s in the outer portion of the iron core[42]. However, because of the weaker gravity experienced by the layers further out and because the information that the core had collapsed propagates outward as a sound wave of finite speed, the neon, carbon and helium shells (as well as the hydrogen envelope) do not participate in the collapse.

The demarcation point for these outer layers is the radius at which the infall velocity is equal to the speed of sound - known as the sonic point, see Fig. 4. At this location in the co-ordinate system of the infalling matter, sound waves remain stationary: they have the same velocity as that of the infalling material. Thus, a disturbance inside the homologous core has no influence beyond the sonic point.

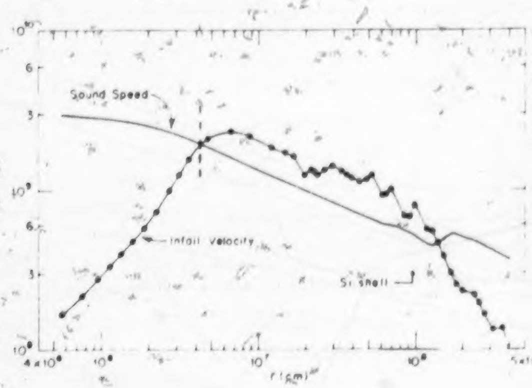

Figure 4. [57] For $r<4\times10^6$ cm, the infall velocity is approximately proportional to distance r from the centre; this is the homologous core. The matter in the core beyond the sonic point (shown as a dotted line) is infalling faster than the local sound speed. Outside the silicon shell the infall is once again subsonic .

The infa!! continues adiabatically until nuclear densities are reached; nuclei then dissolve into a homogeneous fluid of free protons and neutrons. The most striking feature of simulations is the rapid increase of pressure with density as degenerate nucleon interactions in a Fermi fluid become dominant. Above 1.5 ρ_o where ρ_o is the nuclear density (2.3×10^{14} g/cm^3), nucleon pressure exceeds electron pressure. The nucleon pressure at such densities, is commonly derived using the compressibility, K, of nuclear matter (as extrapolated from the energy of the 'breathing mode' of heavy nuclei[19]). For an adiabatic collapse the total pressure, P is given by,

$$P = A\left(\frac{\rho}{\rho_o}\right)^{\Gamma}, \qquad \text{(III.1)}$$

where constant, $A \propto K$ at nuclear densities, and Γ is the polytropic index.

For densities up to that of nuclear matter, the pressure is determined almost completely by relativistic, degenerate electrons, and so infalling material has a polytropic index, Γ_1 slightly less than the 4/3 expected for degenerate electrons (the decrease coming chiefly from electron capture[58] prior to neutrino trapping).

In order to gain a simple physical picture for the reversal of the collapse, I shall employ the hydrodynamic equation of motion for a non-magnetic spherically symmetric system:

$$\frac{d^2r}{dt^2} = -\frac{1}{\rho}\frac{dP}{dr} - \frac{m(r)G}{r^2}, \qquad \text{(III.2)}$$

where d^2r/dt^2 is the deceleration upon the mass element in question; G is the gravitational constant; and m(r) is the mass interior to radius, r. For the motion of an individual element of infalling material, whose density will satisfy, $\rho = \rho_i(r_i/r)^3$, where ρ_i and r_i correspond to values at the onset of collapse, the acceleration on any mass element within the homologously collapsing core, is given by[59],

$$\frac{d^2r}{dt^2} = \frac{m(r)G}{r^2}\left[1-\left(\frac{r_i}{r}\right)^{\Gamma-(4/3)}\right]. \qquad \text{(III.3)}$$

Until nuclear densities are reached, $\Gamma=\Gamma_1$, and the acceleration is of the order G $m(r)/r^2$. However once nuclei are converted to nucleons (at supranuclear densities), Γ rapidly increases (see Fig. 5), and the exponent changes sign: the second term becomes large and the acceleration oppositely directed. The effect of this massive core deceleration is almost as if the infalling matter were striking a 'brick wall".

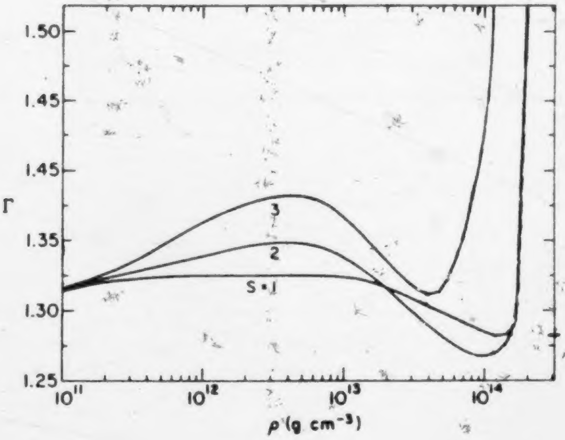

Figure 5. Adiabatic indices as a function of density (at the appropriate entropy)[60]. The graph shows the rapid increase of Γ above 10^{14} g cm^{-3}.

III.3 SHOCK FORMATION

At the core in the heart of the star infalling matter is stopped. This, however, is not instantaneous owing to the compressibility of nuclear matter. Thus momentum carries the central core to a maximum 'scrunch' density, $\rho_s=3\text{-}4\rho_o$ [19,3,61]. After maximum 'scrunch', the core of nuclear matter rebounds. Further oscillations of the core are critically damped by the radiation of pressure waves into the surrounding material[26].

As these pressure waves propagate outward, they slow, partly because the local speed of sound, v, decreases (Goldreich-Weber theory[62] gives, $v = C\rho^{1/6}$, where C is a constant); and partly because they move upstream against a flow of infalling matter that gets steadily faster (Fig. 4). Meanwhile more material falls onto the hard central sphere, so generating further pressure waves which collect at the sonic point building up pressure. This fluctuation in pressure slows the material flowing through the sonic point and creates a discontinuity in velocity. Such a discontinuity is known as a shock wave. Thus shock formation occurs near the sonic point (20-25 km), that is, near the edge of the homologous core (Fig. 4), rather than at the centre of the star.

Unlike the pressure waves that generate it, the shock wave is not pinned to the sonic point by infalling matter, rather its progress is dependent upon its energy. So initially it is a stationary accretion shock. It only begins propagating outward (in spatial co-ordinates) when 0.1-0.2 $M_\odot$ [26]. has fallen through onto the core, adding kinetic energy and thereby raising the shock velocity above that of the infall.

From energy conservation, the energy put into the shock can be estimated[61] as,

$$E_{shock} \sim M_{shock}(E_{max} - E_{min}) - \Delta E_\upsilon \; ; \qquad \text{(III.4)}$$

where M_{shock} is the mass enclosed by the shock when it first forms; where $E_{max}\,M_{shock}$ and $E_{min}\,M_{shock}$ are the total energy of the mass, at maximum core compression and maximum core rarefaction; and where ΔE_υ is the neutrino energy radiated out of M_{shock}

between compression and rarefaction [small due to trapping of neutrinos (§B.2)]. Simulations give the initial shock energy as

$$E_{shock}= 4\text{-}7 \times 10^{51} \text{ ergs}, \qquad \text{(III.5)}$$

the exact value being dependent upon the 'softness' of the nuclear equation of state[26]: the higher the density that the core achieves before bounce, the greater the initial shock energy[63].

Until the outward propagation of the shock wave the main characteristics of the Sk - 69° 202 explosion are agreed upon, but the synopsis from this stage on is highly controversial.

III.4 THE PROMPT SHOCK WAVE

In the simplest scenario, the shock wave continues outwards through the star. Beyond a certain radius, the bifurcation point, all the stellar material is blown off; the matter interior to this point condenses to form a neutron star. This is known as the prompt hydrodynamic explosion. However, in most models of the explosion, energy losses cause the shock to stall before it leaves the iron core and is thus insufficient to remove the stellar envelope (see Fig. 6)[64].

The problem is one of energy dissipation by disintegration, $E_{disintegration}$. This is a measure of how much energy the shock must expend to disintegrate iron-like nuclei to free neutrons and protons as it propagates through the outer core. This is given by,

$$E_{disintegration} = 17 \left(\frac{M_{core}}{M_\odot} - \frac{M_{shock}}{M_\odot}\right) \times 10^{51} \text{ ergs}, \qquad \text{(III.6)}$$

where it has been assumed that the average binding energy of nucleons to nuclei is 8.7 MeV per nucleon (disintegration takes place primarily on iron group nuclei). The actual amount of energy that the shock expends in disintegrating nuclei is less than this because nuclei are not completely dissociated either at the outer edge of M_{shock}, where the shock wave has not yet acquired its maximum energy, or at the outer edge of the core M_{core}, where the post-shock temperatures fall too low to disintegrate nuclei.

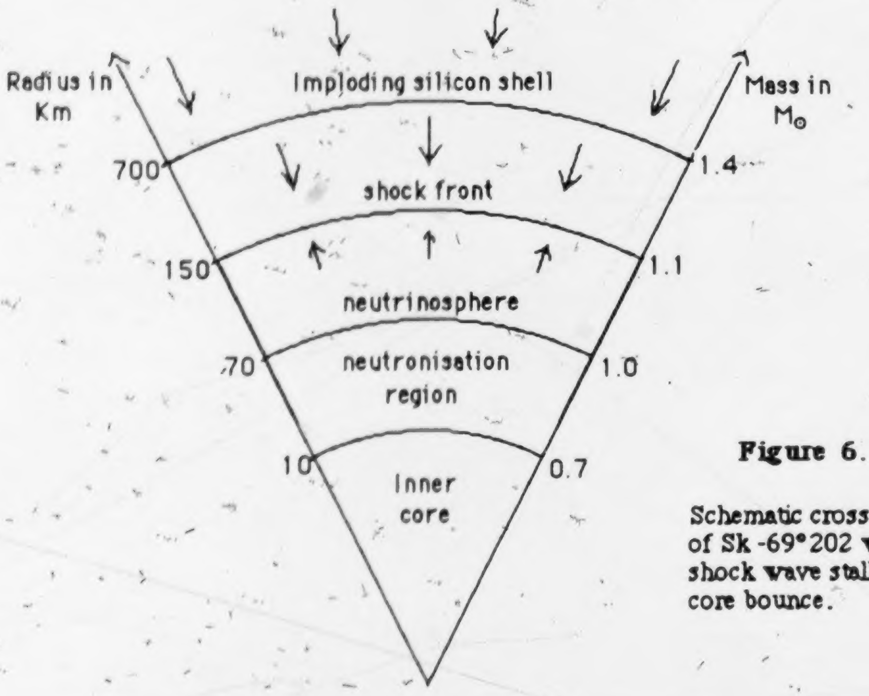

Figure 6.

Schematic cross section of Sk -69°202 when the shock wave stalls after core bounce.

Since models of the shock wave always start in the same region (0.1-0.2 $M_\odot$ outside the homologous inner core), its success or failure is contingent upon the mass between the onset of the shock wave, and the bifurcation point. From observed supernova remnants, this point is the edge of the iron core: the mass of the neutron star remnant in the centre is taken to correspond to the theoretical rearranged mass of the iron core which was in place before implosion. Taking typical values of the mass of the homologous core, 0.7-0.9 $M_\odot$ [§II.1(ii)], conservation of shock wave energy [using (III.5) and (III.6)] requires model iron cores not larger than about 1.3 $M_\odot$. This picture is incomplete, however, because once the shock wave has passed the neutrinosphere, neutrinos which previously support the shock wave, remove further energy [2-3x10^{51} ergs (§III.5)] from the shock.

The most recent calculation[65] gives a maximum iron core mass (M_{core}) of 1.1 $M_{\odot}$ for a successful prompt shock.

It is generally agreed that such an iron core mass is too small; the reasons are twofold. If the neutrinos detected from SN 1987A are taken to herald the birth of a neutron star, then iron core masses of about 1.4 $M_{\odot}$ [§IV.4(ii)] are required. Moreover, models of stellar evolution indicate iron core masses of 1.1 $M_{\odot}$ to correspond to main sequence progenitors of masses between 13 and 15 $M_{\odot}$ [66]. This is at variance with observations of Sk -69° 202 (§II).

If the prompt explosion fails, does Sk -69° 202 disappear inside its event horizon and form a black hole? This might be an exciting event, but it would most likely be dim and not a supernova. To refute this catastrophe, the evolution of the central energy rich core must be considered. In particular, it contains a large fraction of electrons.

After core bounce, the temperature of the core is high enough [40-50 MeV (§B.3)] that electrons are captured by nuclei and protons [neutronisation (II.2)]. The resulting neutrinos diffuse out (§B.4). As electrons are captured, the pressure in the inner core decreases and the inner core contracts; the outer core, between 0.8 $M_{\odot}$ and the neutrinosphere follow. Neutronisation releases about $2\text{-}4\times10^{51}$ ergs as neutrinos until about 300 ms after core bounce: the time for the proto-neutron star to reach hydrostatic equilibrium. This is followed by a release of $1\text{-}5\times10^{53}$ ergs in thermal neutrinos 0.1-10 s after core bounce (§B.4). For several decades, it has been realised that the coupling of even a small fraction of this flux to the comparatively loosely bound mantle ($\sim10^{51}$ ergs) would produce a vigorous explosion.

III.5 THE DELAYED EXPLOSION MECHANISM

When the outgoing shock wave stalls (as it does in most calculations), it lies external to the neutrinosphere - even so, some escaping neutrinos deposit energy as they are scattered by electrons and captured by neutrons and protons. Here I shall describe the ways in which a stalled shock may be revived by neutrino heating.

The disintegration of nuclei, so costly to the prompt shock, actually contributes to the shock wave in another way: the process produces free protons which in turn capture electrons. Although the neutrinos emitted in this process and those emitted by the cooling core are only trapped until the shock front expands beyond the neutrinosphere (2-6 ms)[67], the coupling of a small percentage of this neutrino flux is sufficient to revitalise the shock. Because of its longer time scale, this mechanism has come to be known as the "delayed explosion mechanism"

Momentum deposition by outgoing neutrinos can only be effective in driving the shock wave if the luminosity exceeds the critical "Eddington neutrino luminosity", the value at which the outward force due to neutrino momentum deposition equals the inward force of gravity. Assuming spherical symmetry, the force of neutrino pressure, $F_{\upsilon P}$, of the emitted radiation which acts on the material is

$$F_{\upsilon P} = \frac{\sigma_\upsilon f}{c}, \qquad \text{(III.7)}$$

where the flux is $f = L/4\pi R^2$, and σ_υ, the neutrino scattering cross-section. The attractive gravitational force is,

$$F = \frac{GMA(m_e+m_p)}{R^2} \approx \frac{GMAm_p}{R^2}, \qquad \text{(III.8)}$$

assuming that the opacity in the overlying mantle is dominated by coherent scattering of heavy nuclei with an average atomic mass, A (m_e is the mass of an electron, and m_p the proton mass). Equating (III.7) and (III.8), a critical value for the luminosity of the source is obtained; this is known as the Eddington neutrino luminosity,

$$L_{E\upsilon} = \frac{GM4\pi cAm_p}{\sigma_\upsilon}. \qquad \text{(III.9)}$$

For coherent scattering,

$$\sigma_\upsilon = \frac{1}{16}\sigma_0 \left(\frac{E_\upsilon}{\mathrm{MeV}}\right)^2 A^2 \left[1 - \frac{Z}{A} + (4\sin^2\theta_w - 1)\frac{Z}{A}\right]^2 , \qquad \text{(III.10)}$$

where $\sigma_0 = 3.5 \times 10^{-44}$ cm^2/MeV, where Z is the mass number, and θ_w is the Weinberg angle with a measured value[68] of $0.23^\circ \pm 0.01^\circ$. For Z~26, A~56, then

$$L_{E\upsilon} \sim \frac{5 \times 10^{54}}{\left(\frac{E_\upsilon}{10\ \mathrm{MeV}}\right)^2} \text{ ergs/s.} \qquad \text{(III.11)}$$

To consider the effectiveness of such a mechanism the timescale for neutrino release must be considered. The flux comprises two distinct phases of high neutrino luminosity: there is a burst of neutrinos as the shock breaks out (2-6 ms) of the neutrinosphere[69]; this is followed by the flux of neutrinos diffusing from the proto-neutron star [(0.1-10 s (§B.4)]. I shall first consider the effect of the initial phase of neutrino emission.

The energy lost in this burst of electron neutrinos is 1-2 x10^{51} ergs. But since the burst duration is a few milliseconds, the peak luminosity is enormous, $L_{\upsilon_e} \sim 5 \times 10^{53}$ ergs/s [70]. Although its short duration means that it will be insufficient to support the Eddington neutrino luminosity (III.11) (and hence the shock wave) for long, a fraction of this energy preheats the iron nuclei in front of the shock front. If sufficient energy is deposited by the neutrinos, then the material ahead of the shock will 'pre-dissociate' before the shock arrives. Thus 'prompt' preheating by neutrinos would be a net energy saver for the shock. The importance of this mechanism is difficult to establish due to its sensitive energy dependence [see (III.11)]. Detailed calculations[67] show that, if E_υ=15 MeV, then the disintegration energy, $E_D \sim 1.4$ x10^{51} ergs, whereas if E_υ=10 MeV then $E_D \sim 0$ ergs. Analysis of the neutrino burst spectrum indicates $E_{\bar{\upsilon}_e}$=3-5 MeV [§IV.4(ii)][71]. Although not enough to overcome the losses due to photodisintegration incurred by the prompt shock, its effects must be considered.

In the second phase the binding energy of the proto-neutron star is released [some 2-9x10^{53} ergs (§B.3 & Fig. 9). Although this represents an energy release ~100 times that of the earlier phase, its long timescale [0.1-10 s (§B.4)] means that the Eddington neutrino luminosity (III.11) is not provided.

For both phases of neutrino emission, such heating is insufficient to drive an explosion, but it can have supported the shock. It must be noted that when the prompt shock wave stalls, it is in radius, not in the mass coordinate: outer core layers continue to fall through the shock. So, material behind the shock may become dominated by radiation pressure, if its temperature is maintained by the neutrino flux. When the specific internal energy of this material exceeds the gravitational energy,

$$\frac{aT^4}{3\rho} > \frac{GM}{R}, \qquad \text{(III.12)}$$

expansion occurs[52]. So accretion through the shock can reverse into a neutrino driven wind, the supernova.

In one recent calculation[72] a hot bubble of material, formed at between 5×10^6 cm and 2×10^8 cm, with $T=0.5$ MeV, and $\rho=10^5$ g/cm^3 is sufficient to maintain the pressure behind the shock and thus to remove the envelope. Other computations indicate that this pressure gradient is sufficient to lead to a micro-convective[73] instability with the convective regions encompassing the neutrinosphere. This increases the flux by mixing dense electron-rich matter into less dense regions from which the neutrinos freely stream. It seems that the temperature of the neutrinosphere, upon which the long term mechanism strongly depends, is increased by up to 50% by this convection[50]. To date only one full hydrodynamic calculation has managed to provide a successful delayed explosion. Unfortunately the uniqueness of the model[72] is not known as the calculation is very involved[74]. The checking of this computation by other groups is of the utmost importance.

The effects of rotation on the explosion must be considered [see also §V.4(ii)]. For instance a combination of rotation and nuclear burning in the mantle could provide the energy requirements for a successful detonation. If so, supernova remnants displaying a pronounced anisotropy, e.g. N132D in the Large Magellanic Cloud[75], might occur.

Unfortunately, the initial angular momentum distribution and its coupling to stellar material is very poorly understood. Preliminary calculations agree [76,77] that rotation leads to a lower density at core bounce and so to a less energetic shock wave, but this is partially compensated by higher temperatures (from enhanced convection) which lead to more material undergoing explosive nucleosynthesis.

Despite using similar input physics, many computer simulations of the explosion have given widely conflicting results. On closer inspection this is hardly surprising, when one appreciates the apparent fine tuning of the event. From observations we know that nearly all the binding energy of the newly born neutron star was radiated as neutrinos ($>10^{53}$ ergs). The kinetic energy of the ejecta ($\sim10^{51}$ ergs) and the energy in the electromagnetic radiation ($\sim10^{49}$ ergs) were merely small fractions of the energy inventory. In replicating the explosion, it is the consistent modelling of these small corrections from which we derive our understanding.

Delayed explosions are certainly favoured if the iron core mass exceeds 1.3 $M_\odot$ - the neutrino signal indicates about 1.4 $M_\odot$ [§IV.4(ii)]. Though the simulations of delayed explosions tend to result in less kinetic energy ($< 10^{51}$ ergs) than prompt ones ($>10^{51}$ ergs). Current estimates (e.g.[78,44]) of the explosion energy, based upon light curve and velocity, are in the range 0.6-1.5×10^{51} ergs, for an envelope mass of 9-11 $M_\odot$. The debate is not resolved. Models are, however, far from complete. They have yet to properly incorporate the effects of general relativity, rotation, and departures from spherical symmetry.

It was hoped that SN 1987A would resolve the controversy over the explosive mechanism of massive stars. Unfortunately, most of the observable properties of SN 1987A, e.g., velocity, spectra and light curve, are not sufficiently sensitive to suggest how the star explodes, but register only the fact that about 10^{51} ergs is somehow deposited in the central regions of the star. This must be kept in mind when the neutrino events from SN 1987A are interpreted.

IV. THE NEUTRINO BURST

SN 1987A continues to reveal interesting phenomena and will be scrutinized for many years throughout the electromagnetic spectrum. However, the most exciting and unique aspect of the explosion will remain the detection of neutrinos. This signalled not only the collapse of the supernova's iron core, but also heralded the birth of neutrino astronomy.

Neutrino bursts were recorded in four detectors in the Northern Hemisphere. These pulses arrived on February 23.12(UT) and February 23.32(UT). Photographs taken at February 23.44(UT)[79], show an object in the position of Sk -69° 202 in the Large Magellanic Cloud (LMC) to have brightened since the previous night by at least 8 mag to mag 6.4 (naked-eye brightness). The probability that a strong burst of neutrinos would have arrived coincidentally - within 4.5 hours - with the electromagnetic signal which had a travel time of 1.4×10^9 hours (1.6×10^5 years) is vanishingly small. The neutrinos must have been emitted from the exploding star.

Neutrino signals were detected at Baskan (Soviet Union)[80], Irvine-Michigan-Brookhaven=IMB (USA)[81], Kamiokande (Japan)[82], and MontBlanc (Italy)[83]. The latter two detectors were originally constructed to search for proton decay, but were also well instrumented for detecting neutrinos. The former detectors were constructed for detecting neutrinos from the centre of our Galaxy.

Also in operation on February 23, 1987, was the well known ^{37}Cl experiment at Homestake mine (U.S.A.). It saw one count for the period February 15th to March 1st - consistent with its normal background counting rate[84]. The experimenters thus find that there is no evidence for a positive effect due to neutrinos from SN 1987A. However, its lack of observation yields interesting null constraints for the interpretation of the events seen in the other detectors [§ IV.4(i)].

Table 1. Detector properties[85]

DETECTOR	ACTIVE MASS (tons)	DETECTION THRESHOLD MeV	BACKGROUND PULSE s^{-1}	ERROR IN TIMING s	EFFICIENCY see §B.5 ε
IMB	6800	20	3.5×10^{-6}	±0.05	0.1-0.7
Kamiokande	2140	8.3	0.022	±60	0.15-0.9
Baskan	200	10	0.033	±54	0.6
Mont Blanc	90	5.3	0.01	±0.002	0.5-1.0

IV.1 NEUTRINO DETECTION

The various experiments differ in their volume of detector fluid, threshold energies, efficiencies, and in their method of neutrino detection - see Table 1. However, all the detectors utilized the relatively large cross section [$\sim\left(\frac{E\,\bar{\nu}_e}{\mathrm{MeV}}\right)^2 10^{-43}\,\mathrm{cm}^2$][86] for electron antineutrino($\bar{\nu}_e$) capture on free protons,

$$\bar{\nu}_e + p \dashrightarrow n + e^+ \qquad \text{(IV.1)}$$

$$n + p \dashrightarrow {}^2H_1 + \gamma . \qquad \text{(IV.2)}$$

With a smaller interaction cross section ($< \frac{E\nu_i}{\mathrm{MeV}} 10^{-44}\,\mathrm{cm}^2$)[86] neutrinos of all types, i, scatter on the electrons of the water molecules:

$$\nu_i + e^- \dashrightarrow e^- + \nu_i \; ; \qquad \text{(IV.3)}$$

where i = e, μ, or τ.

The positrons (IV.1) and electrons (IV.3) created by these processes acquire a significant fraction of the energy of the neutrinos, and are thus highly relativistic. In water, however, light itself travels at 3/4 c (water's refractive index is 4/3). The positrons and electrons thus propagate faster than light, create 'shocks', and radiate so-called Cerenkov radiation. It was this Cerenkov radiation that was detected by photomultipliers surrounding the tanks of water in the neutrino observatories and which, in conjunction with analyses of the probability (that what was seen was a chance event or not), constituted the evidence that neutrinos from the LMC supernova had been detected. The intensity of each pulse of Cerenkov radiation measured the energy of the positron (IV.1) / electron (IV.3), and thus the neutrino producing the interaction.

In reaction (IV.1), the protons form neutrons (mass, m_n) and positrons (mass, $\frac{m_n}{1839}$). So the release of positrons has an isotropic angular distribution. This means that capture of electron antineutrinos by free protons in the scintillator, results in the simultaneous emission of isotropic Cerenkov radiation, with an isotropic angular distribution, from positrons. The subsequent reaction (IV.2) also produces photons (delayed coincidence - within 170 μs), these have an energy of 2.2 MeV and were detectable only in the Mont Blanc apparatus[83].

On the other hand, the Cerenkov radiation from electron scattering (IV.3) is not isotropic. Because electrons are light and loosely bound in a molecule, the exit angle of scattered electrons is smaller[87] than $[18.3^{o}(\frac{10\text{MeV}}{E})]^{1/2}$. Thus, cones of photons which are directed away from the LMC, subtending less than about 40^{o}, might have been the signature of electron scattering. As noted, such events may arise from any kind of neutrino.

Table 2. The events ascertained to be from SN 1987A[88].

EXPERIMENT[l]	TIME[j] (UT) (23rd February)	ENERGY[k,i] (MeV)	ANGLE WITH RESPECT TO THE LMC (q^0)
Mont Blanc	2h52m36s.79	6.2±0.9	-
	40s.65	5.8±0.9	-
	41s.01	7.8±1.2	-
	42s.70	7.0±1.1	-
	43s.80	6.8±1.0	-
Baskan	2h52m34s.57	10.0±4.0	-
	7h36m11s.82	12.0±2.4	-
	12s.52	18.0±3.6	-
	13s.53	23.3±4.7	-
	19s.51	17.0±3.4	-
	20s.92	20.1±4.0	-
Kamiokande	2h52m40s	11.4±2.8	15±21
	7h35m35s.00	20.0±2.9	18±18
	35s.11	13.5±3.2	40±27
	35s.30	7.5±2.0	108±32
	35s.32	9.2±2.7	70±30
	35s.51	12.8±2.9	135±23
	36s.54	35.4±8.0	32±16
	36s.73	21.0±4.2	30±18
	36s.92	19.8±3.2	38±22
	44s.22	8.6±2.7	122±30
	45s.43	13.0±2.6	49±26
	47s.44	8.9±1.9	91±39
IMB	7h35m41s.37	41±7	80±10
	41s.79	37±7	44±15
	42s.02	28±6	56±20
	42s.52	39±7	65±20
	42s.94	36±9	33±15
	44s.06	36±6	52±10
	46s.38	19±5	42±20
	46s.96	22±5	104±20

[i] Errors are 1σ, except the Mont Blanc which are 2σ.

[j] Error in time is given in Table 1.

[k] Assumes all events due to $\bar{\nu}_e + p \longrightarrow n + e^+$.

[l] The Mont Blanc[89] and IMB[5] events have been revised since the original reports.

IV.2 ANALYSIS OF THE NEUTRINO DATA

The majority of published opinion accepts the Japanese and American results, distrusts the Italian results and ignores the Soviet results. In order to test the validity of such claims, I wish to first discuss the events (see Table 2) recorded at each detector.

If the events are caused by neutrino radiation, then several necessary but by no means sufficient conditions must be satisfied: (a) the interaction points should lie inside the detector and be uniformly distributed throughout the target mass; (b) the angular distribution of ionizing particles should be isotropic when measuring the inverse β decay (IV.1); (c) when measuring elastic neutrino scattering by electrons, the angular distribution of the ionization particles should be anisotropic, with a strong peak along the incident direction of the neutrino. If the events recorded by several detectors are caused by the same neutrino burst, the following additional constraints come in to play: (d) the events should be simultaneous within the limit of pulses in a group; (e) the signal should be proportional to both the detector mass and the detection efficiency of the appropriate neutrino interaction; (f) the energy spectra of the pulses should be identical when normalized with respect to the detector efficiency; (g) the angular distribution of the pulses should be similar among detectors that register the same type of interaction.

Do the recorded events satisfy the criteria a-c? The data from all four detectors satisfy or at least do not contradict conditions a-c - within the limits of detector capability[58,90,91,61]. Only the obviously anisotropic angular distribution in the IMB detections, [which are simultaneously too broad for reaction (IV.3)], are problematic [§IV.2(ii)].

I shall now proceed to analyse the response of the set of detectors to the two observed bursts (conditions d-f). Although only one set of neutrinos was expected from the collapse of a massive star (§IV.3), it should be noted that in principal a two-stage collapse emitting two bursts is possible (§IV.5). So, I shall treat the events at 2:52 UT and 7:36 UT as arising from two separate times of neutrino emission.

IV.2(i) Neutrinos around 2:52 UT?

First, I shall consider the events near 2:52 UT. The only strong detection was apparent in the Mont Blanc apparatus. A burst of 5 neutrinos was found. For a particular background pulse-rate, m (Table 1), the probability of finding a given number of events, k, within in a given time interval, t, is [86]

$$N_K(m,t) = \sum_{i=k}^{\infty} m \frac{(mt)^{i-1}}{(i-1)!} e^{-mt}, \qquad \text{(IV.4)}$$

Then the background rate, for the experiment to find 5 positrons in a 10 s interval, is once every 11 months. So, one might have expected strong signals in the other detectors.

Kamiokande had a mass of 2140 tons, compared to the 90 tons of the Mont Blanc detector; however, all of the Mont Blanc events were below the detection threshold (8.3 MeV) of the larger instrument. To check their results, the experimenters at Mont Blanc recalibrated their apparatus and found that the recorded energies were in error by less than 15% (2σ). This allows only the 7.8 MeV detection to be relevant to Kamiokande. So it is not surprising that Kamiokande recorded only one neutrino above background ($0.022 s^{-1}$) during this period.

Because of the low energy of the detections no events would be expected in the Baskan and IMB detectors. No events were found in the IMB detector - its threshold energy of ~20 MeV (Table 1) is well above the average energy, 7.5 MeV, apparent from the Kamiokande and Mont Blanc measurements at this epoch. The single event found in the Baskan detector [mass=200 tons, threshold energy 10 MeV (Table 1)] is only nontrivial in conjunction with the other detections: it has a background of $0.033 s^{-1}$. The Mont Blanc and Baskan data lack angular resolution so altogether, the events at 2:52 UT do not contradict any of the conditions d-f.

IV.2(ii) Gravity waves?

According to current understanding, any asymmetry in the collapse of a massive star must be accompanied by gravitational radiation. When the data[92] from the gravitational wave detector in Rome were juxtaposed with events recorded by the Mont Blanc detector, the analysis revealed an approximately sixfold increase, with respect to the background noise, at 2h52m33s.4±0.5 UT. This preceded by 1.4±0.5 s the first of the Mont Blanc events. The background imitation frequency of such events is once every 2 hours. However, no such effect was noted at this time by a similar sensitivity detector at Maryland (U.S.A)[93]. In addition, the magnitude of this effect implies more than 10^{55} ergs (a binding energy equivalent of 100 $M_\odot$) to have been emitted in gravitational waves from the LMC. Furthermore, it must be noted that collapse models allow gravitational radiation to remove less than 1% of the binding energy for reasonable theoretical core collapses[94]. I shall ignore this event.

IV.2(iii) Neutrinos around 7:36 UT?

This time, two of the detections were significant: in Kamiokande, 11 pulses were found over 13 s; and in IMB, 8 pulses were found over 6s. However, in order for the events to be coincident, it is necessary to shift the timing of the Kamiokande detector forward by 6.4s. The ± 1 min uncertainty in its timing makes this possible. According to the equation (IV.4), the rate at which pulses akin to those observed in Kamiokande can arise from statistical fluctuations is of order one every 7×10^7 years. The statistical significance of the IMB detection is even higher. However, these figures are rather optimistic since the working-span of the detectors was only 2 and 4 years, respectively.

In addition to the pulses in the larger detectors, the Baskan apparatus registered 5 events. These data must be shifted by 25.2 s for temporal coherence - this is possible within the uncertainty in timing. However, the coincidence with IMB and Kamiokande is usually taken to be trivial: such an event has an imitation frequency of once every 42 minutes [by (IV.4)]. The Mont Blanc apparatus also found events near this time, but only two. The chance of such a replication due to background was once every 8.3 minutes [by (IV.4)]. Furthermore, these events did not comply with the timing of the pulse from the highly significant IMB detection; it is therefore regarded as background. I thus find that the events do not contradict condition (d) - within the scope of the discussed caveats.

On the basis of Kamiokande's higher sensitivity (Table 1), and higher count rate, I shall consider how many events, k would have been expected in the other detectors:

$$k_i = \sum_{j=1}^{11} \frac{M_i x_i(E_j)}{M_k x_k(E_j)}\,, \qquad \text{(IV.5)}$$

where M_k and x_k are the mass and efficency of the Kamiokande detector; E_j is the energy (in MeV) of the eleven events in the Kamiokande detector; i=2,3,4 refer to the Baskan, IMB, and Mont Blanc detectors respectively (the efficiencies of the detectors are given in §B.5. The results are 0.6, 2.3, and 0.65 respectively for Baskan, IMB, and Mont Blanc - the probabilities[86] of recording the observed pulses are 0.001, 0.01, and 0.3. The experimental data thus seem inconsistent with the magnitude of the Kamiokande effect, and condition (e).

In order to test the energy spectra [condition (f)] for the Kamiokande and IMB events, it is necessary to know something about the source: to describe the expected spectrum of the electron antineutrinos. The shape is dictated by the physics of the explosion, and so is affected by the radiative aspects of the production and transport of the neutrinos (discussed §IV.3). Regardless of which energy spectrum, the Kamiokande or the IMB, is taken as the starting point, several studies have shown that their spectra only overlap on their 95% confidence levels {Table 4 [§IV.4(ii)]}. Accordingly, condition (f) is poorly satisfied.

Even now, there remains debate as to the angular distribution of the Kamiokande and IMB events. As discussed (§IV.1), kinematics dictates that the captures on free protons should produce an isotropic distribution, as opposed to the highly peaked Cherenkov ring recorded from scattering events. One school of thought has even postulated a new particle to explain the structure of the signals: neutral X^0 particles, having masses <20 MeV. These scatter off nuclei to produce the observed photon distribution. But the evidence for, or against, such exotica is scanty[95].

Figure 7. Angular Deflection of Neutrinos

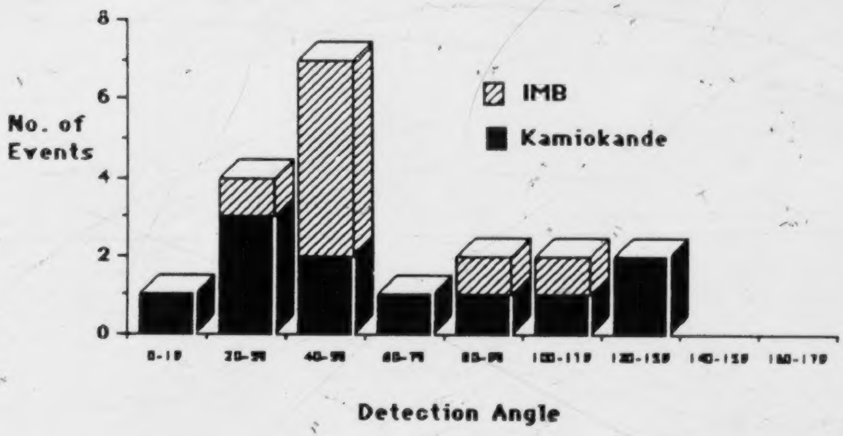

Many authors (e.g. [96]) interpret the forward peaked angles and high energies of the first two Kamiokande events as being due to scattering[97]. However, there is no strong statistical basis for this assumption (see Fig. 7). Furthermore, this would imply that observations do not fit within known neutrino interactions: there is an ~100 times (§IV.1) greater chance of detecting electron antineutrino absorption (IV.1) than any scattering reaction (IV.3). Unfortunately, whether any of these events is a scattering event, cannot be definitively determined from the sparse data.

The IMB data are clearly not fit by an isotropic distribution. This, however, cannot be due to scattering: the events subtend too great an angle to the LMC; and, at the high energies observed in this detector the cross section for scattering reactions (IV.3) is about 250 times (§IV.1) smaller than that for absorption reactions (IV.1). Recently, it has been recognised that for neutrino absorption (i), this detector yields an $\sim 1+0.2\cos\theta$ distribution, not isotropic[98]. The observed distribution is then ~8% probable, so it is not too ($<2\sigma$) unlikely. However, the alternative of some new physics cannot be trivially excluded. In conclusion, condition (g) is barely satisfied.

Regardless of any assumptions about the neutrino source, the following conclusions can be made:

(α) The events near 2:52 UT do not contradict the detection of neutrinos.

(β) Taken separately, the effects near 7:36 UT in the Baskan, Kamiokande, and IMB detectors do not contradict the registration of a neutrino source, but the consistency of these effects is poor.

It must be emphasized that these conclusions are subject to the uncertainties of small number statistics.

In order to discuss how these neutrino events fit into the current understanding of the core collapse of massive stars, it is first necessary to delve into the theoretical prejudices of this standard model.

IV.3 THE STANDARD MODEL

In order to understand whether the neutrino observations fit into the emission expected from a type II core collapse supernova, it is necessary to discuss the standard model. This scenario is based upon detailed numerical models and analytical arguments constructed over the last two decades (§III). Here, I wish to address specifically the expected neutrino signature (Table 3). It may be broken up phenomenologically, into three distinct stages.

Table 3. Sketch of neutrino's timetable for emission

EVENTS	$E(10^{51}$ ergs)	$\Delta t(s)$	SPECIES
Collapse (infall)	0.5-1.5	0.01-0.1	υ_e
Prompt burst	2-4	0.002-0.3	υ_e
*Cooling and neutronisation	200-400	0.1-10	all

*Inside, degenerate 30-80 MeV υ_e (§B.3) ----> Outside, ~10-30 MeV (All species)
$< E_{\upsilon_{\mu,\tau}} >$ ~20-30 MeV
$< E_{\upsilon_e} >$ ~10-15 MeV

(a) As discussed [§II.1(ii)], the core of a massive star is destabilized primarily by electron capture. The rate of electron capture, and thus the release of electron neutrinos increases rapidly from 10^8 g/cm^3 to 10^{11} g/cm^3, when neutrinos become trapped (§B.2). Because the star is 'transparent' to neutrinos until such densities are reached, some of these neutrinos escape as the core implodes. The energy released is some 0.5-1.5 x10^{51} ergs - dependent upon the details of the pre-supernova model[18]. This flux represents at most 1% of the total energy to be released in neutrinos by the supernova. However, because it consists solely of electron neutrinos it should have a distinct signature. In fact, there has been speculation[18] that one or two of the first 2 events recorded by Kamiokande were infall electron neutrinos.

(b) As far as the neutrino luminosity was concerned, the next important stage was shock breakout: the point at which the shock wave burst through the neutrinosphere. This happens at a radius of 30-100 km and a temperature 3-7 MeV. The neutrinos are released copiously for two reasons. The first is that they are carried with the material in the shock wave as it expands to below trapping densities (at which point they are released). The second is that the shock wave dissociates the matter into free neutrons and protons; thus electron capture rates are boosted and neutrino emission is rapid (III.6).

Over a period of ~300 ms, 2-4 x10^{51} ergs, comprising primarily electron neutrinos, is released [though mostly at shock breakout (§III.5)]. At around 200 ms, pair neutrinos from electron-positron annihilations,

$$e^{+} + e^{-} \longrightarrow \bar{\nu} + \nu, \qquad \text{(IV.6)}$$

make their first appearance. These neutrinos are produced in the high temperature ambience of the post-shock material.

(c) The remaining neutrino emission, after the early shock wave, is from the cooling processes of the nascent neutron star. The energy released is governed by the binding energy of the neutron star; and thus depends on its mass and the equation of state for neutron star material. Observation of existing neutron stars (Fig. 9) suggests the release of 1.5-3.5x10^{53} ergs.

The protoneutron star is very hot [30-80 MeV (§B.3)], so neutrino pairs of all flavours are created (B.12). Thus, the binding energy of the neutron star is carried away by neutrinos of all species - not just electron neutrinos from neutronisation. During this phase, the proto-neutron star is opaque to neutrinos: there are ~10^4 mean free paths from the centre to the neutrinosphere. So, neutrinos diffuse slowly from the core (~0.1-10 s) to the neutrinosphere (§B.4). The shape of the energy spectrum may be represented approximately by a cooling black body with an average effective temperature.

For electron neutrinos the neutrinosphere energy is 10-15 MeV. However, since mu and tau neutrinos only interact at these temperatures via the neutral rather than by the charged current interaction (§B.3), their neutrinospheres are deeper in the core. Consequently their average energies (20-30 MeV)[99], are greater than those of the electron neutrino pairs. It should also be noted that since neutrino interaction cross sections are proportional to the square of the energy, the lower energy ones of a given type can escape from deeper in the star (§B.4). Thus, the mu and tau neutrinos have a higher average energy, but since they are not synthesized in electron capture processes, their flux is reduced. Detailed models for the emission (e.g.[56]) indeed find that there is an approximately equal amount of energy carried away by the different neutrino species.

IV.4 HOW WELL DO OBSERVATIONS FIT THE STANDARD MODEL?

I shall now give a detailed discussion of the pulse characteristics of each burst, and consider its compliance with the standard model. Because of the small numbers of events detected, I accord the greatest weight to integral characteristics: the total number of events; the dependence of the total number of detected pulses on time; and the stellar energy carried off in neutrinos.

IV.4(i) Events around 2:52 UT

From the experimental point of view, it has been shown that the detections comprising the initial neutrino burst at around 2:52 UT are not contradictory. But can they be interpreted within the standard model for a cooling proto-neutron star?

Depending upon the choice of nuclear equation of state (EOS), the expected total neutrino energy is (Fig. 9),

$$E_{total} = 1\text{-}9 \times 10^{53} \text{ ergs.} \qquad \text{(IV.7)}$$

The total thermal energy emitted in neutrinos by SN 1987A can be written as,

$$\text{(iv)} \quad \int L_\nu \, dt = N_{all} F 4\pi D^2 \tau. \qquad \text{(IV.8)}$$

The number of free protons in the Mont Blanc experiment[83] was 8.4x10^{30}; if all the neutrinos were due to neutrino absorption (IV.1), for which the cross section is 9.3x10^{-44} $(E\,\bar{\nu}_e/\text{MeV})^2$ cm^2, then the integrated flux, $F\tau$, was $6\pm3\times10^{12} (E\,\bar{\nu}_e/\text{MeV})^{-2}$ ergs cm^{-2}. For a distance, D, to the LMC of 50±7 kpc [3], an average energy of 6.7±0.7 MeV, and an approximate equipartition of energy between species of neutrino [N_{all}=6 (§IV.6(v)], the total energy is $E_{total} = 2.4 \pm 1.5 \times 10^{55}$ ergs. This implies an energy release comparable to the entire rest mass of the Sanduleak star. To check the possibility of a large low energy flux, the Kamiokande experimenters searched[100] for a large signal below the originally determined threshold (8.3 MeV). When it was decreased to 5.6 MeV, the number of candidate events observed over a 17 minute period around the Mont Blanc time was 138±12, compared with an expected 127 background counts.

There is a further problem with such a large flux: the Homestake mine ^{37}Cl experiment, having a threshold flux (F) of 2×10^{11} cm^{-2} [85], would expect several 10's of counts. The ^{37}Cl neutrino detector in Homestake mine found no evidence for a positive effect[85].

In addition to its non compliance within the standard model, there exists a very strong observational constraint upon the initial neutrino events: the early light curve is consistent with calculations for a shock wave starting at the centre of a blue supergiant at the time of the second neutrino burst - but not at the Mont Blanc time (§ V.1)

IV.4(ii) Events around 7:36 UT

At around 7:36 UT neutrino events were recorded in all four detectors. However, the Baskan and Mont Blanc detections do not synchronise with the statistically far more significant Kamiokande and IMB events. So, as previously argued [§IV.2(ii)], only the Kamiokande and IMB pulses are considered.

It is curious that after a 7.3 s gap in the Kamiokande data, neutrinos of rather high energy are observed. Monte Carlo simulations of the neutrino signal have been performed (e.g.[101]); they find that the situation of having a gap of seven seconds duration, with at least three neutrinos following the gap, occurs about 5% of the time. Some authors (e.g.[102]) consider this gap to be physical and they argue that for rapid rotation the core collapse can leave two protoneutron stars which coalesce. This scenario yields two bursts of neutrino radiation several seconds apart. However, it must be noted that the late IMB events partially fill this gap, see Fig. 8. When the statistical significance of the combined data is tested, the agreement between the detectors becomes significant (0.93)[102].

Figure 8. Neutrinos from Kamiokande and IMB

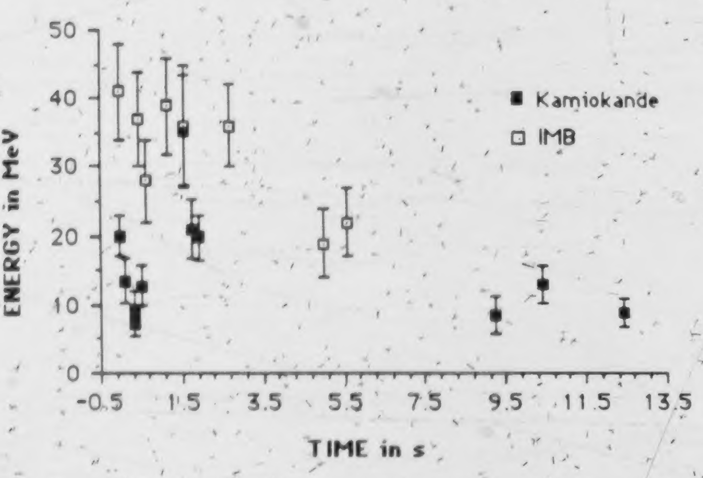

Is it possible to gain any information about the neutrino source from the combined IMB and Kamiokande energy spectra? It certainly seems as if the neutrino source is cooling: almost all the events are concentrated in the first few seconds; and the late-time events are all lower in energy. In addition, the shorter duration of the IMB signal (5.58 s) with respect to the Kamiokande signal (12.44 s) also suggests that the source is cooling since, for a given decay in temperature, an even more rapid decay in the high energy tail of a thermal spectrum (or near thermal spectrum) is expected. The low energy threshold of the Kamiokande detector [8.3 MeV (Table 1)] makes it much more sensitive to this tail than the IMB detector with its higher threshold [20 MeV (Table 1)]. Hence, the IMB signal would be expected to turn off sooner, as it did.

Schematically, this cooling scenario is in accordance with the standard model: a decaying flux and temperature as the proto-neutron star shrinks from an initial radius of

~100 km to one of ~20 km [IV.3(a)-(b)] followed by a longer cooling flux [IV.3(c)]. Unfortunately, there is no conclusive evidence for even one scattering reaction. So, the validity of the standard model fluxes, IV.3(a) and (b) cannot be proven.

In accordance with IV.3(c), the neutrino events can be fit to a black body spectrum, though the distribution of the electron antineutrino energies are more narrowly concentrated around the peak energy than for a blackbody spectrum. This weak consistency of the experiments, has been confirmed many times (see Table 4). Because of the complexities of neutrino production and transport, full hydrodynamical calculations of the spectral and temporal evolution of the neutrino flux from a cooling proto-neutron star remain to be done.

Table 4. Comparison of the temperatures and energies thought to represent the neutrino burst from SN 1987A.

		MODELS					
REFERENCE		101	103	104	77	52	105
TEMPERATURE in MeV	Kamiokande	2.8 ± 0.4	$2.9\pm^{0.9}_{0.7}$	2.7 ± 0.1	$2.8\pm^{1.0}_{0.6}$	2.7 ± 0.7	2.80 ± 0.4
	IMB	4.2 ± 1.0	4.5 ± 0.7	4.2 ± 0.3	$4.5\pm^{1.9}_{1.2}$	4.5 ± 0.7	4.1 ± 1.1
ENERGY $\times10^{52}$ ergs	Kamiokande	$6.3\pm^{4.0}_{3.1}$	$6.3\pm^{8.1}_{3.9}$	7.3 ± 3.0	$6.5\pm^{8.0}_{4.0}$	$7.5\pm^{3.6}_{1.4}$	$6.9\pm^{4.0}_{3.0}$
	IMB	$4.5\pm^{12.4}_{3.4}$	$3.4\pm^{11.6}_{7.4}$	4.5 ± 2.0	$3.5\pm^{11.5}_{2.5}$	$3.4\pm^{4.1}_{1.4}$	$4.5\pm^{120}_{3.4}$

An average of the literature models (Table 4) yields that the effective temperature of the neutrinos was,

$$T_{\bar{\nu}_e}^{IMB} = 4.3\pm^{1.0}_{0.8}\ \text{MeV}$$

$$T_{\bar{\nu}_e}^{K} = 2.8^{+0.6}_{-0.5}\ \text{MeV}. \qquad \text{(IV.9)}$$

Combining these gives,

$$T_{\bar{\nu}_e} = 3.5^{+0.8}_{-0.7}\ \text{MeV}. \qquad \text{(IV.10)}$$

And the energy released in electron neutrinos was,

$$E\,\bar{\nu}_e^{\text{total, IMB}} = 3.9\pm^{7.8}_{3.4}\ \text{x}10^{52}\ \text{ergs}$$

$$E\,\bar{\nu}_e^{\text{total, K}} = 6.8\pm^{5.1}_{3.1}\ \text{x}10^{52}\ \text{ergs.} \qquad \text{(IV.11)}$$

Thus, the total energy liberated by SN 1987A in electron antineutrinos was,

$$E\,\bar{\nu}_e^{\text{tot}} = 5.4\pm^{6.3}_{1.7}\text{x}10^{52}\ \text{ergs.} \qquad \text{(IV.12)}$$

If this energy was divided equally between six species of neutrinos, then the total neutrino energy liberated by SN 1987A was,

$$E_{\nu}^{\text{tot}} = 3.2\pm^{3.8}_{1.0}\ \text{x}10^{53}\ \text{ergs.} \qquad \text{(IV.13)}$$

Such a torrent of neutrino energy corresponds to the binding energy of a $1.4\pm^{0.7}_{0.2}$ $M_\odot$ neutron star, see Fig. 9.

Figure 9 has been removed because of the unavailability of copyright

From [illegible] Bowers [illegible] 1987 [illegible] Suppl. [illegible] 415

Figure 9. Cold neutron star binding energies versus gravitational mass for various equations of state (for explanations of the various models see[106]). The vertical lines denote the masses derived from the binary system discussed below.

Best fits for such neutron star models give, 1.4-1.6 $M_\odot$ (best fit stiff EOS), or 1.3-1.5 $M_\odot$ (best fit soft EOS), depending upon the choice of the equation of state(EOS) for neutron star material[61]. Masses have been determined for several pulsars[107] which are in binary systems. The best known values are for the system PSR 1913+16, thought to consist of two neutron stars, one a pulsar, with masses 1.444 $M_\odot$ and 1.384 $M_\odot$. There is no observational evidence for any pulsar possessing a mass greater than 1.5 $M_\odot$ [107].

Furthermore, the electron antineutrino luminosity:

$$L\,\bar{\nu}_e = (7\pi/4)\sigma_B T\,\bar{\nu}_e{}^4 R\,\bar{\nu}_e{}^2\ , \qquad \text{(IV.14)}$$

where σ_B is the Stefan-Boltzmann constant and 7/4 corrects for spin and Fermi statistics[52], can be used [from (IV.12) in ~13 s)] and gives the radius of the cooling neutrinosphere for electron antineutrinos as, $R_{\bar{\nu}_e} = 19\pm^{38}_{9}$ km. This radius is near those quoted for neutron stars, and near nothing else.

So, it seems as if the neutrinos intercepted by the Kamiokande and IMB detectors had just the properties expected from a standard model core collapse. They have triumphantly confirmed the schematic picture of core collapse, though the data are not sufficient to discriminate between various EOS (Fig. 9) or to validate specific detailed models (§IV.3).

IV.5 BIZARRE POSSIBILITIES

Offsetting the apparent triumph of the neutrinos detected by Kamiokande and IMB, the puzzle of the events recorded at the Mont Blanc detector remains. The signals from Kamiokande and IMB were so significant that there is no doubt they saw the supernova. Could there have been 2 signals?

Many theorists have attempted to find a way of answering this in the affirmative. There are 2 principle difficulties.

(a) The early light curve is consistent with a shock wave starting at the centre of a blue supergiant at the time of the second neutrino burst, but not at the Mont Blanc time (§V.1). So what was the star doing 4.7 hours before it collapsed? Stellar models indicate that it was burning silicon. Its neutrino luminosity would have been immense by conventional standards, about 5×10^{45} ergs/s (for comparison, $L_{\nu\odot} \sim 8\times10^{31}$ ergs/s)[108] but far less than the 10^{54} ergs/s implied by the Mont Blanc detection.

(b) From the experimental point of view, it has been shown [§IV.2(i)] that the Mont Blanc and Kamiokande events around 2:52 UT are not contradictory. However, these measurements signify an energy release of around 10^{55} ergs [§IV.4(i)]: they cannot be explained in terms of the binding energy released from a proto-neutron star, $< 9\times10^{53}$ ergs (Fig. 9).

A number of somewhat speculative scenarios have been developed in order to explain the 4.7 hour delay in the neutrino pulses.

(i) A phase transition to a super-dense state[109].

(ii) Fragmentation of the progenitor on collapse[110].

(iii) The oscillation of a newly formed black hole[111].

IV.5(i) Phase Transition

In the first of these, the initial neutrino burst arises from the collapse of the precursor to a neutron star. The problem of the vast energy implied by the initial burst is avoided by assuming the stellar core to be rapidly rotating in which case, the neutrinosphere would become anisotropic. If viewed pole-on the observed neutrino flux might be many times that observed for a spherically symmetric neutrinosphere, see [§V.4(i)(c)]. The subsequent neutrino event was then caused by the transition of a neutron star into a super-dense state: a pion-condensed star[112,109], a quark star[112,109], or a black hole[110].

It is argued that, during neutrino cooling of the proto-neutron star, a certain critical temperature is reached at which the matter undergoes a drastic rearrangement and new microscopic degrees of freedom are excited. If this phase transition is strong enough, the neutron star becomes unstable and collapses to an ultradense state (pion condensate and/or quark matter). The stability of this newly formed ultradense state is uncertain, and collapse to a black hole may ensue. In all cases, in excess of 10^{51} ergs are released. The present uncertainties in the equation of state for strongly interacting matter leave these possibilities open.

IV.5(ii) Fragmentation on collapse

The second collapse scenario suggests that at the onset of infall, the rotation of the progenitor caused fragmentation into two pieces, one light (1-3 $M_\odot$) and the other heavy (~18 $M_\odot$). The massive component then collapses to form a black hole giving rise to the first burst. Although this would occur on a dynamical scale (~10 ms), the cross section for neutrino interactions is proportional to the square of the energy; hence the large density due to infalling matter makes the escape of high energy neutrinos very difficult. This might concur with the low energy spectrum observed in the initial pulse.

The second burst occurs when, eventually, the lighter fragment coalesces onto the black hole. The time delay results from the gravitational braking as the light component falls onto the black hole with the accompanying emission of gravitational waves [§IV.2(ii)].

IV.5(iii) Black hole

The third scheme for the detonation postulates a failed explosion and invokes the accretion of matter onto the central remnant to lead to the formation of a black hole. Recent papers [113] have shown that if the collapsed mass is higher than the limiting neutron star mass, then static solutions do not exist - the only viable solution is a dynamical oscillatory solution. Figuratively, a black hole turns into a white hole in going through a physical singularity (compression is replaced by expansion). Therefore, any gravitational self-closing, the occurrence of a gravitational grave for matter and energy, does not occur.

Quantum theory implies that such a body oscillates, emitting gravity waves as well as particles and radiation. The release of energy into the high density environment is invoked to cause not only the explosion of the envelope of Sk -69° 202, 4.7 hours after initial collapse, but also the neutrinos recorded in all four detectors. If sufficient mass is ejected, the oscillating black hole may transform into a neutron star[111].

Apart from the lack of existence of precise quantitative models for any of these hypotheses, there are four other major problems:

(a) The standard model predictions, for elemental abundances produced in explosive nucleosynthesis as the early shock wave passes through the ejecta, have been fitted by observation(§V.5).

(b) A preliminary model[77] suggests that a rotating core collapse only reaches densities of ~$4x10^{13}$ g/cm^3. In order to produce a shock wave strong enough to eject the stellar envelope it is necessary for the core to collapse to above nuclear densities (>$3x10^{14}$ g/cm^3 - §II.2)

(c) The large energy release implied by the Mont Blanc pulse is not overcome.

(d) Black hole formation is a dynamical event (~10 ms) - a burst of neutrinos over ten seconds would be unlikely. More likely would be the quick truncation of the emission within (at most) a few seconds[114].

The whole story will have its epilogue when the supernova shell becomes transparent and further observations of the pulsar are possible. In conclusion, it seems possible, though ***not*** straightforward, to invent an astrophysical scenario to explain the 2 neutrino bursts. It is also obvious, however, that the easiest explanation is to dismiss the first pulse as unfortunate background events, and assume that the second pulse signalled the formation of the neutron star.

IV.6 NEUTRINO PROPERTIES

SN 1987A has proved to be an amazing neutrino laboratory. In addition to the lessons in supernova physics, it has placed many limits on the neutrino that are more restrictive than current laboratory limits. Table 5 compares the properties of neutrinos that were obtained from a standard model SN 1987A with those from other observations. Many authors have drawn far reaching conclusions based on the angular distribution and time dependence of the neutrino events. However, I give the greatest weight to integral characteristics: the total number of events; and the dependence of the total number of detected pulses on time.

Table 5. Neutrino properties

PROPERTY	OTHER EXPERIMENTS	SN 1987A
LIFETIME γt_υ in sec where $\gamma = E\upsilon/M\upsilon$	Solar neutrinos $> 5\text{x}10^2$ (^{115})	$> 2\text{x}10^{15}$
MASS in eV/c^2	Tritium β decay expts < 18 (^{116})	model dependent < 16 < 33 (limit)
ELECTRIC CHARGE q/e	10^{-13} (^{115})	$< 10^{-15}$
MAGNETIC MOMENT μ/μ_B	White dwarf cooling rates $< 10^{-11}$ (^{115})	model dependent $< 10^{-13} - 10^{-15}$ $< 10^{-11}$ (limit^{115})
NUMBER OF NEUTRINO FLAVORS	LEP Collider < 4 (^{117})	< 7

IV.6.(i) Neutrino Mass

Relativity implies the photon rest mass to be zero, but no equivalent restrictions exist for the mass of neutrinos. If they have a finite mass, then the most energetic ones will arrive first. But, because the neutrinos diffused [t=0.1-10 s (§B.4)] from the core, they were not emitted at the same time. So, the duration of the burst must be used to estimate the upper bound rest mass. The $\bar{\nu}_e$ rest mass, $m\,\bar{\nu}_e$ can be found simply from,

$$m\,\bar{\nu}_e = E\,\bar{\nu}_e\left(\frac{2c\Delta t}{D}\right)^{0.5}; \qquad \text{(IV.10)}$$

where Δt is the timescale over which the neutrinos were emitted; D is the distance to SN 1987A; the average energy is given by $E\bar{\nu}_e$; and c represents the speed of light. Simplistically, if the entire 13 second spread of the Kamiokande events were due to this effect, then, $m\bar{\nu}_e<30$eV. Alternatively, comprehensive statistical treatments based upon Monte Carlo simulations have been made. These models[116,118] account for the detectors' efficiency at different energies, the uncertainties in the measured energies, and the neutrino interaction cross sections for hot dense matter. By maximizing the joint likelihood function for all the Kamiokande and IMB events, they conclude that the upper limit on the mass of the $\bar{\nu}_e$ is,

$$m\bar{\nu}_e<16 \text{ eV } (2\sigma). \qquad \text{(IV.16)}$$

Neither of these limits ascribes to neutrinos sufficient mass to close the Universe[42].

IV.6(ii) Neutrino lifetime

The notion of an unstable neutrino was proposed in 1972 as a solution to the solar neutrino problem[119]. Because the $\bar{\nu}_e$'s from SN 1987A made it over 50 kpc, they must have a lifetime $\tau\bar{\nu}_e$ such that,

$$\gamma\tau_{\bar{\nu}_e} > 1.6 \times 10^5 \text{ yr}, \qquad \text{(IV.17)}$$

where γ is the relativistic factor ($\gamma=E\bar{\nu}_e/M\bar{\nu}_e$). To decay requires that $m\bar{\nu}_e>0$. Since γ for neutrinos from the Sun is ~0.1 of γ's from SN1987A (assuming $m\bar{\nu}_e=m\nu_e$), neutrino decay cannot be a solution to the solar neutrino problem.

However, there is a loophole in this argument. If, the $\bar{\nu}_e$ is a combination of two mass eigenstates, then the heavier state might decay and the lighter state could be stable. The non-detection[120], of coincident γ rays, from decays in the Earth's atmosphere, $\nu \rightarrow x + \gamma$, implies that fewer than 1 in 10^{10} of the supernova's $\bar{\nu}_e$ could have decayed producing a γ ray. This is widely perceived to rule out[121] neutrino decay as an explanation of the solar neutrino problem.

IV.6(iii) Magnetic moment

An anomalous magnetic moment ($>10^{-10}\ \mu_B$) has been suggested as an explanation for the suppressed count rate in the solar neutrino experiment[122]. If the SN 1987A neutrinos had a non-zero magnetic moment, then their interactions with the electric and magnetic fields present in the collapse could have influenced the observed pulse structure. Several refined but model-dependent arguments have been developed which restrict the magnetic moment to $<10^{-13}$ to$10^{-15}\ \mu_B$ (e.g.[123]). However, there is a general consensus that the observed neutrino signal would have been very different if the magnetic moment were $>10^{-11}\ \mu_B$. In future neutrino detections from stellar collapses, a finite magnetic moment, might be a very good diagnostic of collapse characteristics - e.g., electron density, electric, and magnetic fields.

IV.6(iv) Neutrino charge

If the value of neutrino charge is non zero, then different neutrinos of different energies will have different paths in the galactic and intergalactic magnetic fields. Higher energy $\bar{\nu}_e$'s will move along a straighter path and therefore arrive at Earth before lower energy $\bar{\nu}_e$'s - even for massless $\bar{\nu}_e$'s. The absolute value of any charge (independent of mass) must be $\leq 10^{-15}$e, where e is the electron charge, otherwise the burst would have been spread by more than 13 s on its 160,000 yr flight to the Earth[124]. This limit is substantially smaller than the limit, $q\ \bar{\nu}_e \geq 10^{-13}$ e obtained from solar neutrinos[125].

IV.6(v) Neutrino flavours

In principle, the total energy carried off by all the species of neutrinos cannot exceed the binding energy of the neutron star remnant. Thus, the number of neutrino flavours may be derived using the luminosity of the detected electron antineutrinos. This argument relies on the appropriate partition[126] of energy between all flavours of neutrino: the more flavours, the smaller the yield per flavour. So from equation (iv),

$$N_{\text{flavour}} < \frac{E_{\text{max binding}}}{E_{\text{min observed}(\bar{\nu}_e)}} \sim \frac{9\text{x}10^{53}}{5.4\text{x}10^{52}}, \qquad \text{(IV.18)}$$

is obtained; where N_{flavour}, is the number of neutrino flavours. Substituting $5.4\text{x}10^{52}$ ergs (IV.12) and $9\text{x}10^{53}$ ergs (Fig. 9) in (IV.18) gives $N_{\text{flavour}} < 12$. The accepted limit[127], using $3.5\text{x}10^{53}$ ergs as an upper limit to the binding energy, is $N_{\nu} \leq 7$. This is less restrictive than limits obtained from Big Bang nucleosynthesis and from laboratory measurements.

IV.6(vi) Special relativity

Special relativity requires that the limiting velocity for all forms of radiation is the same: independent of the source velocity. With a generous estimate of 10 hr for the uncertainty of the coincidence in arrival times between the first photons and the first burst of neutrinos; the speed of photons and of neutrinos cannot differ by more than 1 part in 10^8 - the speed of light itself[128] is known to 1 part in 10^{10}.

However, if the source velocity is considered then a much stronger constraint may be obtained. From the inferred $\bar{\nu}_e$ temperature, ~3.5 MeV (IV.10), the core nucleons must have had a thermal velocity of about 0.1c. In order that the neutrino pulse was sufficiently independent of its source to arrive within the observed 13 s, special relativity is found[129] to be correct to better than 1 part in 10^{11}. This is, by a factor of 100, the most precise test of special relativity to date.

IV.6(vii) The weak equivalence principle

The gravitational field of our Galaxy causes about a 5 month time delay[130] in the transit time of photons from SN 1987A. The observation of a neutrino burst within a few hours of the associated photon burst from SN 1987A demonstrates that both radiations follow the same trajectories in the gravitational field of our Galaxy. A range of paths of different gravitational potentials has been found from the galactic rotation curve[131]. These indicate that photons and neutrinos move along the same trajectories to an accuracy of better than 0.2%[132]. The accuracy of this test, unfortunately, depends on the poorly known mass distribution in the outer parts of the Galaxy. In spite of this, the test is the first verification of the weak equivalence principle for relativistic particles.

IV.6(viii) Other interactions

If the Kamiokande and IMB detections at 7:56 UT are taken to represent the neutrinos from a proto-neutron star, then the neutrinos travelled ~50 kpc without apparent attenuation. This means that any unknown reactions they might have undergone can be constrained[127],

$$\sigma_{\mathrm{unknown}} < 10^{-25}. \qquad \text{(IV.18)}$$

Majorons and axions, proposed light particles, might have carried off the bulk of the supernova's binding energy - they did not. This limits any interactions neutrinos may have outside the standard Weinberg-Salam model. In particular, an axion mass of 10^{-3} to 2 eV is excluded(e.g.[133]). SN 1987A has also tightly constrained many other hypothesised particles encumbent in weak[134], and supersymmetry[135] interactions.

IV.7 CONCLUSION

There are many lessons from the history of science which tell us that a lack of theoretical understanding can lead to a misjudgment of observational data. With this in mind, the observed Kamiokande and IMB neutrinos do seem to suggest that the basic ideas are essentially correct: massive stars do collapse, emitting most of their gravitational binding energy in the form of thermal neutrinos. The data thus verify the basic tenets of stellar core collapse theory developed over the last 20 years.

SN 1987A has allowed model-independent estimates of upper limits on the electron antineutrino rest mass, which are equivalent to the best limits from terrestrial experiments. Similarly, good upper limits on the neutrino charge and magnetic dipole moment have been derived. Furthermore, the properties and existence of a zoo of hypothetical particles, inaccessible to laboratory experiments, can be constrained. SN 1987A has provided the best test to date of special relativity and the weak principle of equivalence. However, a collapse not fifty but five kiloparsecs away in our own Galaxy, promises to incite a revolution in the physics of both supernovae and neutrinos. A factor of ten decrease in distance leads to a factor of one hundred increase in the integrated signal. What could not be learned about supernova physics and fundamental physics with one thousand events?

IV.8 THE FUTURE?

Neutrino detectors now hold the possibility for use as early warning devices for astronomers observing in the electromagnetic spectrum. The scientific community has been educated by SN 1987A in the simple steps: upgrade phototubes, expand data buffers, reduce dead times, maintain accurate clocks, coordinate and link the international detectors to ensure that at least one is on-line at all times. For example, at IMB the analysis of a thousand neutrino events now takes only a few minutes. Global transmission of such information would allow an international, multi-pronged approach to measurements of the transition from collapsing star to supernova.

Table 6. Sample future detector event totals [from the Galactic centre (8.5 kpc)][136]

DETECTOR	TOTAL#	INFALL ν_e's	PROMPT ν_e's	ν_m's
Super Kamiokande	4770	4	4	210
Kamiokande	318	0.4	0.4	14
Homestake	5.7	0.15	0.15	-
ICARUS	169	3.6	3.6	2.5
Sudbury Neutrino Observatory	1179	4.1	4.1	500

The future looks good for supernova neutrino detection. Around the world, many large mass detectors are being built or planned. Table 6 depicts the predicted number of events from a collapse at the galactic centre in proposed or extant neutrino telescopes. Since these detectors are designed for multipurpose use, it can also be expected that solar neutrinos, ultra-high energy neutrinos, WIMPS, monopoles, massive neutrinos, photinos, etc, will (if they exist) be observable. It is expected that neutrino detectors will play a crucial role in the development of astrophysics and cosmology.

The thousands of events expected should not only revolutionise our ideas about neutrinos and core collapse, but also give us the direction of the event. For example, Super - Kamiokande would give some 200 elastic scattering (direction indicating §IV.1) events - this is enough to point direction with a 2° accuracy[137]. For a supernova in our galactic centre, the direction will be vital: the event will probably be invisible to other detectors. The rate of stellar collapse in the galactic core is once every 12 to 20 years[138]. Do we have the patience to wait?

V. THE AFTERMATH

In this chapter, I will discuss the sequence of events from SN 1987A with a higher time resolution. When, on February 24.23 UT Ian Shelton, University of Toronto, Las Campanas station, communicated to the astronomical community the possibility of a new supernova in the Large Magellanic Cloud, astronomers in the Southern Hemisphere immediately began to search for recent photographs of the region - to determine exactly when Sk -69° 202 had started to brighten. Serendipitously, on February 23.44 UT, Ron McNaught, of Siding Spring observatory had photographed[79] the supernova at a visual magnitude, V of 6.4; only 3.4 hours earlier it had been observed[79] by Shelton at a visual magnitude greater than 12.1. It transpired that McNaught's photograph was taken only 3.2 hours after the detection of the neutrino burst by Kamiokande, IMB, and Baskan (§IV). A second crucial observation[139] was made. Alan Jones (Nelson, New Zealand), who easily discovered the supernova visually on Feb 24.37 UT with a finder telescope, did not notice the object with the same instrument on Feb 23.39 UT suggesting that the supernova was fainter than V=7.5 at this time. These early data points have proved invaluable in constraining models of the early evolution of SN 1987A. The chronology of the early events is given in table 7.

Table 7. The early chronology of SN 1987A

DATE UT 1987	REF	EVENT
January 24	140	Observations of the field of Sk -69° 202 were identical to V=14.5
February 22	140	Observations of the field of Sk -69° 202 were identical to V=14.5
February 23.101	140	$M > 12.1$
23.124	(§IV)	Mont Blanc and Kamiokande neutrino events
23.316	(§IV)	Kamiokande, IMB, and Baskan neutrino events
23.390	139	$M > 7.5$
23.444	79	$V=6.36\pm0.1$
23.621	79	$V=6.11\pm0.1$
24.122	79	$V= 5.0\pm0.1$ (Shelton's discovery photograph)
24.313	79	$V=4.77\pm0.1$
24.4		IAUC announcing the discovery of the Supernova
24.8		Major instruments became trained upon SN 1987A, eg. IUE

V.1 EARLY CONSTRAINTS

The first day of SN 1987A was thus characterized by a rapid rise in its optical brightness, although the optical detection of a typical type II supernovae was not expected until several days after the neutrino detection.

The increase in luminosity is expected to occur when the shock wave produced by the core bounce (§III.4) reaches the outermost regions of the star, that is, when,

$$\tau \sim \frac{R_0}{v_0}, \qquad (V.1),$$

where v_0 is the envelope expansion velocity, $v_0 \sim \left(\frac{2E_0}{M_{env}}\right)^{0.5}$. So, the rise time is,

$$\tau \sim \frac{R_0}{\left(\frac{2E_0}{M_{env}}\right)^{0.5}} \qquad (V.2)$$

Sk -69° 202 was a B3Ia supergiant and therefore had a radius, R_0 of some 3×10^{12} cm (§II). For a shock wave energy, $E_0 \sim 10^{51}$ ergs (§III.5), and $M_{env} \sim 10\ M_\odot$ (§III.5), an outbreak time of 2.6 hours is obtained - this concurs with McNaught's detection 3.2 hours (and Jones's non-detection 30 minutes) after the fiducial neutrino time. The reason for SN 1987A's unusually fast rise in luminosity was its compactness: the shock wave had to travel ~40-50 $R_\odot$ (§II) as compared to the ~1000 $R_\odot$ typical for type II supernovae of 20 $M_\odot$.

The early observations may also be used to constrain the neutrino detections. A full hydrodynamical simulation[141] finds the time of shock outbreak to be, Feb 23.16±0.024; this excludes the Mont Blanc time of Feb 23.124 though, if Jones' non-detection is ignored, then the small variation in the early data points is insufficient to eliminate the Mont Blanc time. However, if the Baskan time is taken to be real, the emergent shock wave would be expected to give velocities and effective temperatures 2/3 those observed from SN 1987A.

Further evidence for the compact nature of Sk -69° 202 came from observations made in South Africa[142] and Chile[143] on February 25 which showed broad absorption features of the Balmer series extending up to 3×10^4 km/s (0.1 c). The presence of hydrogen made SN 1987A a Type II supernova, but the very high velocity (typically 1.5×10^4 km/s for Type II) indicated that it was distinct from most members of its class. The easiest explanation for such velocities is that the progenitor of SN 1987A was more compact than those of previously observed Type II supernovae.

At the same time another effect of the compact progenitor star became apparent. Since the velocity of the ejecta was twice that of normal supernovae, much of the ejecta's energy was consumed in expansion - rather than released as radiation as it would be in a more typical red supergiant explosion. The early luminosity can be approximated by,

$$L \sim \frac{E_{thermal}}{\tau_{diffusion}} \qquad (V.3)$$

If the envelope expands adiabatically then,

$$E_{thermal}(t) \sim \frac{E_o R_o}{2R(t)} \qquad (V.4)$$

The diffusion time scale (Thompson) can be written as,

$$\tau_{diffusion} \sim \frac{3\kappa}{4\pi c}\,\frac{M_{env}}{R}\,. \qquad (V.5)$$

The opacity, κ, is dominated by electron scattering (from the hydrogen envelope ionised by the shock wave) and is thus 0.4 $cm^2\,g^{-1}$. Combining (V.4), (V.5), and (V.3) gives,

$$L \sim \frac{2\pi c E_o R_o}{3\kappa M_{env}} \qquad (V.6)$$

This gives a somewhat lower (3×10^{40} ergs/s) than the observed value [6×10^{41} ergs/s (Fig. 10)] because it neglects the steep density profile in the outer envelope which leads to the outermost layers becoming highly relativistic[144].

The early luminosity was less than a tenth that of other type II supernovae at a similar age. This is not wholly unexpected: for a red supergiant explosion, all the parameters in equation (V.6) would be the same, except the initial radius, R_0, which would be about 20 times that inferred for Sk -69° 202.

V.1(i) The ultraviolet flash

The electromagnetic display commenced when the shock wave from the collapse of the iron core broke through the hydrogen envelope. If, the supernova is approximated as an homologously expanding sphere of uniform density with internal energy uniformly distributed throughout, then the velocity of the gas is given by

$$v(r) \sim \frac{R}{R(t)} v_0, \qquad \text{(V.7)}$$

the radius of the outer surface is $R(t) \sim v_0 t$, and t is the time elapsed since the explosion. The radiation temperature immediately after the passage of the shock wave can be obtained if an equipartition between the radiant and kinetic energy is assumed[42]: $(4/3)\pi R_0^3 a T_0^4 \sim E_0$, where a is the radiation constant, then rearranging gives

$$T_0 \sim \left(\frac{3E_0}{8\pi a R_0^3}\right)^{0.25} \sim 3\times10^6\ \mathrm{K}. \qquad \text{(V.8)}$$

Although this was not directly observed, the ionisation stages seen by IUE in the circumstellar envelope constrain the temperature[145] at shock break out to be $4\text{-}8\times10^5$ K. This is in good agreement with hydrodynamical models which yield $2\text{-}8\times10^5$ K (e.g.[12]). Continuing this approximation for opaque regions of the supernova, the interior temperature varies as $T(t) \propto R(t)^{-1}$, then,

$$T(t) \sim \frac{R_0 T_0 \left(\frac{M_{env}}{E_0}\right)^{0.5}}{t}. \qquad \text{(V.9)}$$

So even without any consideration of the energy that has been radiated away, the interior of the supernova should become relatively cool within a few months.

The first accurate photometric measurements[146] taken 35 hours after core collapse showed the temperature to have already dropped to 1.5×10^4 K. This dramatic decrease continued as the long diffusion time scale of the envelope meant that most of the internal energy was used in expansion. So the nearly adiabatic expansion of SN 1987A led to a fast decrease in the effective temperature and a fast increase in the radius. The rapid decrease in the effective temperature and the photospheric velocity led to extremely rapid spectral evolution.

A prompt radio burst also accompanied the epoch of shock break out.This emission reached a maximum (0.12 Jy) in only a few days before it faded with a similar timescale to become undetectable after 50 days. The rise time (months to years) and the luminosity were very much less ($\sim 10^3$) than for other well-studied type II supernovae, such as SN 1979C (950 days at 1.4 GHz) or SN 1980K(190 days at 1.4 GHz)[49]. Polarization measurements indicated that the physical process of the radio emission in SN 1987A and in these other much brighter radio supernovae appears to be the same: synchrotron radiation from the interaction of the ejecta with the surrounding circumstellar medium[147].

V.1(ii) The distance to SN 1987A

This can be found by using a distance dependent spectroscopic angular radius (the Baade method):

$$\theta_s = \frac{vt + R_0}{D}, \qquad (V.10)$$

where v is the velocity of matter at the photosphere, t is the time since explosion, and D is the distance. Ordinarily, the time of explosion is not known, but is derived simultaneously with the distance by considering several observation times. For SN 1987A, however, the explosion time is known with considerable accuracy from the neutrino observations. Since the early photometric observations of SN 1987A can be fitted to blackbody curves extremely well[148], the spectroscopic angular size[3] can be derived. This can then be compared with the size deduced from measurements of the velocity of the photosphere (using early line profiles) and a distance to SN 1987A derived. The method yields 55±5 kpc; the accepted value of the distance to the Large Magellanic cloud is 50±7 kpc [3].

Extending this model, several groups have developed model atmospheres for SN 1987A. These have given 49±6 kpc [149], 43±4 kpc [150], and 48±4 kpc [151]. Combining such estimates may in future provide a distance to supernovae that is independent of the many steps on the extragalactic distance ladder.

V.2 TO THE PEAK

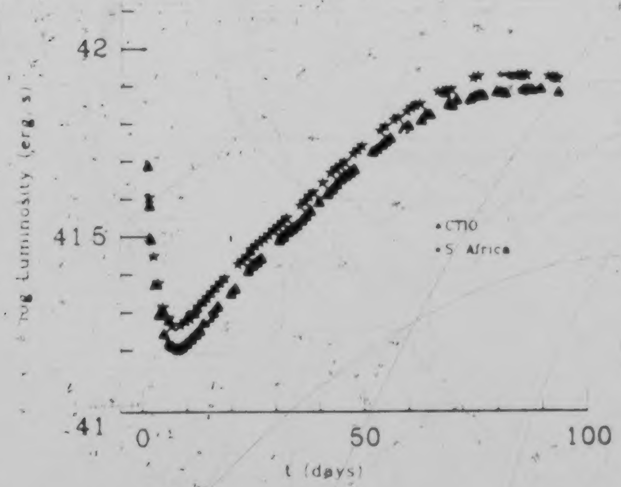

Figure 10. The early light curve[152]

As the evolution proceeded, one of the major tasks for astronomers, was the measurement of the bolometric light curve. This is the energy radiated at infrared, optical, and ultraviolet wavelengths (M to U wavelength bands) as a function of time. The early light curve (Fig. 10) was produced by the release of the radiation field established in the outer layers of the star by the shock wave. Once the temperature had fallen to about 7000 K, the hydrogen in the envelope ionised by the initial shock wave began to slowly recombine in an inward propagating wave. This process liberated energy. However, the dramatic upturn in the light curve resulted from a change in the opacity of the envelope.

Previously dominated by scattering from free electrons, the recombination of these electrons together with the decreasing density (from the rapid expansion) led to a large increase in the envelope's optical depth.

Assuming adiabatic cooling the observed recombination time may be illustrated by rearranging equation (V.9):

$$t \sim \frac{R_0 T_0 \left(\frac{M_{env}}{E_0}\right)^{0.5}}{T(t)} \qquad \text{(V.11)}$$

For typical values, e.g., $T_0 \sim 5 \times 10^5$ K, $T(t) \sim 7000$ K. This gives a time of 11 days in reasonable agreement with the observed 7-9 days (Fig. 10).

This hydrogen recombination lasted until the wave encountered the helium mantle. In principle, this epoch could be deduced from the spectroscopic history: when was the slowest moving hydrogen observed? In practice this cannot be easily resolved since different hydrogen lines originated from different photospheres. Most observers (e.g.[49]) cite the Brackett hydrogen lines at 2.1×10^3 km/s as suggestive of the cessation of hydrogen recombination, some 25 to 40 days after the explosion.

The energy released as a result of recombination of the envelope can be estimated. For an envelope with an helium mass fraction, Y (typically 0.3)[78] and hydrogen mass fraction, X=1-Y, this is,

$$\varepsilon_{rec} = 1.60 \times 10^{-12} \left[13.6(1-Y)N_A - 24.58Y(N_A/4)\right] \text{ ergs/g}, \qquad \text{(V.12)}$$

$$= 5.4 \times 10^{12} \text{ ergs/g},$$

where N_A is Avogadro's number, and the ionization energies for hydrogen and helium[153] have been used. For an hydrogen envelope of 10 $M_\odot$, then 1×10^{47} ergs will be released. The average brightness due to volume recombination will be

$$\frac{1 \times 10^{47} \text{ ergs}}{20 \text{ days}} \sim 6 \times 10^{40} \text{ ergs/s}, \qquad \text{(V.13)}$$

so the actual energy release due to recombination had only a small effect on the light curve.

1

As the wave continued propagating into the star, heavier elements were able to recombine and so the opacity of the envelope continued to decline rapidly. Were there no other source of energy besides the initial shock wave, the bolometric luminosity of SN 1987A should now have begun to decline: the energy release from recombination and the resultant decrease in the opacity of the helium mantle would be insufficient to sustain the light curve. But it increased steadily and smoothly to reach maximum luminosity 85 days after core collapse. What powered this emission? There were two possibilities for the energy source.

(a) Radioactivity from the decay of ^{56}Ni produced in explosive nucleosynthesis (suspected as the power source for the light curves of previously observed type II supernovae).

(b) Energy from a central remnant, e.g. a pulsar.

Once the bolometric light curve had climbed to maximum, SN 1987A was no longer under-luminous in comparison with other type II supernovae, e.g.SN 1967L[49]. This seems to verify the expected similarity between its energy release upon core implosion and that released by other type II supernovae. The key to SN 1987A's reduced early luminosity was the compactness of its progenitor: a blue rather than a red supergiant. Subsequently other supernovae have been discovered[154]/re-evaluated[155] - to check if they had not been missed because of selection effects. However, it does appear that these dim events are uncommon relative to the more flamboyant red supergiant explosions: only a small fraction of all presently evolving massive stars occur in galaxies where the metallicity is sufficiently low to produce subluminous type II supernovae[156]. So everything that is learnt from the evolution of SN 1987A with regard to the products of nucleosynthesis and the central remnant must be tempered by its unusual progenitor.

V.2(i) Early Spectra

The spectrum from SN 1987A evolved very rapidly in the first few months, see Fig. 12. The wavelength of the blueshifted Hα absorption line, which on Feb 25th corresponded to a Doppler velocity $v \sim 1.7 \times 10^4$ km/s, shifted to the red and by April 17th corresponded to $v \sim 6 \times 10^3$ km/s. The fact that the velocity decreased does not imply that the supernova was decelerating; rather, it implies that the Hα absorption line was formed in progressively deeper, more slowly expanding layers of the envelope as the transparency of the envelope increased.

Figure 11. Spectra of SN 1987A during the first few months[53]

As the recombination wave propagated inward, absorption lines of neutral Na and singly ionized Ca, Fe, Ti, Sc, Br and Sr began to appear and strengthen (e.g. Fig. 12). However, models of stellar evolution allow Ba and Sr to be mixed out only as far as the helium layer in the atmospheres of most stars and indeed, (because of the opaque nature of such a deep region) they normally show up only *very* weakly in the spectrum. These elements are produced by the 's-process': iron nuclei are converted to heavier elements through the slow addition of neutrons. Since the iron core is formed only in the last days of stellar evolution, such an overabundance of these heavy elements suggests that there was considerable mixing (§V.6) - either in the progenitor, or else in the supernova fireball itself.

Figure 12. The spectral evolution at optical wavelengths during the first month of SN 1987A [49].

V.3 OVER THE HILL

After about day 85, SN 1987A released insufficient energy to maintain its prodigious light curve. By day 125 a steady decline in the bolometric luminosity set in, allowing astronomers to resolve the problem of the central energy source. The bolometric light curve followed an exponential decline having a characteristic decay rate very close to the laboratory value for the radioactive isotope ^{56}Co (Fig. 13). Detailed models (e.g.[12]) find that this radioactive energy had actually been powering the light curve since about day 20. The early luminosity had increased until, at maximum, the escape and generation of energy became the same. The timing of this 'bump' in the light curve was dictated by a combination of the rate of release of radioactive energy and the increase in transparency of the envelope due to recombination.

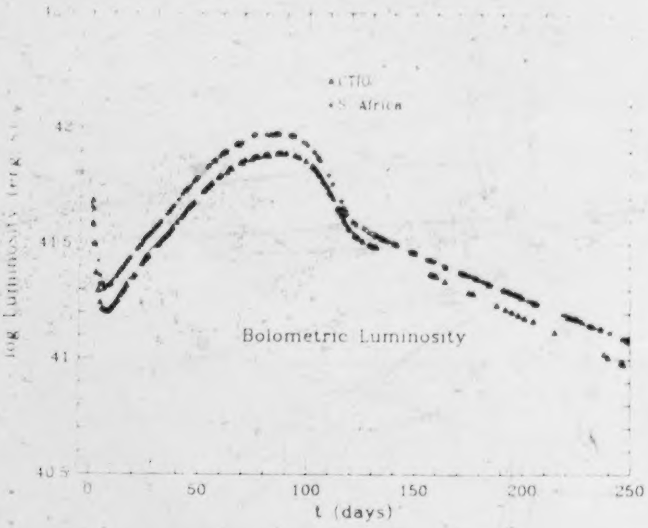

Figure 13. The bolometric light curve until day 250 [157].

From July 1987, the 'linear' phase had a half life of 71-80 days, in good accord with the 78.76 day laboratory half life for ^{56}Ni decay by electron capture to ^{56}Fe:

$$^{56}Ni_{28} + e^- \xrightarrow[\tau_{1/2} = 7 \text{ days}]{} {}^{56}Co_{27} + \gamma + \upsilon_e$$

$$^{56}Co_{27} + e^- \xrightarrow[\tau_{1/2} = 79 \text{ days}]{} {}^{56}Fe_{26} + \gamma + \upsilon_e. \tag{V.14}$$

The gamma-rays released by the decay of ^{56}Co have energies 847 keV (100%), 1038 keV (14%), 1238 keV (68%), 1772 keV (16%), and 2599 keV (17%)[158].

The rate of energy released corresponds to the rate of decay, $\dot{N}$ with the decay Q value. Since the rate of decay is

$$-\dot{N}(t) = \lambda N_0 \exp(-\lambda t), \tag{V.15}$$

the rate of energy release can be written as,

$$\dot{E}(t) = Q\dot{N}(t) = Q\lambda N_0 \exp(-\lambda t), \tag{V.16}$$

where $\lambda=\ln(2/\tau_{1/2})$ is the decay rate of the nucleus. For $^{56}Co_{27}$ the Q value is 3.695 MeV (ignoring the contribution of neutrinos)[159]. The initial mass of radioactive nuclei, M can be calculated: $M=N_0Am_p$, where N_0 is the initial number of nuclei, m_p the proton mass, and A the atomic mass. If the contribution of ^{56}Ni to the light curve is ignored (since $\tau_{1/2}=7$ days), then the total mass of ^{56}Co, and hence the total mass of ^{56}Ni, can be calculated by rearranging equation (V.15) and substituting $N_0=M/Am_p$:

$$M \sim \frac{Am_p\dot{E}(t)}{Q_{Co}\lambda_{Co}(e^{-t/\tau_{Co}})} \qquad (V.17)$$

From Figure 13., I calculate (§C) the original mass of ^{56}Ni to be 0.076 $M_\odot$, in good agreement with the accepted value of 0.075 $M_\odot$ (e.g.[7]).

How did such disjoint mechanisms as the release of trapped energy by a recombination front, and the diffusion of radioactive energy, dovetail to produce such a smooth evolution to maximum light? For this radioactive decay energy to affect the light curve, the nickel, freshly synthesized by the shock wave at the base of the ejecta (§V.5), must have somehow distributed itself throughout the envelope; or perhaps some portions of the envelope became optically thin very quickly, allowing the effective photosphere to include some material from deep regions of the supernova. These possibilities will be addressed in §V.4.

V.3(i) Spectral Evolution

Invoking 0.075 $M_\odot$ of ^{56}Ni to explain the light curve led immediately to the prediction that gamma-rays [from radioactive decay (V.13)] should become visible as the optical depth of the expanding ejecta decreased. The expectation from preliminary models was that gamma ray lines should turn up sometime in early 1988 with a 3 month warning signal: a hard X-ray continuum of nuclear decay photons degraded by multiple scatterings. However, in early August 1987 X-rays were recorded by the Mir[160] and Ginga[161] satellites. The very hard spectrum observed in both cases, peaking around 20 keV, was consistent with scattered gamma-rays from ^{56}Co decay. Prior to SN 1987A, only one other young supernova, SN 1980K, had been discovered in X-rays; however, this supernova gave little spectral information.

Under these circumstances gamma-rays should also have been detected earlier than predicted. Once again observations overtook predictions. The Solar Maximum Mission[162] registered a small flux of gamma-rays in late August 1987. By the beginning of September 1987, a series of experiments, satellite and balloon borne, began to detect the characteristic 847 and 1238 keV lines that accompany ^{56}Co decay to ^{56}Fe. These hard line emissions have persisted to this day [§V.6(ii)].

As SN 1987A continued to expand, the spectrum evolved from that of a star (continuum) to a nebula (discrete emission lines). This was demonstrated by the Kuiper airborne telescope observations (e.g. see Fig. 14) in the infrared (where the optical depth was greatest). During the fall of 1987 and the spring of 1988 these revealed a veritable zoo of ions: FeI, FeII, CoII, N, NiI, NiII, ArII, CII, OII, NeII, MgII, UII, KII, CaII, AlI, CO, SiO and a host of long wavelength hydrogen lines[163]. The strengths of these lines (except carbon and oxygen lines) have been such that production by the progenitor can be excluded. Such abundances must have arisen during explosive nucleosynthesis deep inside the star (§V.5).

Figure 14. The infrared spectrum taken in mid-April (day 410), 1988 from the Kuiper Airborne Observatory[164].

Figure 14 has been removed because of the unavailability of copyright

Witteborn, F. et al. 1988. Preprint, submitted to

In addition, line profiles, particularly those of Ni, Co, Fe, and Ar showed velocities of ~3000 km/s: twice as fast as could be expected without mixing. This is an indication that macroscopic mixing has occurred (§V.4). Furthermore, the cobalt feature was particularly interesting because the observed line strength agreed[5] with the abundance of radioactive ^{56}Co ions expected to be present based upon the initial creation of 0.075 $M_\odot$ of ^{56}Ni that is required to explain the light curve.

V.4 MIXING

Well-observed supernovae remnants, e.g. Cas A, show a clumpy, chemically inhomogeneous structure throughout their ejecta. While there did exist theoretical indications that this was due to instabilities of the propagating shock wave, such observations were commonly taken to be a result of the ejecta's expansion into an inhomogeneous circumstellar medium. Models of supernova envelopes that were constructed before SN 1987A, employed a separation of elements into concentric shells; they comprised an outermost hydrogen envelope surrounding distinct layers composed mainly of He, C, O, Si, and Fe, respectively (that is, an expanded version of Fig. 1). So models upon which predictions of electromagnetic fluxes were based, relied on an isotropic stratification of the internal composition in velocity space. However, there is much evidence that suggests this has not been maintained and that large scale mixing has taken place in the envelope of SN 1987A. This evidence includes the following:

(a) the smoothness of the bolometric light curve [§V.3(i)];

(b) the early appearance of x and gamma-rays [§V.3(i)];

(c) and the strengths of the spectral lines produced by heavy elements observed at infrared and gamma ray wavelengths [§V.3(i)].

All of the above observational features appear to stem from the unexpected distribution of the radioactive energy in the envelope of SN 1987A. This begs the question, how did the radioactive elements synthesized (§V.5) deep in the star find their way out so quickly? The mixing can be attributed to 3 processes: (i) the ejecta are asymmetric; (ii) Rayleigh-Taylor mixing occurred as the helium core moved into the low density hydrogen envelope; and (iii) the formation of Nickel bubbles mixed the envelope. I shall consider these mechanisms in turn.

V.4(i) Asymmetry

The spherical symmetry of the progenitor may have been broken in a number of ways:

(a) rotation of the progenitor may have mixed the helium core and mantle, thus altering the density profile of the envelope with respect to a concentric shell model;

(b) the progenitor's rotation may have led to enhanced oxygen burning during the propagation of the early shock wave through the envelope (§II.6);

(c) an asymmetry in the core collapse and bounce may have produced an explosive asymmetry that was able to propagate to the envelope.

That the ejecta are asymmetric is certain. During the first few months several groups measured the polarisation in both continuum and line emissions of the envelope. From this data several models (see^5) found a ratio between the minor and major axes of the envelope of 1.1±0.1. By December 1989 this had increased to 1.4±0.1 inclined along an E-W axis (Fig. 27).

Are the mechanisms (a) to (c) capable of producing the large scale asymmetry observed? The propagation of the initial shock wave through an already mixed envelope certainly enhances mixing. However, the magnitude of (a) is highly model dependent: for a 2% perturbation in the initial density composition of the ejecta, calculations find a 15-20%

Mechanism (b) would increase the temperature of the mass outside the original iron core (§II.6). This is expected to allow more explosive nucleosynthesis than for a non-rotating explosion. The prediction from such a model is that less oxygen should be observed in the supernova ejecta (for which there is some evidence)[77] but, unfortunately, abundance determinations from line strengths are not as yet sufficiently accurate to prove or disprove this scenario. In regard to mechanism (c), pulsars are known to have typical space velocities of the order of 200 km/s. Since their progenitor population does not have such a large velocity, the velocity would appear to be associated with the formation of a neutron star[167]. So it is plausible that the pulsars receive their velocities as a result of an asymmetry in the initial explosion mechanism. At present, it is not possible to eliminate any of scenarios (a)-(c).

Limits on the influence of rotation can be inferred from the neutrino burst (§IV). For rapid rotation, the neutrinosphere of the proto-neutron star is expected to suffer considerable flattening; an observer will detect as much as a threefold[168] increase in the neutrino flux if the neutron star is seen pole-on (because a greater surface area is viewed) - as compared to an equatorial observation. Because of the reasonable agreement between the observed and expected neutrino fluxes [§IV.4(ii)], the case of extreme differential rotation seems unlikely though it is not possible to make quantitative statements within the confines of the present neutrino models and the small number of events detected. The evidence certainly indicates rotation has played a significant, though not dominant, role in the evolution of the ejecta.

V.4(ii) Clumping

As the shock wave propagated outward it encountered a number of different density regions in the envelope - in particular the increment in density between the hydrogen and helium burning layers. Shock propagation through a sharp density gradient necessitates partial reflection (known as the reverse shock wave), which in turn leads to a density inversion. Since March 1988, Cobalt line profiles have appeared as double peaks, this is qualitatively consistent with the line splitting expected from the radioactive decay of atoms which have been given different velocities by the shock wave[169]. Three-dimensional models for simple polytropes [170,165,171] have shown that the development of a density inversion in the ejecta leads to Rayleigh-Taylor instabilities which enable the formation of a fragmented structure, see Fig. 15. Furthermore, the associated mixing between the core and envelope materials produces a non-spherical distribution of elements.

[illegible]

[illegible] Müller E. 1989

Figure 15. Cross section of a model[172] for the expanding supernova ejecta. The Figure shows density contours (5% spacing) at 9814 s after the explosion. The "mushroom head" shapes are characteristic of the Rayleigh-Taylor instability and represent the penetration of heavier elements into the helium mantle.

So, if the heavy elements become localized in clumps, then a large fraction of the high energy flux from their radioactive decay is able to escape through the hydrogen and helium regions of the envelope without substantial absorption. This effectively reduces the opacity. In addition, it should aid the 'bubble' mixing process [§V.4(iii)], by providing paths of lower resistance for the expansion of the hot radioactive bubble that is modelled to develop during the first few months of the explosion.

Moreover, as the outer ejecta sweep up the circumstellar medium surrounding SN 1987A, this too will become Rayleigh-Taylor unstable and so fragmentation is likely in all regions of the supernova envelope. The 'ragged' appearance of known supernova remnants indicates that clumping is a common phenomenon, e.g., Cas A. It is thought that the time dependence of gamma ray line profiles will provide the most explicit test for clumping.

V.4(iii) Blowing bubbles

After the passage of the reverse shock [§V.4(ii)], the elements heavier than helium are modelled[12] to be moving at 1000-2000 km/s. Such a velocity corresponds to a kinetic energy density of about 2×10^{16} ergs/g. However, this is less than the energy released by the decay of ^{56}Ni (3.0×10^{16} ergs/g) and of ^{56}Co (6.4×10^{16} ergs/g). If all this radioactive decay energy were deposited in an homologously expanding sphere and radiation transport were neglected, then the edge of the expanding sphere would be moving at ~4500 km/s. Taking the total energy available from the decay of 0.075 $M_\odot$ of ^{56}Ni to ^{56}Fe and subtracting the fraction that came out in the bolometric light curve after day 40 (when the light no longer came from shock deposited energy), it has been estimated[173] that 45% of the radioactive energy did work expanding the core and thus did not appear in the light curve. This argument leads to an upper bound to the velocity of the heavy elements of 3000-4000 km/s.

Since the velocity gradient in the region where radioactive isotopes form is only a few hundred km/s, the decay of ^{56}Ni and ^{56}Co has dynamic consequences. The energy released causes the constituents of this region to reduce their density (expansion) faster than any of the surrounding layers. A density inversion then develops. This region of low density is known as the nickel bubble and pushes material ahead in a dense shell. Hydrodynamical calculations[174,165] show this situation to be Rayleigh-Taylor unstable and indicate that bubbles of nickel-cobalt rich material penetrate the overlying layers and lead to extensive mixing.

The turn-on of gamma-rays and X-rays appears to mark the epoch when the first nickel bubbles reached moderate optical depth. Existing fragmentation [§V.4(ii)] provided paths of lower resistance for the passage of bubbles, thereby enhancing existing clumps and allowing the earlier escape of radioactive decay energy. From late August 1987 gamma ray lines of 1238 keV and 847 keV [characteristic of ^{56}Co decay (V.13)] were observed [§V.3(i)]. These indicated velocities of up to 3000 km/s, sufficient for the material to have overtaken the slower moving material at the base of the hydrogen envelope [~ 2100 km/s (§V.2)]. It is unlikely that appreciable cobalt could be mixed so quickly into the envelope in the star without the aid of a mechanism such as the nickel bubbles.

In order to satisfy the conditions described in [§V.4(i)-(iii)], significant mixing is required in the envelope. Compare Figure 16, which shows a model of SN 1987A neglecting mixing, with Figure 17 which is a recent mixed model. Indeed, mixed models have been used to provide clear correlations with most aspects of SN 1987A. They can therefore be used as a guide to suggest the future evolution of the remnant.

Figure 16. A model[175] of the ejecta with no mixing.

Figure 16 has been removed because of the unavailability of copyright.

From Woosley, S.E. 1988, Proc. of 14th Texas Symposium on Relativistic Astrophysics, in press

Figure 17. A model[7] where mixing has been added in order to agree with the light curve and early appearence of X-rays and Gamma-rays.

Figure 17 has been removed because of the unavailability of copyright.

From Woosley, S.E. 1988, Proc. of 14th Texas Symposium on Relativistic Astrophysics, in press

From the numerous and diverse observations of the ejecta, each of the proposed mixing scenarios appears to contribute to the ejecta's departure from a cohesive spherical shell. It is important that all 3 instability mechanisms ultimately be included in one sequential series of calculations.

V.5 EXPLOSIVE NUCLEOSYNTHESIS

As the shock wave generated by core bounce (§III.4) propagated through the silicon and oxygen rich layers, explosive nucleosynthesis took place. The peak temperature behind the shock exceeded 5×10^9 K and so materials originally composed of Si, S, and Ca burned to form iron group elements. The silicon layer produced mostly radioactive ^{56}Ni and lesser amounts of other radioactive species, e.g., ^{57}Ni and ^{44}Ti. In the oxygen rich layer the products were mostly Si, S, Ca and ^{56}Ni. Without explosive nucleosynthesis in the silicon and oxygen layers of Sk -69° 202, only a trace of the observed 0.075 $M_\odot$ of ^{56}Ni would have been produced in the explosion of Sk -69° 202, see Fig. 19.

Figure 18 has been removed because of the unavailability of copyright.

From [illegible] Hashimoto M. Nomoto [illegible]

Figure 19. The composition of the ejecta after nucleosynthesis[176]. Mass exterior to the dotted line is ejected; mass interior to this point falls back onto the neutron star.

Figure 19 has been removed because of the unavailability of copyright.

From [illegible] Hashimoto M. Nomoto [illegible]

Figure 18. The composition of the ejecta before nucleosynthesis[176].

The synthesis of radioactive nuclides has been very important to the evolution of SN 1987A. In particular, models for the production of ^{56}Ni during explosive nucleosynthesis can be directly compared with the observation of 0.075 $M_{\odot}$. Assuming an homogeneous density and temperature distribution behind the shock (this is borne out in detailed calculations, e.g.[159]), the supernova's kinetic energy can be equated to its thermal energy inside the radius of the shock front:

$$E_{SN} \sim \frac{4\pi}{3} R^3 a T^4. \tag{V.18}$$

For $T=5\times10^9$K and $E_{SN}=10^{51}$ ergs, the result is R=3700 km. For evolutionary models[12,159], this radius corresponds to 1.7 $M_{\odot}$ (Fig. 19). In order to comply with the observed abundance of ^{56}Ni and the expected mass fraction of ^{56}Ni produced at this temperature, a mass cut[176] at 1.60±0.05 $M_{\odot}$ (baryonic mass) is required[159]. This corresponds to a neutron star mass of 1.43±0.05 $M_{\odot}$. Although this conclusion is dependent on a somewhat uncertain presupernova model, it is in agreement with that inferred from the neutrino burst [§IV.4(ii)].

The propagation of the shock wave through the star led to very high temperatures throughout Sk -69° 202. However, once it reached the carbon layer, its density became too low to cause further explosive processing. The expected abundances of the silicon, oxygen, neon and carbon burning have been modelled (Fig. 19). The masses of radioactive nuclides (other than ^{56}Ni), produced in the silicon layer are expected to be determined from their contributions to the light curve and their gamma-ray emissions (§VI). However, for the non-radioactive nuclides direct comparison between the calculated abundance and observation suffers from complications. Until the ejecta become optically thin at all wavelengths (this is unlikely for clumpy ejecta [§V.4(ii)], astronomers will not be certain if the total mass of an element is being viewed. In addition, only certain ionization energies are observed. However, in order to determine the total mass of a given element, it is necessary to make assumptions about the temperature and density of the ejecta. This is difficult given the mixed clumpy nature of the envelope (§V.4).

V.6 LATER EVOLUTION

From July 1987 to June 1988, the bolometric light curve declined with a characteristic decay rate close to the laboratory value for ^{56}Co. This agreement, together with the close correlation of mixed models (§V.4) has received even stronger support from the continued detection of gamma-rays characteristic of those from the radioactive decay of ^{56}Co (V.13). However, in June 1988 the bolometric luminosity of SN 1987A fell consistently below radioactive decay predictions (see Fig. 20). Although X-ray and gamma-ray luminosities were not included in the bolometric light curve (see Figs. 22&23), infrared spectra at this time indicated another process - dust formation.

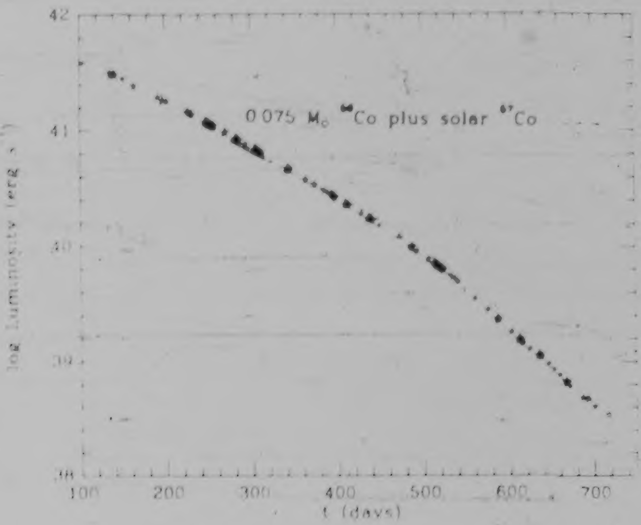

Figure 20. The bolometric light curve from day 100 to day 750 [177]

V.6(i) Dust formation

The formation of dust grains in the gas ejected from supernovae had been considered to explain the isotopic abundance anomalies of heavy elements found in meteorites (carbonaceous chondrites[178]). Observations of previous supernovae were insufficient to distinguish whether thermal infrared emissions had been caused by newly formed grains in the expanding ejecta or by the pre-existing circumstellar grains around the progenitor.

Once the supernova's ejecta cool to below 1800 K, it is expected that dust grains would start to form in the ejecta. Such condensation occurs first for graphite at 1790 K, and then for a number[179] of species of oxidic grains at around 1500 K, e.g., Al_2O_3, Mg_2SiO_2, and Fe_3O_4. If there were no destruction of dust grains, then the large increase in the opacity of the envelope leads to absorption of the bulk of the supernova's radiation (and re-emission at much longer wavelengths). However, it is expected that high energy photons from radioactive decays heat up, and thus destroy, the dust grains. If the ejecta are broken into clumps, then dust grains are, to some degree, protected from energetic radiations.

From about day 530 to day 730, observations[180] in the optical and infrared revealed that line peaks shifted bluewards by several hundred km/s and that the line intensities decreased (e.g. Fig. 21).

Figure 21. The temporal behaviour of the Si I and Mg I emission lines[181]. Note the sudden decrease around day 530

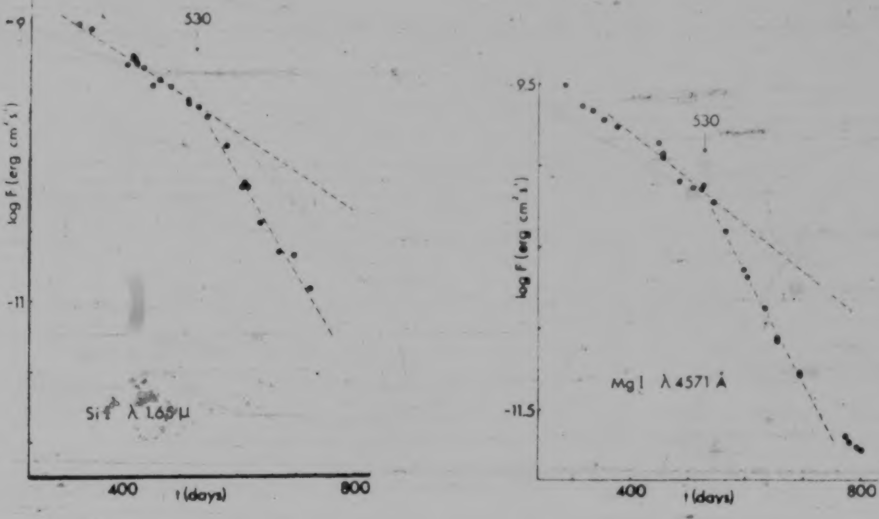

This observation, in varying degrees, was apparent in all emission lines in the wavelength interval 3.7-10 μm. This is thought to be the spectroscopic signature of dust distributed over a finite region in the envelope, where the far (receding) side would be more obscured by the greater path length through dust than the near (approaching) side. Around day 530 there was also an increase in the apparent decline of the bolometric light curve (Fig. 20). Although the far infrared flux actually rapidly increased relative to the optical and near infrared the full effect of this was not established due to difficulties in integrating the far infrared flux[182]. The simultaneous dimming in the optical, brightening in the far infrared, and the sudden blue shifting of emission lines, is strongly suggestive that dust has formed local to the supernova.

Far infrared observations from day 632 distinguished the flat continuum[183] expected from the thermal emission of graphite (with silicates contributing <20%). As of day 1000 more than 80% of the supernova's energy was emitted as infrared and far infrared radiation[184]. Results of the spectra from such wavebands are eagerly awaited.

V.6(ii) The evolution of high energy emissions

Past observations of X-rays and gamma-rays in supernovae have been dominated by the emission, either of a central pulsar, or of fast moving ejecta interacting with circumstellar material. While this may be so at some level in SN1987A, there are radio observations [§V.1(i)] that suggest the circumstellar medium around SN 1987A is very tenuous and so would not be expected to generate substantial high energy radiation. The dominant source of both X-rays and gamma-rays is something not directly observed before from supernovae - *radioactivity*.

The early turn on of gamma-rays, characteristic of the radioactive decay of ^{56}Co [§V.3(i)], in August 1987 when the envelope was expected to be optically thick, has been accounted for by allowing some radioactive material produced in the explosion to be mixed from the inner region of the ejecta into the envelope. These spherically symmetric models, have been continously adjusted to fit the bolometric light curve, the X-ray light curve, and the gamma ray light curve. Until about day 300, these models corresponded well with observation. However, in order to accord with the still increasing X-ray and gamma-ray fluxes after this epoch, several models have invoked the effects of a clumpy structure[§V.4(ii)]. If the heavy elements are in clumps, then a large fraction of X-rays could be transported through the hydrogen and helium regions without suffering much absorption; this would effectively alter the opacity. Recent calculations show[185] that a decrease by about a factor of 9 in the absorption (modelling clumping) of high energy emissions will allow predictions to agree with Ginga data until about day 500. However, after this the continuing steady flux measured in 16-28 keV by Ginga can not be explained by any realistic radioactive model, see below[186].

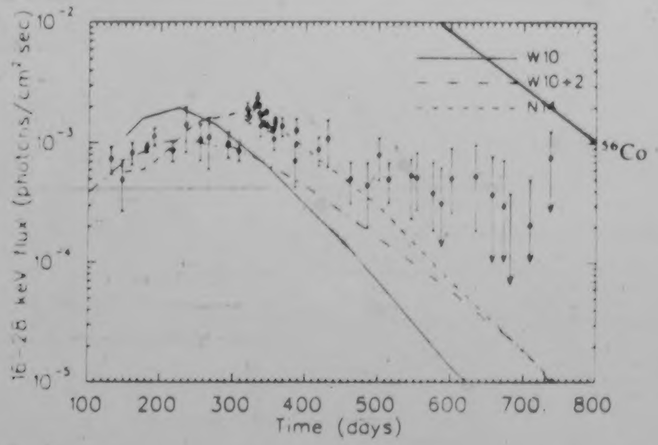

Figure 22. The X-ray light curve. The models N14, W10, and W10+2 correspond to highly mixed models of the ejecta which had been able to explain other observations of the ejecta[187]. The total energy released by the decay of ^{56}Co is shown for reference.

The evolution of the gamma-ray flux has been close to that expected for spherically symmetric mixed models (Fig. 23). However, the recent observed line profiles have not, (Fig. 24). The peak energies of the 847, 1238, and 2599 keV emission lines (V.14) are considerably lower (4.9σ) than predicted; and the line widths are consistently greater (2.9σ) than predicted. The large widths associated with the line profiles imply high velocities for the ^{56}Co material. Apart from being further evidence for mixing of the ejecta, this suggests that the ejecta are transparent. However, the line flux measurements on day

613 are ~50% of those produced by the 0.075 $M_{\odot}$ of ^{56}Co determined from the bolometric light curve. This paradox may be due to clumping: if the supernova contains dense knots or filaments which are optically thick it may be possible to see the receding backside of the supernova.

[illegible] has been removed because of the [illegible] of copyright.

[illegible]

Figure 23. The gamma-ray light curve. All of the measurements are in reasonably good agreement with the mixed model 10 HMM (Fig. 17). 5L is a model with no mixing and the dotted line represents the unattenuated flux from ^{56}Co [188]

Figure 24. GRIS data[188] for the 847 keV line from the decay of ^{56}Co in SN 1987A are shown for day 613.

Figure 24 has been removed because of the [illegible] of copyright.

[illegible]

V.6(iii) The end of the line

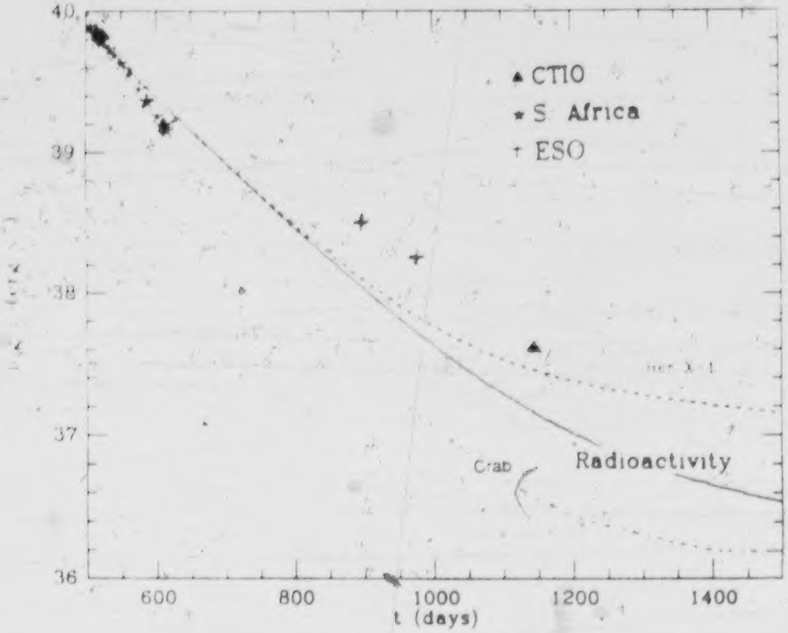

Figure 25. The bolometric light curve since day 500. The expected contributions of both a Her X-1 - like and Crab - like pulsar, embedded in SN 1987A are shown[189].

Since about day 900 measurements have deviated from radioactive predictions. This implies that a hitherto undetected energy source is now contributing significantly to the energy output. Using the solar ratio of $^{57}Fe/^{56}Fe$ and the known production of mass 56 in SN 1987A, the contribution of radioactive ^{57}Co from

$$^{57}\mathrm{Ni} \xrightarrow[\tau_{1/2}=36\ \mathrm{hours}]{} {}^{57}\mathrm{Co} \xrightarrow[\tau_{1/2}=271\ \mathrm{days}]{} {}^{57}\mathrm{Fe} \qquad (V.19)$$

is expected to become the most important radioactive nuclide once most of the ^{56}Co has decayed (§V.10). However, if the upturn in the light curve were due to ^{57}Co, then the original amount would have to be 4-6 times the anticipated[159] 0.0017 $M_\odot$. On the other hand, a thermal echo from external dust seems unlikely since it would coincidentally need to have a colour temperature (150-180 K) similar to that of the supernova's emission. Pulsar emission, absorbed and re-radiated, is a possible explanation.

V.7 THE BEAST WITHIN

In 1932 James Chadwick announced to the scientific world his discovery of the neutron, and by 1934 Baade and Zwicky had put forward the concept of the neutron star. This hypothesis was brilliantly confirmed in 1967 when pulsars, promptly identified as spinning neutron stars left over from supernova explosions, were detected in the Crab and Vela nebulae. Since then, 437 pulsars (until 1987)[190] have been identified, and a further 30 examples[191] where plerionic radio, or non-thermal X-ray emission, indirectly implies the presence of an active neutron star.

The neutrino burst from SN 1987A is strong evidence for the birth of a neutron star [§IV.4(ii)]. Recent observations indicate that SN 1987A is emitting more radiation than expected; this has appeared in the bolometric light curve (Fig. 25), in the X-ray flux (Fig. 22), and in the gamma-ray flux (Fig. 23). But as yet no pulsed radiation has been found.

Pulses of optical radiation were actually detected[192] in January 1989. However, they have since been reported[193], February 1990, as instrumental error. Despite the frustration of calculations carried out upon the basis of this bogus detection, it did focus detailed attention on all aspects of young pulsars. In §V.7(iv)&(v), I shall briefly discuss some of the more novel ideas that arose.

V.7(i) Spin Rate

The distribution of pulsars has led to the prediction[194] that most pulsars are born spinning at around 0.1 s . The few pulsars that have been detected with periods of 1.6 to 10 ms are believed to have been "spun-up" by accretion from companion stars, though this conclusion is uncertain[167].

How fast is the neutron star in SN 1987A spinning? If Sk -69° 202 was a typical BO star when it was on the main sequence, then observations (see[102]) suggest a rotation period of 2 days. If the star was rotating rigidly and the collapse of the core conserved angular momentum, then,

$$MR_0^2\Omega \sim MR^2\omega, \qquad (V.20)$$

where R_0 and R are the respective radii of the core and neutron star, and Ω and ω are their respective angular frequencies. Since $R/R_0 \sim 200$, a rotation period of about 5 s is expected.

However, a neutron star in SN 1987A is also likely to have been spun-up by accretion. This is expected to occur when the reverse shock [§V.4(ii)] arrives back at the core and increases the density of the core gases. Because Sk -69° 202 was a blue supergiant, the time scale for the reverse shock to reach the core is ~100 times shorter than for a red supergiant[167]. This means that the surface of the neutron star is still sufficiently hot (~10^{10} K) to radiate accretion energy as neutrinos (though below detection limits). So, ~$0.1M_\odot$ is allowed to accrete onto the neutron star before radiation pressure causes the gas to return to uniform expansion (1-2 hours)[167]. The amount of "spin-up" provided by this accretion has yet to be calculated. But it is accepted that a neutron star in SN 1987A will be rotating faster than one left from a red supergiant whose progenitor had a similar period of rotation.

V.7(ii) Luminosity of a pulsar

Although now limited by radiation pressure, accretion is expected to continue and might contribute to the light curve. In order to give a limit to the accretion, the Eddington luminosity (§III.5) may again be used - this time for photons - then,

$$L_E = \frac{GM4\pi cm_p}{\sigma_T}. \qquad (V.21)$$

Since the surrounds of the neutron star are fully ionized Compton scattering is the principal source of opacity and so the Thompson scattering cross-section may be used. For $\sigma_T = 6.65\times10^{-29}$ m^2 and M~1.4 $M_\odot$, then, $L_E \sim 2\times10^{38}$ ergs/s. This is well above the current luminosity, see Fig. 25, so the remnant is not accreting near the Eddington luminosity.

It has often been suggested (e.g.[12]) that the pulsar has not been observed because the infall pressure of accretion has been larger than the magnetic dipole pressure. This situation requires a mass accretion rate[167] of $M > 3\times10^{-5}\ M_{\odot}\ yr^{-1}$. However, the luminosity of an accreting neutron star is given by,

$$L = \frac{GMM}{R}\ ; \qquad \text{(V.22)}$$

inserting the above mass accretion rate, $M=1.4\ M_{\odot}$, and $R=10^6$cm, a luminosity of $\sim10^{41}$ ergs/s is obtained. This is well above the current luminosity and so pulsar activity is not strangled by the accretion.

In addition to luminosity generated by accretion, neutron stars radiate energy as a rotating magnetic dipole. This is possible because of their magnetic fields, typically 10^{12} G. Such high magnetic fields are expected in neutron stars since they involve the collapse of stellar material which is ionized and thus a good conductor. The magnetic flux through, say, the radial plane of the star, is conserved so that

$$B = B_o\left(\frac{R_c}{R}\right)^2\ ; \qquad \text{(V.23)}$$

where B_o and B are the magnetic fields at corresponding points in the star before and after collapse. When a normal star of core radius, $R_c\sim10^{11}$ cm collapses to form a neutron star of $R\sim10^6$ cm, the star's magnetic field will increase from typically 100 G to at least 10^{12} G - this is borne out by observations of X-ray pulsars[195].

A rotating magnetic dipole will radiate if its dipole moment makes an angle θ with the rotation axis. The luminosity of a rotating dipole[196],

$$L = \frac{B^2\omega^4R^6\sin^2\theta}{6c^3}\ , \qquad \text{(V.24)}$$

is in excellent agreement with well-observed pulsars. They appear to have the same radius [§IV.4(ii)], so luminosities scale as $B^2\omega^4$. Figure 25 shows what the well observed pulsars Her X-1 and the Crab pulsar would look like if embedded in SN 1987A.

Although the input from a typical pulsar nebula may now be discernible [§V.6(iii)], the question still foremost in the minds of astronomers is: when will pulsations from the remnant become observable? Pulsar beam widths are given by $\sin^{-1}(\omega R/c)^{0.5}$ for a rotating magnetic dipole model[197] so perhaps we do not live in the path swept out by the rotating beams of the pulsar. Even if we do live in the beamwidth, the pulsed emission may be faint. If the Crab is taken as a guide, less than 10^{-9} of the total spin-down energy is likely to be emitted as pulsed emission[198]. Because SN 1987A is young, the inner regions of its ejecta are still 'hot' (both in the radioactive and thermal sense), such pulsed emission would be most likely at X-ray wavelengths. Unfortunately, the detection limit of current satellites[199], such as Ginga and Mir-Kvant, is 3×10^{36} ergs/s. However, balloon flights[200] using CCD X-ray imaging spectrometers are currently able to detect 1×10^{36} ergs/s; and similar devices on the recently launched ROSAT and BBXT telescopes should within the next year be able to detect around 10^{34} ergs/s.

V.7(iii) Black hole?

The neutrino data did not eliminate the possibility of black hole formation (§IV:5). Furthermore, if $\sim 0.1 M_\odot$ is accreted onto a neutron star within a few hours of the explosion [§V.7(i)], this may be sufficient to cause a neutron star to collapse to a black hole. The argument that the ejection of substantial ^{56}Ni implies little mass fallback is not full proof for the accretion after the reverse shock since the ^{56}Ni is expected to mix with outer core layers. If a black hole is present in SN 1987A, then its rate of accretion will be very sensitive to the unknown angular momentum of the progenitor (far more so than for a magnetic rotating neutron star[201]). It should be noted that the observed luminosity of Cygnus X-1 is $\sim 7 \times 10^{37}$ ergs/s - though this would have to be scaled to SN 1987A. With so little known, it is difficult to eliminate the possibility of a black hole.

V.7(iv) Neutron star vibration

Historically, neutron star vibrations were rejected as an explanation of pulsars because their vibrational periods are much shorter than the vast majority of measured pulsar periods. In addition, observed pulsars appear to endure for thousands to millions of years. Such persistence is natural for neutron star rotation but difficult for vibrational oscillations - they are expected to be damped within a few hundred years. However, this need not pose a problem for a newborn pulsar because radial modes excited at the time of formation may not have been damped out.

The period of the fundamental mode of vibration, P is comparable to the free fall time, t_{ff}, therefore,

$$P \sim t_{ff} = \left(\frac{3\pi}{G\rho}\right)^{0.5} , \qquad (V.25)$$

where ρ is the average density. For neutronic material $\rho = 2.5 \times 10^{14}$ g/cm^3, so the period associated with this fundamental mode is of the order 10^{-4} s. If exotic [e.g. §V.7(v)] material is not important in the neutron star, then a damping time of about 100 years is expected[202]. Perhaps neutron star vibrations will be detected from SN 1987A; more likely, astronomers will have to wait for neutron star formation in an object with a smaller obscuring envelope surrounding it.

V.7(v) Strange star?

Another possibility given serious consideration following the bogus detection of a pulsar in SN 1987A was the formation of a 'strange star'. The proto-neutron star reaches densities for which it is conceivable that a high-strangeness quark-gluon plasma could appear. QCD calculations suggest that three flavour quark matter, or strange matter, is absolutely stable (e.g.[203]) - the ground state of hadrons. There is a variety of routes for nascent neutron stars to convert to strange matter, for example[204]: via formation of 2 flavour matter; clustering of Lambda particles; kaon condensates; burning of neutron matter; and sparking by cosmic rays. Once a 'strangelet' has formed, strange matter will swallow nuclear matter in the surroundings if, as it seems, it is a lower energy state. This conversion is thought to be explosive.

Advocates of strange stars compute (e.g.[205]) not only that the 2 stages of collapse to strange matter would overcome the energy problems in envelope ejection commonly precluding more conventional models (§III.4&5), but also explain the hiatus in the neutrino detections from Kamiokande between 3 s and 10 s [§IV.4(ii)]. Strange stars may also offer an explanation[205] for ultra energetic gamma ray bursters and Centauro event primaries. Though strange matter *may* explain these mysteries, none of the above can really be construed as evidence for it.

The structure of these objects has been widely discussed. It has been shown that for models between 1-2 $M_\odot$, the radius and gravitational red shift are almost indistinguishable from those expected for a neutron star. However, the cooling of strange stars is far more efficient than for neutron stars: the surface temperature after 3 years are anticipated to be, $T_{strange} \sim 10^5$ K [206], whereas $T_{neutron} \sim 4 \times 10^6$ K [199]. New X-ray satellites (§V.10), should eventually be able to distinguish this.

The appearance of strange matter might close the global evolution of massive stars: from birth to death these undergo a series of quantum mechanical tunnellings ending with matter at the absolute minimum energy. There is a price to pay. If the strange matter theory is correct then *all* supernova explosions produce strange ***not*** neutron stars. The bizarre possibility exists that there may be no neutron stars in the universe and that all the pulsars may be identified as spinning strange stars.

One way or another the beast should eventually come out of its lair.

And when it does, we will be waiting.

Ready to learn.

V.8 CIRCUMSTELLAR MATERIAL

Stellar evolution studies (§II) suggest that Sk -69° 202, the progenitor of SN 1987A, began its main sequence lifetime as a massive (~20 $M_\odot$) O type star. Such a massive star is likely to have a strong stellar wind - especially once it evolves off the main sequence and becomes first blue, then red, and then blue again during its supergiant phases. The shocks formed by the interaction of these winds with the interstellar medium produce an 'interstellar bubble' consisting of a relatively warm, low density cavity created by the wind from the red supergiant phase; this surrounds a relatively dense shell of material where the stellar winds from the red and blue supergiant phases have interacted; inside this is a low density region remaining from the blue supergiant phase. In §II.2(i), I discussed the evidence for this structure with regards to ultraviolet and optical observations; in §V.8(ii), I wish to discuss the expected structure with regards to the light echoes from SN 1987A. But first I shall address a less certain observation of the circumstellar surroundings: the so-called 'mystery spot', or sometimes 'son of supernova'.

V.8(i) The mystery spot

Speckle interferometric observations by AAO and CTIO [207] from March 25th until April 14th 1987 reported the presence of a companion object close to the supernova. Pre-outburst photos showed clearly that the progenitor had been the brightest star in the field. However, this mystery spot was only a factor 12 fainter than the supernova, making it an astounding 150 times brighter than Sk -69° 202 had been prior to explosion. The spot, a mere 0".06 (19 light days)[208] away, at an angle of 194±2°, was clearly associated with the supernova. Perhaps the spot arose from the interaction of the ejecta with circumstellar material? Since the outermost ejecta had a velocity of less than 0.2 c and the spot was recorded after only 30 days, ejection from the supernova seems unlikely. It seemed equally unlikely that it was a cloud of gas or dust illuminated by the ultraviolet flash [§V.1(i)]: since the radius of the spot was less than 0".02, it did not cover enough solid angle ($\Delta\Omega/4\pi<0.02$) to account for its brightness (~0.1 times that of the supernova). A model of fluorescence by circumstellar material has also been considered, this model[209] can reach the required luminosity if the cloud is moving at ~0.1 c towards the supernova. This seems highly unlikely - the only plausible mechanism for material to reach such velocities is in another supernova!

A different scenario relies on the ejection of a jet of material from the collapse of a rapidly rotating Sk -69° 202. Core collapse simulations can be manipulated[210] (using rotation) to give a bounce which ejects some 0.007 $M_\odot$ along the poles at a velocity of 0.6 c. The emission is then produced by synchrotron emission in the vicinity of the bow shock. Although 2 blobs of material are expected from such a model, the luminosity ratio between them is large because of relativistic effects - and only one is seen. However, if the spot resulted from a jet, then it would be difficult to understand the lack of radio, gamma-ray and X-ray emissions that should be very intense if material were ejected directly from the core. Moreover, in addition to the energy problems encountered when modelling rotating collapses (§III.5), this scenario must be sufficiently contrived to allow recoil of the other jet of material near the line of sight to the supernova.

The properties of the mystery spot certainly appear very bizarre; this has led to examination of the detection itself. At the time of detection SN 1987A was essentially a point source. The reported intensity of the mystery spot is almost identical to that of the first Airy ring (neither of the reports shows the first autocorrelation function in their data). So, perhaps the spot appeared from careless use of the autocorrelation functions in the deconvolution process. The novelty of speckle methods leads some astronomers (e.g.[211]) to doubt the reality of the detection.

Although it has not re-appeared in quite the initial style, the spot has enjoyed partial confirmation. Since its appearance, several knots of optical emission have been observed[212]. Although these have been more numerous on the opposite side of the supernova, they have been consistent with the axis of symmetry of the spot - though not that of the supernova (E-W). In particular, one confirmed optical knot would be consistent with the position of the spot, were it moving radially from the supernova with a velocity about one third that of the speed of light from the time of the explosion[213,214]. Perhaps this is yet another coincidence, perhaps not. The possible reappearance of 'son of spot' must be treated with caution. For now at least, the nature of the mystery spot remains just that, a mystery.

V.8(ii) Echoes

The initial ultraviolet flash is the source of many ionization features, known as echoes. These appear in two forms; either by the 'light echoes' from the gas and dust illuminated by the supernova radiation, or by radiation from shocks that occur when the supernova's ejecta strike the circumstellar matter.

From the history of the progenitor (§II.2) astronomers expect to be able to distinguish three spherical regions in the environment of Sk -69° 202 (Fig. 26).

Figure 26. Expected Circumstellar environment

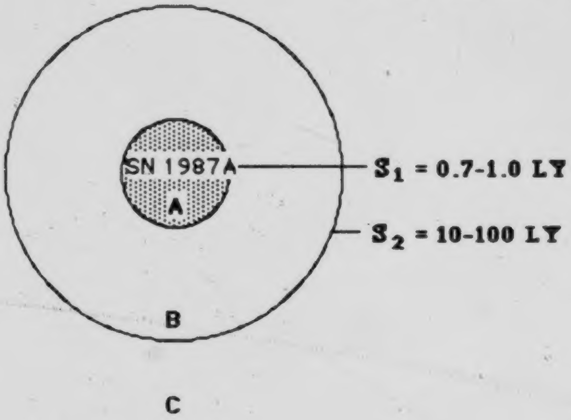

(A) A tenuous inner cavity, evacuated of dust by the fast hot wind from the progenitor in its blue supergiant phase. The radius of this cavity is expected to be given by a shell (s_1) of red supergiant wind swept-up by the blue supergiant wind. This is estimated as 0.7-1.0 light years [§II.2(iii)] and is expected to produce a light echo.

(B) A region of free streaming wind from the red supergiant phase. Its radius will be given by a shell (s_2) of interstellar material and mass loss from the main sequence phases of Sk -69° 202 swept up by the red supergiant wind. This is expected to have a radius of 10-65 light years - depending upon the length of time that Sk -69° 202 spent as a red supergiant (6×10^5-1×10^6 yr) and the velocity of its red supergiant wind (5-20 km/s) - and is also expected to produce an observable light echo.

(C) A region where the interstellar medium is mixed[215] with the mass loss from Sk -69° 202 during its main sequence phases.

When the initial blast wave of fast [~0.1c (§V.1)] moving ejecta gets to shell s_1, in 7-10 yr, it is expected to heat the ambient material to $\sim4\times10^6$ K. The cooling time for this gas is estimated as 20 years, and so the X-ray luminosity is expected to increase as the shock traverses the shell[216]. Although these fireworks are still some time away, there are plenty of light echoes pertaining to regions (B) and (C) to investigate.

The light from the supernova can be scattered by dust grains creating an optical reflection nebula; it can also be absorbed by the grains and re-emitted as thermal infrared radiation. There is strong evidence for scattered echoes at both optical and infrared wavelengths. These appear as rings of emission and as weak diffuse emission - these structures are shown in Fig. 27[217].

As the supernova fades, fainter sources of smaller angular-size should become resolvable. It is hoped that the episodes of mass loss from Sk -69° 202 will become clearly discernible - these are expected to greatly constrain our rather uncertain knowledge of the evolution of the progenitor (§II.2).

Figure 27 The circumstellar environment of SN 1987A in December 1989

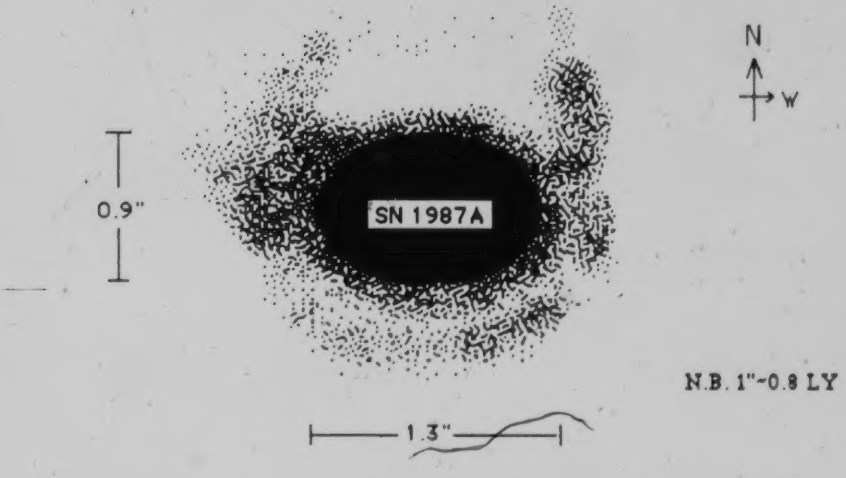

The clearest circumstellar features from SN 1987A have been the outermost light echoes. The evolution of these three circular arcs is shown in table 8. Their circularity implies that the scattering material is distributed in plane sheets[218] nearly normal to, and in front of, the supernova.

Table 8. The evolution of light echoes[219]

	ANGULAR RADII"		
DATE	**INNER**	**MIDDLE**	**OUTER**
16/8/87			32.8
13/2/88		32	52
16/3/88		32.9	55.7
20/3/88		32.8	54
6/10/88	7.94	x	x
12/11/88		43.3	72.5
15/12/88	8.4	x	x
24/1/89	9.5	46	78
5/2/89	8.1	48.4	79-83.4
18/10/89	9	x	x

x-Data not given for this region

The outer two light echoes arise from region (C) and are not thought to be related to Sk -69° 202; rather, they are remnants of the interstellar shells (§V.9) created by previous supernovae in the Large Magellanic Cloud. The inner arc (8".0-9".5) is particularly interesting. This corresponds to a shell of material ~15 light years from SN 1987A; it may have its origin in the deceleration of the pre-supernova red supergiant wind by the surrounding medium (shell S_2 in Fig. 26).

If the spectrum from this echo can be obtained and compared to those of the larger arcs, then it may be possible to differentiate between the scattering from circumstellar grains and that from interstellar grains. Such a comparison should be able to distinguish the origin of this shell. Spectra from the outermost light echo have been obtained. Figure 28 shows the light echo to have a spectrum very similar to that recorded from SN 1987A in September 1987. It is hoped that similar ultraviolet measurements may uncover the spectrum of the initial ultraviolet flash - an epoch that went undetected by astronomers.

Figure 28. The spectrum obtained from the outer light echo in September 1989 compared to spectra of the supernova near maximum light (May 1987)[220].

Figure 28 has been removed because of the unavailability of copyright

From: Sonneborn R, Fransson B, Stathakis R, [illegible] [illegible], 51

V.9 THE INTERSTELLAR MEDIUM TOWARDS SN 1987A

SN 1987A outshone all other sources in the Large Magellanic Cloud (LMC) by about 5 magnitudes at ultraviolet wavelengths. This meant that uncertainties in measuring interstellar lines were much smaller than for typical measurements of absorption towards the Large Magellanic Cloud. An excellent series of high dispersion spectra was obtained. The principal result was the discovery of line profiles which suggested a wide variety of ionization conditions.

(a) Clouds with velocity, v~0 km/s were of galactic origin;

(b) Clouds with v=50-150 km/s were located in the galactic halo;

(c) Material at v>150 km/s was associated with the LMC.

(d) A feature with v=294 km/s was consistent [§II.2(ii)] with a shell of material in front of Sk -69° 202.

Measurements[49] demonstrated some 29 discrete clouds along the line of sight to the supernova. So, these observations extended the hypothesis from 21 cm radio survey observations that the LMC gas is contained in 3 overlapping sheets of gas (two of the radio sheets were confirmed)[221].

Although the interstellar absorption spectrum towards SN 1987A appeared similar to those towards other LMC stars, strong lines of highly ionised species (e.g. AlIII, SiIV, and CIV) have been identified[222] which, because of their high velocities, can most likely be attributed to the LMC. There are several possible reasons for this. The original high energy flash [§V.1(i)] of radiation produced a region of increased ionization around SN 1987A. However, the density of this evacuated region [§V.1(i)] is less than that required to satisfy the ionisation flux inferred from the CIV and SiIV lines[222,223]. On the other hand, the supernova may lie deeper in the LMC than other previous stars used for the spectroscopic analysis of the line of sight to the LMC. But the most popular explanation for the high ionisation is that the explosion occurred inside a pre-existing bubble of hot gas generated by previous supernovae events in the region. As the light echoes from more distant gas clouds are received, it should be possible to map the existence of any such bubble.

Another 'first' for SN 1987A, was the detection[224] of forbidden FeX distributed between 205-370 km/s. This implies a blob of very hot gas ~10^6 K. Since no significant variations in its absorption were seen over several months, it seems unlikely that it is associated with SN 1987A. Rather, it is interpreted as arising from the supergiant HII region 30 Doradus - where the combined effects of previous supernovae appear to have produced superbubbles in the interstellar medium[225]

SN 1987A has provided the first possibility to directly measure the lithium abundance of an external galaxy. Lithium 7 is one of the light nuclei produced in the standard hot big bang model of the universe whose primordial abundance has remained controversial. Two entirely different values can be obtained by employing different methods. Very high resolution (S:N~1000) spectrographic measurements[226] from SN 1987A have given a value of $Li/H < 0.8x10^{-10}$ consistent with that derived from observations of dwarfs in the galactic halo[225]. This implies that the abundance $Li/H = 1x10^{-9}$ found in the galactic interstellar medium is due to the enhancement of Lithium as a result of stellar activity and cosmic rays in the local region[227].

This SN 1987A derived abundance is marginally consistent with standard big bang nucleosynthesis and places severe constraints on alternative cosmological models. The resulting baryon to photon ratio is $2\text{-}3x10^{-10}$ which implies that the nucleons fall short by a factor 14-160 to close the universe[227]. Attempts to improve on these present limits of the interstellar medium by repeated observations of the supernova have proved ineffective: since September 1987, the supernova's spectrum has developed sufficient intrinsic structure to make the determination of weak interstellar lines progressively more difficult and subjective.

VI. THE FUTURE?

During the next few years a roster of radioactivities will remain a salient energy source for the light curve of SN 1987A, see Figure 29. By day 1200 the burden of energy generation will have shifted to ^{57}Co [§V.6(iii)] and then after about day 1400 to

$${}^{44}\mathrm{Ti} \xrightarrow[\tau_{1/2}=54\ \mathrm{yr}]{} {}^{44}\mathrm{Sc} \xrightarrow[\tau_{1/2}=2.6\ \mathrm{yr}]{} {}^{44}\mathrm{Ca}\,.\ [228] \tag{V.27}$$

The latter decay is accompanied not only by gamma-ray emission, but also by the creation of a positron having an average kinetic energy of 700 keV. Even a small disordered magnetic field could trap the positrons in the ejecta long enough for them to deposit their kinetic energy; thus the decay of ^{44}Ti may power the supernova long after it becomes transparent to gamma-rays. But ^{44}Ti is also interesting because it is synthesized in the deepest region that is thought to have been ejected by the supernova (Fig.19). Therefore, its abundance is most sensitive to matter falling back during and after the explosion [§V.7(i)] - much would be learnt from its detection at any level. If the suggested amount of ^{44}Ti has been ejected ($2\mathrm{x}10^{-4}\ M_{\odot}$), the luminosity of SN 1987A will not decrease below 10^{36} ergs/s for many years.

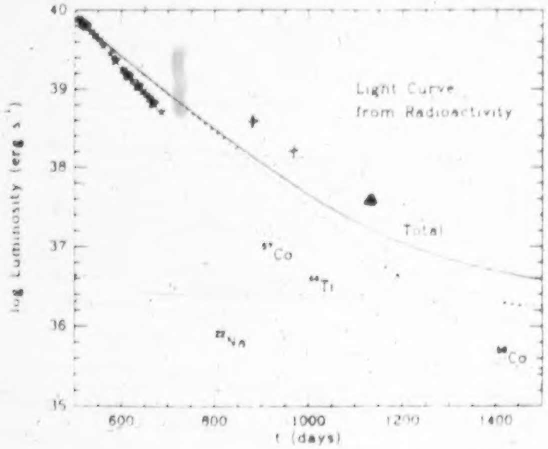

Figure 29. The contribution of long lived radoactivities to the light curve of SN 1987A[189].

If there is a neutron star in the middle of SN 1987A, and there are compelling reasons to believe that there is, then within the next few years it should provide a contribution to the light curve - if it does not at the moment - that will be in excess of that from radioactive decay. In addition to the radiation from accretion and/or particle acceleration, models for the thermal cooling of neutron stars indicate that the surface radiation should remain strong enough 1-3x10^{35} ergs/s [199] to be detected by BBXT, ROSAT (~10^{34} ergs/s), AXAF[~10^{32} ergs/s (1996)], and other future X-ray satellites within the next 100 years. However, as of January 1990, this emission will have decreased (~4x10^{35} ergs/s) significantly below the detection limit of Ginga (3x10^{36} ergs/s). Observation of these X-ray lines, strongly redshifted in the gravitational field of the star, would place constraints upon the equation of state of neutronic matter. This shift is given by $\Delta\lambda \sim -GM\lambda/Rc^2$, where R and M are the respective radius and mass of the neutron star[229].

What will be the future development of the spectrum from SN 1987A? As its luminosity continues to decrease, the interior will certainly become cooler and more neutral and several molecular species, such as H_2, OH, and H_2O are expected to appear. A time will come when the heating from the interior will drop below the saturated high temperature cooling produced by fine structure lines. When this happens, an "infrared catastrophe" is expected[230]: the interior temperature will drop to T<100 K and much of the luminosity will appear as infrared emission lines rather than optical radiation. SN 1987A will become highly unusual - a cold molecular cloud illuminated from within by radioactivity and probably, by a compact X-ray source.

With regard to nucleosynthesis, detailed comparisons of synthetic and observed spectra will, for the first time, allow an accurate determination of the elemental abundances ejected from a supernova. This will certainly increase the understanding of how galaxies become enriched with heavy elements.

SN 1987A has given astronomers the chance to add supernovae to the calibration of the extragalactic distance ladder [§V.1(i)]. Atmospheric models (e.g.[149]) for the spectrum of SN 1987A may in future be combined with observations of other type II supernovae to yield distances with errors of less than 10%. This error is small by extragalactic standards. One of the principal tasks ahead will be to improve the distance estimates to other type II's for which good observations are available. Since type II supernovae are ~10000 times brighter than Cepheids, the method can easily be extended to more distant galaxies. Supernovae may become a fundamental component of the extragalactic distance scale.

Because of its proximity, observations of SN 1987A will be possible at all wavelengths for decades to come. Direct measurements of the decay of radioactive elements, the birth of a pulsar, the circumstellar medium left by Sk -69° 202, and the dynamic evolution of a young supernova remnant all beckon.

REFERENCES

---

[1] Pannekoek, A., 1961, *A history of astronomy*, London, Allen and Unwin.

[2] *Time*, 1987, March 23.

[3] Branch, D., 1987, *Ap. J.*, 320, L25.

[4] Number 202 in the declination band -69° of the astronomer, Nicholas Sanduleak, who first catalogued it.

[5] Hillebrandt, W., Hofflich, P., 1988, *Reports on Progress in Physics*, 52, 11, 1421.

[6] White, G.L., Malin, D., 1988, *Proc. of E.S.O Workshop on SN 1987A*, ed. Danziger, I.J.,11.

[7] Woosley, S.E., 1988, *Proc. of 14th Texas Symposium on Relativistic Astrophysics*, in press.

[8] Woosley, S.E., Weaver, T.A., 1986, *Ann. Rev. Astron.*, 24, 205.

[9] Lucke, P.B., Hodge, P., 1970, *Astron. Astrophys.*, 182, L31.

[10] This scenario has been compiled primarily from[11,14,24].

[11] Bethe, H.A., Brown, G., 1985, *Sci. Am.*, 252, 60.

[12] Adapted from Woolsey, S.E., 1988, *Ap. J.*, 330, 218.

[13] Arnett, D., 1989, *Ap. J.*, 343, 834.

[14] Woosley, S.E., Phillips, M.M., 1988, *Science*, 240, 750.

[15] Bowers, R., Deeming, T., 1984, *Astrophysics I*, Jones and Bartlett, 236.

[16] Compiled using[12,24].

[17] Above $5\text{x}10^9$ K processes are simplified becuase strong and electromagnetic interactions reach equilibrium. Therefore only weak interactions and, of course, gravity need to be considered.

[18] Cooperstein, J., 1988, *Physics Reports*, 163, 1-3, 99.

[19] Bethe, H.A., Brown, G.E., Appelgate, J., Lattimer, J.M., 1979, *Nuc. Phys.*, A324, 487.

[20] Chandrasekhar, S., 1939, *An Introduction to the Study of Stellar Structure*, University of Chicago Press, Chicago, Illinois.

[21] Imshennik, V.S., Nadezhin, D.K., 1979, *Ann. Rev. in Space Physics*, 39, 75.

[22] Bruenn, S. W., 1987, *Ast. & Space Sci*, 143, 15.

---

[23] Baron, E., Cooperstein, J., Kahanna. S., 1985, *Nuc. Phys.*, A440, 744.

[24] Hillebrandt, W., Hoflich, P., 1989, *Astronomy, Cosmology and Fundamental Physics*, ed. Caffo, Kluwer Academic, 331.

[25] Bethe, H., 1988, *Ann. Rev. Nuc.and Part. Sci.*, 38, 15

[26] Brown, G.E., Bethe, H.A., Baym, G., 1982, A375, *Nuc. Phys.*, 481.

[27] Castella, A., 1987, *Proc. of E.S.O Workshop on SN 1987A*, ed. Danziger, I.J., 101.

[28] Panagia, N., 1987, *Proc. of E.S.O Workshop on SN 1987A*, ed. Danziger, I.J., 55.

[29] Fransson, C., Casstella, A., Gilmozzi, R., Kirshner, R.P., Pangia, N., *Ap. J.*, 1989, 336, 429.

[30] For neighbouring LMC blue supergiant stars N/O=0.55 and N/C=0.31 (uncertainties of a factor of 2-3) relative to solar values (Truran, J.W., Weiss, A.,1990, *Comm. Astrophys.*,14, 4, 195).

[31] D'Odorico, S., Baade, D., 1989, *The Messenger*, 56, 36.

[32] Kudritzki, R.P., Pauldrach, A., Puls, J., 1986, *Astron. Astrophys.*, 298.

[33] Gouiffes, G., Wampler, E.J., Baade, D., Wang, L.F., 1989, *The Messenger*, 58, 12.

[34] Gaskell, C.M, Keel, W.C., 1987, *SN 1987A in the Large Magellanic Cloud*, ed. Kafatos, M., Michalitsianos, A., 13.

[35] Filippenko, A.V., 1990, *IAUC.*, 5003.

[36] Saio, H., Nomoto, K., 1988, *Ap. J.*, 334, 388.

[37] Langer, N., El Eid, M.F., Baraffe, I., 1989, *Astron. Astrophys.*, 224, L17.

[38] A star devoid of its hydrogen envelope that emits principally in the ultraviolet[42].

[39] Humphreys, R.M., 1984, *in Proc. I.A.U. Symp. No. 105*, ed. Maeder, A., Renzini, Reidel, 279.

[40] Barkat, Z., Wheeler, J.C., 1988, *Ap. J.*, 332, 247.

[41] Tuchman, Y., Wheeler, J.C., 1989, *Ap. J.*, 344, 835.

[42] Arnett, W.D., Bahcall, J.N., Kirshner, R.P., Woosley, S.E., 1989. *Ann. Rev. Astron. Astrophys.*, 27, 639.

[43] The emitting mass of the observations in §II.2 is in the range 0.05-0.1 $M_\odot$ [29].

[44] Shigeyama, T., Nomoto, K., 1989, submitted to *Ap. J.* (October 1989).

---

[45] Dufour, R.J., Shields, G.A., Talbot, R.J., 1982, *Ap. J.*, 252, 461.

[46] If electron scattering is taken to be dominant then the opacity,

$\kappa \sim 0.4Z/A$, where Z is the average degree of ionization and A, the average atomic weight (Axelrod, T.S., 1987, *Proc. of the 108th I.A.U.-Colloquim*, ed. Nomoto, K., Springer-Verlag, 375).

[47] Moffat, A.F.J., Niemela, V.S., Phillips, M.M., Chu, Y., Seggewiss, W., 1987, *Ap. J.*, 312, 612.

[48] Humphreys, R.M., McElroy, D.B., 1988, *Ap. J.*, 284, 565.

[49] Dopita, M.A., 1988, *Space Sci. Rev.*, 46, 225.

[50] Wilson, J.R., Mayle, R.W., 1988, *Physics Reports*, 163, Nos.1-3, 63.

[51] Weiss, A., 1989, *Ap. J.*, 339, 365.

[52] Lattimer, J.M., 1988, *Nuclear Physics*, A478, 221c.

[53] McCray, R., Li, W.H.,1987, *Proc. of Yellow Mountain Summer School on the Structure and Evolution of Galaxies*, ed. Fang, L.Z., World Sci., 8.

[54] van den Bergh, S., 1988, Paper presented at the *White Research Conference on SN 1987A* (Canberra, Australia).

[55] From[56].

[56] Hillebrandt, W., 1988, *Neutrinos*, ed. Klapdor, H.V., Springer Verlag, Berlin Heidelberg, 287.

[57] Adapted from[106].

[58] The polytropic index is reduced by 0.01 to 0.06 - dependent on the neutrino transport employed[7].

[59] Bowers, R., Deeming, T., 1984, *Astrophysics I*, Jones and Bartlett, 278.

[60] Adapted from Lamb, D.Q., Lattimer, J.M., Pethnick, C.J., Ravenhall, D.G., 1978, *Phys. Rev. Lett.*, 41, 1623.

[61] Bruenn, S.W., 1989, *Ap. J.*, 341, 385.

[62] Goldreich, P., Weber, S., *Ap. J.*,1980, 238, 991.

[63] Perhaps more physically, the initial shock wave represents the gravitational binding energy of the homologous core after it comes to rest (as corrected for the energy stored in the excited states of nuclei that have not yet undergone neutronisation).

---

[64] Adapted from [56].

[65] Aufdereide, M., Bethe, H.A., Brown, G.E., Weaver, T.A., Woosley, S.E., 1990, submitted to *Ap. J.*.

[66] Hillebrandt, W., Nomoto, K, Wolff, R.G., 1984, *Astron. Astrophys.*, 133, 175.

[67] Ray, A., Kar, K., 1989, *Phys. Rev. Lett.*, 63, 22., 2435.

[68] Shapiro, S.L., Teukolsky, S., 1983, *Black Holes, White Dwarfs, and Neutron Stars*, John Wiley and sons, 311.

[69] Analogous to the ultraviolet flash exhibited by SN 1987A when the shock hit the photosphere [§V.1(i)].

[70] Mayle, R., Wilson, J.R., Schrammn, D.N., 1987, *Ap. J.*, 318, 288.

[71] Where E $\bar{\nu}_e$ is the average energy of the neutrinosphere. Accounting for the energy dependence of the weak interaction cross section, the Fermi-Dirac distribution function gives the average energy of electron antineutrinos as, E $\bar{\nu}_e$=3.15T $\bar{\nu}_e$, where T $\bar{\nu}_e$ is the effective temperature of the neutrinosphere (in MeV) [52].

[72] Colgate, S., 1989, *Nature*, 341, 489. refers to Wilson, J.M., 1989, *The Nuclear Equation of State*, Springer, Berlin, in press.

[73] Microconvection describes the limit where most convective blobs have a size much smaller than the entire region of instability. Numerical studies show this to dominate over its counterpart, ie. macro-convection[50].

[74] Fukugita, M., 1989, Preprint RIFP-824 (summary talk for *International Workshop in Weak Interactions and Neutrinos*, Ginosar, The Sea of Galilee, Israel, 9-14 April 1989).

[75] Lasker, B.M., 1980, *Ap. J.*, 237, 765.

[76] Bodenheimer, P., Woosley, S.E., 1983, *Ap. J.*, 269, 281.

[77] Hillebrandt, W., Hoflich, P., Janka, H.T., 1989, *Astronomy, Cosmology and Fundamental Physics*, Kluwer Academic Publishers, 327.

[78] Bethe, H.A., Pizzochero, P., 1990, *Ap. J.*, 350, L33.

[79] Krunkel, W., Madore, B., Bateson, F.M., McNaught, R.H., 1987, *IAUC.*, 4316.

[80] Alexeyev, E.N., Alexseeva, L., Volchenko, V.I., Krivosheina, I.V., 1987, *JETP. Lett.*, 45, 589.

---

[81] Bionta, R.M., (and 37 coauthors), 1987, *Phys. Rev. Lett.*, 58, 1494.

[82] Hirata, K., (and 23 coauthors), 1987, *Phys.Rev.Lett.*, 58, 1490.

[83] Aglietta, M., (and 19 coauthors), 1987, *Europhys. Lett.*, 3, 1315.

[84] Fireman, E.L., 1989, *Ap. J.*, 349, 241.

[85] From [86, 83, 81, 82, 83] and references in §B.5.

[86] Dadykin, V.L., Zatwespin, G.T., Ryazhskaya, O.G., 1989, *Sov. Phys. Usp.*, 32, 5, 459.

[87] Krivoruchenko, M.I., 1989, *Z. Phys. C - Particles and Fields*, 44, 633.

[88] Same refs. as[85].

[89] Aglietta, M., (and 19 coauthors), 1987, *SN 1987A in the Large Magellanic Cloud*, ed. Kafatos, M., Michalitsianos, A., 207.

[90] Aglietta, M., (and 19 coauthors), 1987, *Europhys. Lett.* , 12, 1321.

[91] Alexeyev, E.N., 1987, *Proc. of E.S.O Workshop on SN 1987A*, ed. Danziger, I.J., 237.

[92] Armaldi, E., (and 13 coauthors), 1987, *Europhys. Lett.*, 3, 1325.

[93] Aglietta, M., (and 19 coauthors), *The Standard Model Supernova*, Editions Frontieres, 717.

[94] Neutrino radiation damps out most of the non-sphericity in the core (Shapiro, S.L., 1978, in *Gravitational Radiation*, ed Smarr, L., Oxford University press, 355).

[95] Laboratory searches will have to await new 'difficult' experiments (van der Velde, 1988, *Phys. Rev. D*, 39, 6, 1492).

[96] LoSecco, J.M., *Phys. Rev. D*, 39, 4, 1013.

[97] Unfortunately, the Homestake mine experiment's sensitivity cannot put a useful limit on this hypothesis[85].

[98] Schramm, D.N., 1989, *FERMILAB-Conf-89/27-A*.

[99] Giovanoni, P.M., Ellison, D.C., Bruenn, S.W., 1989, *Ap. J.*, 342, 416.

[100] Hirata, K.S., (and 23 coauthors), 1988, *Phys. Rev. D*, 38, 2, 448.

[101] Lattimer, J.M., Yahil, A., 1989, *Ap. J.*, 340, 426.

[102] Nakamura, T., Fukugita, M., 1989, *Ap. J.*, 337, 466.

---

[103] Janka, H-T., Hillebrandt, W., 1989, *Astron. Astrophys.*, 224, 49.

[104] Schramm, D.N., 1987, *Comments in Nuc. Part. Phys.*, 17, 5, 239.

[105] Lattimer, J.M., Yahil, A., 1987, *SN 1987A in the Large Magellanic Cloud*, ed. Kafatos, M., Michalitsianos, 209.

[106] From Arnett, W.D., Bowers, R.L., 1977, *Ap. J. Suppl.*, 33, 415.

[107] Kahanna, S., 1989, *Ann. Rev. Nuc. Part. Sci.*, 39, 243.

[108] Wolfstein, L., Beier, E.W., 1989, *Physics Today*, July, 28.

[109] Guo-Chen, Y., Hong, L., 1988, *Nuovo Cimento*, 102 B, No.5, 485.

[110] Berezinsky, V.S., Castagnoli, C., Dokuchaev, V.I., Galeotti, P., 1988, *Nuovo Cimento*, 11C, 3, 287.

[111] Tomozawa, Y., 1989, Prepint *RIFP-810* (May 1989).

[112] Haubold, H.J., Kaempfer, B., Senatorov, A.V., Voskresenski, D.N., 1988, *Astron. Astrophys.*, L22.

[113] Gertsenshtein, M.E., 1989, *Nuovo Cimento*, 12C, 6, 835.

[114] Burrows, A., 1987, *Proc. of E.S.O Workshop on SN 1987A*, ed. Danziger, I.J., 322.

[115] Dar, A., 1987, *SN 1987A in the Large Magellanic Cloud*, ed. Kafatos, M., Michalitsianos, A., 220.

[116] Fritschi, M., (and 5 coauthors), 1988, *Nucl. Phys. A.*, 478, 425.

[116] Burrows, A., 1988, *Ap. J.*, 328, L51.

[117] Barrow, J.D., Dombey, N., 1989, *New Scientist*, 28th October, 30.

[118] Spergel, D.N., Bachall, J.N., 1988, *Phys. Lett. B*, 200, 366.

[119] Bachall, J.N., 1987, *Phys Rev. Lett.*, 59, 1864.

[120] From the detectors on board the Solar Maximum Misssion and the Pioneer Venus Orbiter.

[121] Although if electron antineutrinos and electron neutrinos are unstable but admixed sufficiently with other neutrinos that are stable, then they could have generated the observed neutrino signals. However, this is not testable (Soares, J.M., Wolfstein, L., 1989, *Phys. Rev. D*, 40, 11, 3666.

[122] Okun, L.B., 1986, Preprint *TAUP*, 1543.

[123] Blinnikov, S.I., Okun, L.B., 1988, *Sov. Astron. Lett.*, 14, 5, 368.

[124] Barbiellini, G., Cocconi, G., 1987, *Nature*, 329, 21.

---

[125] Bernstein, J., Rudman, M., 1963, *Phys. Rev.*, 132, 1227.

[126] The distribution of total neutrino energy into the different flavours uses a theoretical estimate, which is uncertain by as much as 50%[74].

[127] Kolb, E.W., Schramm, D.S., Turner, M.S., 1989, *FERMILAB*-Pub-89/97-A.

[128] Lang, K.R., 1980, *Astrophysical Formulae*, Springer-Verlag, preface.

[129] Brecher, K., Yun, J.L., 1989, 173rd *AAS. Meeting*, 15.08.

[130] Known as the Shapiro delay.

[131] Krauss, L.M., Tremaine, S., 1988, *Phys. Rev. Lett.*, 60, 176.

[132] Longo, M.J., 1988, *Phys. Rev. Lett.*, 60, 3, 173.

[133] Turner, M.S., 1989, *Fermi lab-conf*-89/104-a.

[134] Aharonov, Y., Avignone, F.T., Nussinov, S., 1989, *Phys. Rev. D*, 39, 3, 985.

[135] Grifols, J.A., Masso, E., 1990, *Nuc. Phys.*, B331, 244.

[136] Adapted from; Burrows, A., 1989, *Weak and Electromagnetic Interactions in Nuclei*, in press.

[137] Koshiba, M., 1989, *Astronomy, Cosmology and Fundamental Physics*, ed. Caffo, M., Kluwer Academic Publishers, 317.

[138] Fang, Li-Zhi, Huang, J., 1990, *FERMILAB*-Pub-90/24/A.

[139] Jones, A., 1987, *IAUC.*, 4340.

[140] Garrison, R., Shelton, I., 1987, *IAUC.*, 4330.

[141] They account for the expected power law density structure of the envelope and the variations in density as the shock wave passes through the various layers and that once the optical depth drops below 3 in the hydrogen envelope, photons emitted by the shock can diffuse to the surface before the shocked matter (Arnett, W.D., 1988, *Ap. J.*, 331, 337.).

[142] Warner, B., 1987, *IAUC.*, 4316.

[143] Madore, B., 1987, *IAUC.*, 4317.

[144] The physical analogy for this effect is a whip-lash, in which the disturbance moves more and more rapidly down the whip (becoming thinner) until it becomes supersonic - it cracks!

---

[145] Fransson, C., Lunquist, P., 1990, *Astron. Astrophys.*, in press.

[146] Castella, A., (and 6 coauthors), 1987, *Astron. Astrophys.*, 177, L29.

[147] Storey, M.C., Manchester, R.N., 1987, *Nature*, 330, 327.

[148] Blanco, V.M., (and 11 coauthors), 1987, *Ap. J.*, 320, 589.

[149] Eastman, R.G., Kirshner, R.P., 1989, *Ap. J.*, 347, 771.

[150] Chilukuri, M., Wagoner, R.V., 1987, *Proc. of the 108th I.A.U.-Colloquim*, ed. Nomoto, K., Springer-Verlag, 295.

[151] Hofflich, P., 1987, *Proc. of the 108th I.A.U.-Colloquim*, ed. Nomoto, K., Springer-Verlag, 388.

[152] Adapted from[12].

[153] Since double ionization of He only occurs for very high temperatures corresponding to the very early phases of the supernova only its first ionization potential is used.

[154] The spectrum of SN 1990H has exhibited a spectrum (Perlmutter, S., (and 5 collaborators) , 1990, *IAUC* , 4992.) and a light curve (Filippenko, A.V., 1990, *IAUC*., 5003.) very similar to SN 1987A.

[155] Young, T.R., Branch, D., 1989, *Ap. J.*, 342, L79.

[156] van den Bergh, S., McClure, R.D., *Ap. J. Lett.*, submitted.

[157] Adapted from[12].

[158] The numbers in parentheses correspond to percentage of decays in which a gamma-ray of a particular energy is given off[159].

[159] Thielemann, F-K., Hasimoto, M., Nomoto, K., 1989, *Ap. J.*, 349, 222.

[160] Sunyaev, R., (and 33 coauthors), 1987, *Nature*, 330, 227.

[161] Dotanl, T., (and 36 coauthors), 1987, *Nature*, 330, 230.

[162] Matz, S.M., (and 7 coauthors), 1988, *Nature*, 331, 416.

[163] Rank, D.M., (and 6 coauthors), 1988, *Nature*, 331, 505.

[164] Witteborn, F., (and 14 coauthors), 1988, Preprint, submitted to *Ap. J.*.

[165] Benz, W., Thielemann, F-K., 1990 , *Ap. J.*, 348, L20.

[166] Nagasawa, M., Nakumura, T., Miyama, S., 1988, *Pub. Ast. Soc. Japan.*, 40, 691.

---

[167] Chevalier, R.A., 1989, *Ap. J.*, 346, 847.

[168] For the highest possible rotation rate (Janka, H-T., Monchmeter, R., 1988, *Astron. Astrophys.*, 209, L5).

[169] Rester, A.C., (and 6 coauthors), 1989, *Ap. J.*, 342, L71.

[170] Arnett, D., Fryxell, B., Muller, E., 1989, *Ap. J.*, 342, L63.

[171] Ebisuzaki, T., Shegeyama, T., Nomoto, K., 1989, *Ap. J.*, 344, L65.

[172] From[170]

[173] Whitelock, P.A., (and 21 coauthors), 1988, *MNRAS.*, 234, 5P.

[174] Arnett, D., Fryxell, B., Muller, E., 1989, *Ap. J.*, 341, L63.

[175] Adapted from[7].

[176] Adapted from[159].

[177] Adapted from[7].

[178] Clayton, D.D., 1982, *Quart J.R.A.S.*, 23, 174.

[179] Kozasa, T., Hasegawa, H., Nomoto, K., 1989, *Ap. J.*, 344, 325.

[180] Danziger, I.J., Lucy, L.B., Bouchet, P., Gouiffres, C., 1989, *ESO*. Preprint, 680.

[181] Adapted from[180].

[182] see[180].

[183] Moseley, S.H., (and 5 coauthors), 1989, *Nature*, 340, 697.

[184] Bouchet, P., 1990, *Messenger*, 59, 39.

[185] Kumagai, S., (and 6 coauthors), 1989, *Ap. J.*, 345, 412.

[186] Adapted from The, L-S., Burrows, A., Bussard, R., 1990, *Ap. J.*, 352, 731.

[187] Details of these models can be found in[186].

[188] From Tueller, J., (and 6 coauthors), 1990, *Ap. J.*, 351, L41.

[189] Adapted from[217,201].

[190] Thielheim, K.O., 1989, *Fund. Cosmic Phys.*, 13, 357.

[191] Kassim, N.E., Weiler, K.W., 1990, *Nature*, 343, 146.

---

[192] Middleditch, J., (and 13 collaborators), 1989, *IAUC.*, 4735.

[193] Middleditch, J., 1990, *AAS. Meeting* (February 24).

[194] Middleditch, J., 1989, *Computers in Physics*, Jul / Aug, 14.

[195] Shapiro, S.L., Teukolsky, S.A., 1983, *Black Holes, White Dwarfs, and Neutron Stars*, John Wiley & Sons, 382.

[196] Connors, M., 1979, *Pulsars and Aligned Rotators* (University of Alberta Thesis), 4-11.

[197] Bowers, R., Deeming, T., 1984, *Astrophysics I*, Jones and Bartlett, 311. The actual mechanism by which pulsars convert the rotational energy of a neutron star into the observed pulses is poorly understood. This model is merely the most compelling of the current theories.

[198] Shapiro, S.L., Teukolsky, S.A., 1983, *Black Holes, White Dwarfs, and Neutron Stars*, John Wiley & Sons, 280.

[199] Tsurata, S., Nomoto, K., 1988, *Astro. Lett. and Commun.*, 27, 241.

[200] Burrows, D.N., Nonsek, J.A., Berthiaume, G.D., Garmire, G.P., 1989, *Ap. J.*, 347, 1114.

[201] Woosley, S.E., Pinto, P.A., Hartmann, D., 1989, *Ap. J.*, 346, 395.

[202] Wang, Q., Chen, T.T., Hamilton, M., Ruderman, K., Shaham, J., 1989, *Nature*, 338, 319.

[203] Witten, E., 1984, *Phys. Rev.*, 30, 2, 272.

[204] Friemann, J.A., Olinto, A.V., *FERMILAB*-Pub-89/129-A.

[205] Benvenuto, O.G., Horvath, J.E., 1989, *Phys. Rev.*, 63, 7, 716.

[206] Friemann, J.A., Olinto, A.V., *FERMILAB*-Pub-89/129-A.

[207] Anglo-Australian Observatory (Mielke, W.P.S., Marcher, S.J., Morgan B.L., 1987, *IAUC* , 4391 and 4394; and by the same authors, 1987, *Nature*, 329, 608) and the Cerro Tololo Interamerican Observatory (Nisenson, P., Karvoska, M., Miyama, S., 1988, *IAUC* , 4382).

[208] This is the minimum separation of the object from the supernova: it is not known where along the line of sight the reflector lies.

[209] Felton, J.E., Dwek, E., Valdrovandi, S.M., 1989, *Ap. J.*, 340, 943.

[210] Rees, M.J., 1987, *Nature*, 207.

---

[211] Wood, P.R., (and 5 coauthors), 1989, *Ap. J.*, 339, 1073.

[212] Suntzeff, N.B., 1988, *Nature*, 334, 135.

[213] Wood, P.R., Faulkner, D.J., 1989, *IAUC.*, 4739.

[214] Karovska, M., Nisenson, P., Papaliolios, C., Standley, C., Heathcote, S., 1989, *IAUC.*, 4752.

[215] Sk -69° 202 left the main sequence $\sim 10^6$ years ago and so any shell structure that this phase produced is expected to have been dispersed.

[216] Chevalier, R.A., Liang, E.P., 1989, *Ap. J.*, 344, 322.

[217] This figure was constructed using D'Odorico, S., Tarenghi, M., 1990, *Messenger*, 59, 39 and Crotts, A., Krunkel, W., 1990, *IAUC*, 4948.

[218] These sheets must have a large radius of curvature; the most plausible origin would seem to be blast waves from previous supernovae having swept up interstellar material.

[219] Measurements 16/8/87-20/11/88, Deal, A., Hutsmekes, D., Remy, M., Surdej, J., Van Drow, E., 1990, *Astron. Astrophys.*, 229, 427. Then in order of occurrence, Crotts, A., Krunkel, W., 1989, IAUC, 4741; Bond, H.E., Pangia, N., Gilmozzi, R., Meakes, M., 1989, *IAUC*, 4733; Wood, P.R., Faulkner, D.J., 1989, *IAUC*, 4739; Crotts, A., Krunkel, W., 1990, *IAUC*, 4948.

[220] Cannon, R., Dickens, B., Stathakis, R., 1989, *AAO. Newsletter*, 51.

[221] Molaro, P., Vladilo, G., Avila, G., D'Odorico, S., 1989, *Ap. J.*, 339, L63.

[222] Dupree, A.K., (and 5 coauthors), 1987, *Ap. J.*, 320, 597.

[223] Savage, B.D., Jenkins, E.B., Joseph, C.L., Boer, K.S., 1989, *Ap. J.*, 345, 393.

[224] Wang, Q., Hamilton, T., Hefland, D.J., 1989, *Nature*, 341, 309.

[225] Pettini, M., Stathakis, R., D'Odorico, S., Molaro, P., Vladilo, G., Prepint *AAO*.

[226] Sahu, K.C., Sahu, M., Pottasch, S.R., 1988, *Astron. Astrophys.*, 207, L1.

[227] Hogan, C., 1989, *Nature*, 339, 15.

228 These decays should be recognised by the characteristic gamma-ray lines they emit which are expected ($\sim 1\text{x}10^{-4}$) photons cm^{-2} s^{-1} to be within the detection limit, ~2x10-5 photons cm^{-2} s^{-1}, of the new Gamma-Ray Observatory (GRO)[185].

---

[229] Lang, K.R., 1980, *Astrophysical Formulae*, Springer-Verlag, 194.

[230] Colgan, S.W.J., Hollenbach, D.J., 1988, *Ap. J.*, 329, L25.

[231] Lang, K.R., 1980, *Astrophysical Formulae*, Springer-Verlag, 512.

[232] Lang, K.R., 1980, *Astrophysical Formulae*, Springer-Verlag, 84.

[233] From Alexeyev, E.N., 1988, *The Standard Model Supernova* , Editions Frontieres, 739.

BIBLIOGRAPHY

Aglietta, M., (and 19 coauthors), 1987, *Europhys. Lett.* , 12, 1321.

Aglietta, M., (and 19 coauthors), 1987, *Europhys. Lett.*, 3, 1315.

Aglietta, M., (and 19 coauthors), 1987, *SN 1987A in the Large Magellanic Cloud*, ed. Kafatos, M., Michalitsianos, A., 207.

Aglietta, M., (and 19 coauthors), *The Standard Model Supernova*, Editions Frontieres, 717.

Aharonov, Y., Avignone, F.T., Nussinov, S., 1989, *Phys. Rev. D*, 39, 3, 985.

Alexeyev, E.N., 1987, *Proc. of E.S.O Workshop on SN 1987A*, ed. Danziger, I.J., 237.

Alexeyev, E.N., Alexseeva, L., Volchenko, V.I., Krivosheina, I.V., 1987, *JETP. Lett.*, 45, 589.

Armaldi, E., (and 13 coauthors), 1987, *Europhys. Lett.*, 3, 1325.

Arnett, W.D., 1988, *Ap. J.*, 331, 337.

Arnett, W.D., 1989, *Ap. J.*, 343, 834.

Arnett, W.D., Bahcall, J.N., Kirshner, R.P., Woosley, S.E., 1989. *Ann. Rev. Astron. Astrophys.*, 27, 639.

Arnett, W.D., Bowers, R.L., 1977, *Ap. J. Suppl.*, 33, 415.

Arnett, W.D., Fryxell, B., Muller, E., 1989, *Ap. J.*, 342, L63.

Aufdereide, M., Bethe, H.A., Brown, G.E., Weaver, T.A., Woosley, S.E., 1990, submitted to *Ap. J.*.

Axelrod, T.S., 1987, *Proc. of the 108th I.A.U.-Colloquim*, ed. Nomoto, K., Springer-Verlag, 375.

Bachall, J.N., 1987, *Phys Rev. Lett.*, 59, 1864.

Barbiellini, G., Cocconi, G., 1987, *Nature*, 329, 21.

Barkat, Z., Wheeler, J.C., 1988, *Ap. J.*, 332, 247.

Baron, E., Cooperstein, J., Kahanna, S., 1985, *Nuc. Phys.*, A440, 744.

Barrow, J.D., Dombey, N., 1989, *New Scientist*, 28th October, 30.

Benvenuto, O.G., Horvath, J.E., 1989, *Phys. Rev.*, 63, 7, 716.

Benz, W., Thielemann, F-K., 1990 , *Ap. J.*, 348, L20.

Berezinsky, V.S., Castagnoli, C., Dokuchaev, V.I., Galeotti, P., 1988, *Nuovo Cimento*, 11C, 3, 287.

Bernstein, J., Rudman, M., 1963, *Phys. Rev.*, 132, 1227.

Bethe, H.A., 1988, *Ann. Rev. Nuc.and Part. Sci.*, 38, 15.

Bethe, H.A., Brown, G., 1985, *Sci. Am.*, 252, 60.

Bethe, H.A., Brown, G.E., Appelgate, J., Lattimer, J.M., 1979, *Nuc. Phys.*, A324, 487.

Bethe, H.A., Pizzochero, P., 1990, *Ap. J.*, 350, L33.

Bionta, R.M., (and 37 coauthors), 1987, *Phys. Rev. Lett.*, 58, 1494.

Blanco, V.M., (and 11 coauthors), 1987, *Ap. J.*, 320, 589.

Blinnikov, S.I., Okun, L.B., 1988, *Sov. Astron. Lett.*, 14, 5, 368.

Bodenheimer, P., Woosley, S.E., 1983, *Ap. J.*, 269, 281.

Bond, H.E., Pangia, N., Gilmozzi, R., Meakes, M., 1989, *IAUC*, 4733.

Bouchet, P., 1990, *Messenger*, 59, 39.

Bowers, R., Deeming, T., 1984, *Astrophysics I*, Jones and Bartlett.

Branch, D., 1987, *Ap. J.*, 320, L25.

Brecher, K., Yun, J.L., 1989, 173rd *AAS. Meeting*, 15.08.

Brown, G.E., Bethe, H.A., Baym, G., 1982, A375, *Nuc. Phys.*, 481.

Bruenn, S. W., 1987, *Ast. & Space Sci*, 143, 15.

Bruenn, S.W., 1989, *Ap. J.*, 341, 385.

Burrows, A., 1987, *Proc. of E.S.O Workshop on SN 1987A*, ed. Danziger, I.J., 322.

Burrows, A., 1988, *Ap. J.*, 328, L51.

Burrows, A., 1989, *Weak and Electromagnetic Interactions in Nuclei*, in press.

Burrows, D.N., Nonsek, J.A., Berthiaume, G.D., Garmire, G.P., 1989, *Ap. J.*, 347, 1114.

Cannon, R., Dickens, B., Stathakis, R., 1989, *AAO. Newsletter*, 51.

Castella, A., (and 6 coauthors), 1987, *Astron. Astrophys.*, 177, L29.

Castella, A., 1987, *Proc. of E.S.O Workshop on SN 1987A*, ed. Danziger, I.J., 101.

Chandrasekhar, S., 1939, *An Introduction to the Study of Stellar Structure*, University of Chicago Press, Chicago, Illinois.

Chevalier, R.A., 1989, *Ap. J.*, 346, 847.

Chevalier, R.A., Liang, E.P., 1989, *Ap. J.*, 344, 322.

Chilukuri, M., Wagoner, R.V., 1987, *Proc. of the* 108^{th} *I.A.U.-Colloquim*, ed. Nomoto, K., Springer-Verlag, 295.

Clayton, D.D., 1982, *Quart J.R.A.S.*, 23, 174.

Colgan, S.W.J., Hollenbach, D.J., 1988, *Ap. J.*, 329, L25.

Colgate, S., 1989, *Nature*, 341, 489. refers to Wilson, J.M., 1989, *The Nuclear Equation of State*, Springer, Berlin, in press.

Connors, M., 1979, *Pulsars and Aligned Rotators* (University of Alberta Thesis), 4-11.

Cooperstein, J., 1988, *Physics Reports*, 163, 1-3, 99.

Crotts, A., Krunkel, W., 1989, IAUC, 4741.

Crotts, A., Krunkel, W., 1990, *IAUC*, 4948.

D'Odorico, S., Baade, D., 1989, *The Messenger*, 56, 36.

D'Odorico, S., Tarenghi, M., 1990, *Messenger*, 59, 39

Dadykin, V.L., Zatwespin, G.T., Ryazhskaya, O.G., 1989, *Sov. Phys. Usp.*, 32, 5, 459.

Danziger, I.J., Lucy, L.B., Bouchet, P., Gouiffres, C., 1989, *ESO*. Preprint, 680.

Dar, A., 1987, *SN 1987A in the Large Magellanic Cloud*, ed. Kafatos, M., Michalitsianos, A., 220.

Deal, A., Hutsmekes, D., Remy, M., Surdej, J., Van Drow, E., 1990, *Astron. Astrophys.*, 229, 427.

Dopita, M.A., 1988, *Space Sci. Rev.*, 46, 225.

Dotani, T., (and 36 coauthors), 1987, *Nature*, 330, 230.

Dufour, R.J., Shields, G.A., Talbot, R.J., 1982, *Ap. J.*, 252, 461.

Dupree, A.K., (and 5 coauthors), 1987, *Ap. J.*, 320, 597.

Eastman, R.G., Kirshner, R.P., 1989, *Ap. J.*, 347, 771.

Ebisuzaki, T., Shegeyama, T., Nomoto, K., 1989, *Ap. J.*, 344, L65.

Fang, Li-Zhi, Huang, J., 1990, *FERMILAB*-Pub-90/24/A.

Felton, J.E., Dwek, E., Valdrovandi, S.M., 1989, *Ap. J.*, 340, 943.

Filippenko, A.V., 1990, *IAUC*., 5003.

Fireman, E.L., 1989, *Ap. J.*, 349, 241.

Fransson, C., Casstella, A., Gilmozzi, R., Kirshner, R.P., Pangia, N., *Ap. J.*, 1989, 336, 429.

Fransson, C., Lunquist, P., 1990, *Astron. Astrophys.*, in press.

Friemann, J.A., Olinto, A.V., *FERMILAB*-Pub-89/129-A.

Fritschi, M., (and 5 coauthors), 1988, *Nucl. Phys. A.*, 478, 425.

Fukugita, M., 1989, Preprint RIFP-824 (summary talk for *International Workshop in Weak Interactions and Neutrinos*, Ginosar, The Sea of Galilee, Israel, 9-14 April 1989).

Garrison, R., Shelton, I., 1987, *IAUC.*, 4330.

Gaskell, C.M, Keel, W.C., 1987, *SN 1987A in the Large Magellanic Cloud*, ed. Kafatos, M., Michalitsianos, A., 13.

Gertsenshtein, M.E., 1989, *Nuovo Cimento*, 12C, 6, 835.

Giovanoni, P.M., Ellison, D.C., Bruenn, S.W., 1989, *Ap. J.*, 342, 416.

Goldreich, P., Weber, S., *Ap. J.*,1980, 238, 991.

Gouiffes, G., Wampler, E.J., Baade, D., Wang, L.F., 1989, *The Messenger*, 58, 12.

Grifols, J.A., Masso, E., 1990, *Nuc. Phys.*, B331, 244.

Guo-Chen, Y., Hong, L., 1988, *Nuovo Cimento*, 102 B, No.5, 485.

Haubold, H.J., Kaempfer, B., Senatorov, A.V., Voskresenski, D.N., 1988, *Astron. Astrophys.*, L22.

Hillebrandt, W., 1988, *Neutrinos*, ed. Klapdor, H.V., Springer Verlag, Berlin Heidelberg, 287.

Hillebrandt, W., Hofflich, P., 1988, *Reports on Progress in Physics*, 52, 11, 1421.

Hillebrandt, W., Hoflich, P., 1989, *Astronomy, Cosmology and Fundamental Physics*, ed. Caffo, Kluwer Academic, 331.

Hillebrandt, W., Nomoto, K, Wolff, R.G., 1984, *Astron. Astrophys.*, 133, 175.

Hirata, K.S., (and 23 coauthors), 1987, *Phys.Rev.Lett.*, 58, 1490.

Hirata, K.S., (and 23 coauthors), 1988, *Phys. Rev. D*, 38, 2, 448.

Hofflich, P., 1987, *Proc. of the 108th I.A.U.-Colloquim*, ed. Nomoto, K., Springer-Verlag, 388.

Hogan, C., 1989, *Nature*, 339, 15.

Humphreys, R.M., 1984, *in Proc. I.A.U. Symp. No. 105*, ed. Maeder, A., Renzini, Reidel, 279.

Humphreys, R.M., McElroy, D.B., 1988, *Ap. J.*, 284, 565.

Imshennik, V.S., Nadezhin, D.K., 1979, *Ann. Rev. in Space Physics*, 39, 75.

Janka, H-T., Hillebrandt, W., 1989, *Astron. Astrophys.*, 224, 49.

Janka, H-T., Monchmeter, R., 1988, *Astron. Astrophys.*, 209, L5.

Jones, A., 1987, *IAUC.*, 4340.

Kahanna, S., 1989, *Ann. Rev. Nuc. Part. Sci.*, 39, 243.

Karovska, M., Nisenson, P., Papaliolios, C., Standley, C., Heathcote, S., 1989, *IAUC.*, 4752.

Kassim, N.E., Weiler, K.W., 1990, *Nature*, 343, 146.

Kolb, E.W., Schramm, D.S., Turner, M.S., 1989, *FERMILAB*-Pub-89/97-A.

Koshiba, M., 1989, *Astronomy, Cosmology and Fundamental Physics*, ed. Caffo, M., Kluwer Academic Publishers, 317.

Kozasa, T., Hasegawa, H., Nomoto, K., 1989, *Ap. J.*, 344, 325.

Krauss, L.M., Tremaine, S., 1988, *Phys. Rev. Lett.*, 60, 176.

Krivoruchenko, M.I., 1989, *Z. Phys. C - Particles and Fields*, 44, 633.

Krunkel, W., Madore, B., Bateson, F.M., McNaught, R.H., 1987, *IAUC.*, 4316.

Kudritzki, R.P., Pauldrach, A., Puls, J., 1986, *Astron. Astrophys.*, 298.

Kumagai, S., (and 6 coauthors), 1989, *Ap. J.*, 345, 412.

Lamb, D.Q., Lattimer, J.M., Pethnick, C.J., Ravenhall, D.G., 1978, *Phys. Rev. Lett.*, 41, 1623.

Lang, K.R., 1980, *Astrophysical Formulae*, Springer-Verlag.

Langer, N., El Eid, M.F., Baraffe, I., 1989, *Astron. Astrophys.*, 224, L17.

Lasker, B.M., 1980, *Ap. J.*, 237, 765.

Lattimer, J.M., 1988, *Nuclear Physics*, A478, 221c.

Lattimer, J.M., Yahil, A., 1987, *SN 1987A in the Large Magellanic Cloud*, ed. Kafatos, M., Michalitsianos, 209.

Lattimer, J.M., Yahil, A., 1989, *Ap. J.*, 340, 426.

Longo, M.J., 1988, *Phys. Rev. Lett.*, 60, 3, 173.

LoSecco, J.M., *Phys. Rev. D*, 39, 4, 1013.

Lucke, P.B., Hodge, P., 1970, *Astron. Astrophys.*, 182, L31.

Madore, B., 1987, *IAUC.*, 4317.

Matz, S.M., (and 7 coauthors), 1988, *Nature*, 331, 416.

Mayle, R., Wilson, J.R., Schrammn, D.N., 1987, *Ap. J.*, 318, 288.

McCray, R., Li, W.H.,1987, *Proc. of Yellow Mountain Summer School on the Structure and Evolution of Galaxies*, ed. Fang, L.Z., World Sci., 8.

Middleditch, J., (and 13 collaborators), 1989, *IAUC.*, 4735.

Middleditch, J., 1989, *Computers in Physics*, Jul / Aug, 14.

Middleditch, J., 1990, *AAS. Meeting* (February 24).

Mielke, W.P.S., Marcher, S.J., Morgan B.L., 1987, *IAUC* , 4391.

Mielke, W.P.S., Marcher, S.J., Morgan B.L., 1987, *IAUC* , 4394.

Mielke, W.P.S., Marcher, S.J., Morgan B.L., 1987, *Nature*, 329, 608.

Moffat, A.F.J., Niemela, V.S., Phillips, M.M., Chu, Y., Seggewiss, W., 1987, *Ap. J.*, 312, 612.

Molaro, P., Vladilo, G., Avila, G., D'Odorico, S., 1989, *Ap. J.*, 339, L63.

Moseley, S.H., (and 5 coauthors), 1989, *Nature*, 340, 697.

Nagasawa, M., Nakumura, T., Miyama, S., 1988, *Pub. Ast. Soc. Japan.*, 40, 691.

Nakamura, T., Fukugita, M., 1989, *Ap. J.*, 337, 466.

Nisenson, P., Karvoska, M., Miyama, S., 1988, *IAUC* , 4382.

Okun, L.B., 1986, Preprint *TAUP*, 1543.

Panagia, N., 1987, *Proc. of E.S.O Workshop on SN 1987A*, ed. Danziger, I.J., 55.

Pannekoek, A., 1961, *A history of astronomy*, London, Allen and Unwin.

Perlmutter, S., (and 5 collaborators), 1990, *IAUC* , 4992.

Pettini, M., Stathakis, R., D'Odorico, S., Molaro, P., Vladilo, G., Prepint *AAO*.

Rank, D.M., (and 6 coauthors), 1988, *Nature*, 331, 505.

Ray, A., Kar, K., 1989, *Phys. Rev. Lett.*, 63, 22., 2435.

Rees, M.J., 1987, *Nature*, 207.

Rester, A.C., (and 6 coauthors), 1989, *Ap. J.*, 342, L71.

Sahu, K.C., Sahu, M., Pottasch, S.R., 1988, *Astron. Astrophys.*, 207, L1.

Saio, H., Nomoto, K., 1988, *Ap. J.*, 334, 388.

Savage, B.D., Jenkins, E.B., Joseph, C.L., Boer, K.S., 1989, *Ap. J.*, 345, 393.

Schramm, D.N., 1987, *Comments in Nuc. Part. Phys.*, 17, 5, 239.

Schramm, D.N., 1989, *FERMILAB-Conf-89/27-A*.

Shapiro, S.L., 1978, in *Gravitational Radiation*, ed Smarr, L., Oxford University press, 355.

Shapiro, S.L., Teukolsky, S., 1983, *Black Holes, White Dwarfs, and Neutron Stars*, John Wiley and sons.

Shigeyama, T., Nomoto, K., 1989, submitted to *Ap. J.* (October 1989).

Spergel, D.N., Bachall, J.N., 1988, *Phys. Lett. B*, 200, 366.

Storey, M.C., Manchester, R.N., 1987, *Nature*, 330, 327.

Suntzeff, N.B., 1988, *Nature*, 334, 135.

Sunyaev, R., (and 33 coauthors), 1987, *Nature*, 330, 227.

The, L-S., Burrows, A., Bussard, R., 1990, *Ap. J.*, 352, 731.

Thielemann, F-K., Hasimoto, M., Nomoto, K., 1989, *Ap. J.*, 349, 222.

Thielheim, K.O., 1989, *Fund. Cosmic Phys.*, 13, 357.

Time, 1987, March 23.

Tomozawa, Y., 1989, Prepint *RIFP-810* (May 1989).

Truran, J.W., Weiss, A.,1990, *Comm. Astrophys.*,14, 4, 195.

Tsurata, S., Nomoto, K., 1988, *Astro. Lett. and Commun.*, 27, 241.

Tuchman, Y., Wheeler, J.C., 1989, *Ap. J.*, 344, 835.

Tueller, J., (and 6 coauthors), 1990, *Ap. J.*, 351, L41.

Turner, M.S., 1989, *Fermi lab-conf*-89/104-a.

van den Bergh, S., 1988, Paper presented at the *White Research Conference on SN 1987A* (Canberra, Australia).

van den Bergh, S., McClure, R.D., *Ap. J. Lett.*, submitted.

van der Velde, 1988, *Phys. Rev. D*, 39, 6, 1492.

Wang, Q., Chen, T.T., Hamilton, M., Ruderman, K., Shaham, J., 1989, *Nature*, 338, 319.

Wang, Q., Hamilton, T., Hefland, D.J., 1989, *Nature*, 341, 309.

Warner, B., 1987, *IAUC.*, 4316.

Weiss, A., 1989, *Ap. J.*, 339, 365.

White, G.L., Malin, D., 1988, *Proc. of E.S.O Workshop on SN 1987A*, ed. Danziger, I.J.,11.

Whitelock, P.A., (and 21 coauthors), 1988, *MNRAS.*, 234, 5P.

Wilson, J.R., Mayle, R.W., 1988, *Physics Reports*, 163, Nos.1-3, 63.

Witteborn, F., (and 14 coauthors), 1988, Preprint, submitted to *Ap. J.*.

Witten, E., 1984, *Phys. Rev.*, 30, 2, 272.

Wolfstein, L., Beier, E.W., 1989, *Physics Today*, July, 28.

Wood, P.R., (and 5 coauthors), 1989, *Ap. J.*, 339, 1073.

Wood, P.R., Faulkner, D.J., 1989, *IAUC.*, 4739.

Woolsey, S.E., 1988, *Ap. J.*, 330, 218.

Woosley, S.E., 1988, *Proc. of 14th Texas Symposium on Relativistic Astrophysics*, in press.

Woosley, S.E., Phillips, M.M., 1988, *Science*, 240, 750.

Woosley, S.E., Pinto, P.A., Hartmann, D., 1989, *Ap. J.*, 346, 395.

Woosley, S.E., Weaver, T.A., 1986, *Ann. Rev. Astron.*, 24, 205.

Young, T.R., Branch, D., 1989, *Ap. J.*, 342, L79.

APPENDICES

APPENDIX A - Mass loss and Rotation

A.1 Mass Loss

If helium becomes degenerate during its nuclear burning, as numerical calculations suggest it may, then a thermal runaway known as a 'helium flash' results. This prodigious energy release rapidly lifts the electron degeneracy and allows the region to expand. Most of the increased luminosity appears as envelope expansion. Repeated flashes caused by thermally unstable helium shell sources set up relaxation oscillations in the envelope. If a flash is strong enough, some of the envelope will be accelerated to escape velocities. Furthermore, as the envelope expands, the gas cools and radiative energy losses may lead to a significant under pressure. If a series of strong flashes occurs, then mass ejection may accompany them. However, observations [§V.8(ii)] are not sufficiently detailed to restrict the above scenario.

A.2 Rotation

The effects of rotation upon stellar evolution seem to be fourfold.

(a) The contribution of centrifugal force will lead to a decrease in the internal pressure of a rotating star, relative to an identical non-rotating star. The reduced interior temperature will reduce the rate of nuclear burning, giving a subluminous star.

(b) The equipotentials are closer together along the rotational axis than toward the equator. This leads to meridional circulation. It has the consequences not only of significant energy transfer by means of circulation currents but also rotational mixing.

(c) The reduction of effective gravity and increased turbulence leads to enhanced mass loss.

(d) Rotation interacts with convection causing the inner core to rotate more rapidly than the outer envelope. This results from conservation of angular momentum whereby a falling convective shell will tend to increase its angular velocity, whereas a rising shell will tend to decrease its velocity. Convection tends to make the angular momentum per unit mass constant, thereby demanding a greater rotational velocity for the central portion.

APPENDIX B - Neutrinos

B.1 Core infall

During core infall the principal reactions are electron capture,

$$e^- + p <--> n + \upsilon_e.$$

$$e^- + A(Z,N) <--> A(Z-1,N+1) + \upsilon_e. \qquad (II.2)$$

and photodisintegration of iron group nuclei,

$$^{56}Fe <--> 13\alpha + 4n. \qquad (II.3)$$

Hence large numbers of electron neutrinos are produced.

When the central core is destabilised by the above reactions, it has a density of about 10^8 g/cm^3 and a temperature of about 10^9 K; this corresponds to a mean free path,

$$\lambda_{\upsilon_e} = \frac{1}{n\sigma_{\upsilon_e}}. \qquad (B.1)$$

Until nuclear densities are reached the opacity for electron neutrinos is dominated by scattering off neutrons - for which the average cross section[56] is,

$$\sigma_{\upsilon_e} \sim N^2\left(\frac{E_{\upsilon_e}}{MeV}\right]^2 x 10^{-44}\ cm^2, \qquad (B.2)$$

where N is the average number of neutrons in each heavy nucleus - typically 30 for the iron group nuclei predominant at this stage of collapse; and where n is the number density of an heavy nucleus with mass number, A, that is, $n = \rho N_A/A$.

The mean free path,

$$\lambda_{\upsilon_e} \sim A[N^2 N_A \rho\left(\frac{E_{\upsilon_e}}{MeV}\right)^2 x 10^{-44}]^{-1}, \qquad (B.3)$$

is then of the order of 10^{13} cm and thus much greater than the radius of the star's central high density core, $\sim 10^8$ cm. Thus, the neutrinos escape freely from the star. However, only milliseconds later the neutrinos become trapped by the rapidly increasing densities.

B.2 Neutrino trapping density

The neutrino trapping density is commonly defined as the density when the timescales for neutrino diffusion,

$$\tau_{diff} \sim \frac{\lambda_{\upsilon_e} N_{scatt}}{c}, \qquad (B.4)$$

and for collapse[231]

$$\tau_{grav} = \frac{1}{(\pi\ G\rho)^{0.5}}, \qquad (B.5)$$

became the same. Since the number of scatterings, N_{scatt}, experienced by the neutrino prior to escape will be $N_{scatt} >> 1$, then for coherent scattering (expected), the neutrino trajectory can be described by the random walk relation:

$$\lambda_{\upsilon} N_{scatt} \sim R^2. \qquad (B.6)$$

Substituting N_{scatt} from (B.6) and (B.3) into (B.4) and equating with the timescale for collapse (B.5) gives,

$$\frac{1}{(\pi\ G\rho)^{0.5}} = \frac{R^2 N^2 N_A \rho_{trap} \left(\frac{E_{\upsilon_e}}{MeV}\right)^2}{Ac}. \qquad (B.7)$$

Rearranging, yields the trapping density as,

$$\rho_{trap} = \left[\frac{A\ c}{R^2 N^2 N_A \left(\frac{E_{\upsilon_e}}{MeV}\right)^2 x10^{-44} (\pi G)^{0.5}}\right]^{2/3}. \qquad (B.8)$$

By this stage A had increased[56] to about 100 and N to about 50. For $E_{\upsilon_e} \sim 5$ MeV and, R ~ $2x10^7$cm [104], this gives,

$$\rho_{trap} \sim 1x10^{11}\ g/cm^3, \qquad (B.9)$$

which is within a factor 2 of the values found by detailed hydrodynamic calculations where allowance is made for the central concentration, electron capture onto heavy nuclei, and neutrino downscattering.

B.3 Core collapse

The core continues to collapse until the density (ρ_c) reaches 3 -4 times that of an atomic nucleus ($2.5x10^{14}$ g/cm^3). Because the collapse is nearly adiabatic (Fig. 5), the central temperature (T_c), can be well approximated by $T_c \sim T_{trap}(\rho_c/\rho_{trap})^{1/3}$; where T_{trap} and ρ_{trap} are about 1.5 MeV and 10^{11} g/cm^3, respectively. Thus,

$$T_c = 40\text{-}45 \text{ MeV}. \tag{B.10}$$

More detailed models[74] yield from 30 MeV to 80MeV.

The gravitational binding energy, E_B, released as the iron core collapses from a radius of about 2000 km to 10-20 km is

$$E_B \sim \frac{GM_{core}^2}{R} = 3x10^{53} \left(\frac{M_{core}}{M_{\odot}} \right)^2 \left(\frac{10 \text{ km}}{R} \right). \tag{B.11}$$

Because neutrinos are initially trapped, the bulk of the liberated gravitational energy must be converted into other forms of internal energy, i.e., thermal energy, energy of nuclear excited states, bounce kinetic energy, etc. Rather than being immediately released in escaping electron neutrinos. The hot (B.10) ambient medium allows neutrinos af all flavours to be produced and interact through neutral reactions (above 15 MeV), as well as through charged reactions. Neutrinos are created by the following reactions[232];

(a) $e^+ + e^- \text{-->} \nu_i + \bar{\nu}_i$,

(b) plasmon $\text{-->} \nu_i + \bar{\nu}_i$,

(c) $e^- + \gamma \text{-->} e^{-'} + \nu_i + \bar{\nu}_i$;

(d) $e^- + (Z,A) \text{-->} (Z,A)' + e^- + \nu_i + \bar{\nu}_i$. (B.12)

They are scattered and absorped by the following reactions[232];

(e) $\nu + (Z,A) \text{-->} (Z,A)' + \nu'$,

(f) $\nu + (n,p) \text{-->} (n,p) + \nu$,

(g) $\nu + e^{\pm} \text{-->} e^{\pm} + \nu$,

(h) $\nu_e + n \text{-->} e^- + p$,

(i) $\bar{\upsilon}_e + p \dashrightarrow e^+ + n$,

(j) $\upsilon_i + \bar{\upsilon}_i \dashrightarrow 2\gamma$. (B.13)

B.4 Neutrinos escape

To calculate the diffusion time for electron antineutrinos at nuclear densities, I will again use (B.4). The main source of opacity for $\bar{\upsilon}_e$'s is absorption on protons, so the number density becomes, $n = (N_A)\rho Y_p$; where Y_p is the fraction of protons. Hence,

$$\tau_{diff} \sim \frac{R^2 N_A \rho Y_p \sigma_\upsilon}{c}. \qquad \text{(B.14)}$$

From collapse calculations $Y_p \sim 0.2$; the cross section for absoption on protons is[86], $\sigma \bar{\upsilon}_e = 9\left(\frac{T\upsilon_e}{MeV}\right]^2 x 10^{-43}\ cm^2$. Using $T\bar{\upsilon}_e \sim 40$ MeV (B.10), and where $R\bar{\upsilon}_e \sim 19$ km [§IV.4(ii)] for the protoneutron star;

I obtain $\tau_{diff} = 4$ s.

Because of the plethora of neutrino interactions (i)-(j) and lack of regard for time evolution, my calculation is highly simplified; though it does give essentially the same result as calculations employing neutrino transport from a cooling neutron star [0.1-10 s (e.g.[74])]. And of course, the 13 s apparent from the Kamiokande results.

The mu and tau neutrinos only interact via the neutral rather than the charged reactions, so the only mechanism for energy exchange was through scattering reactions. Their cross sections for interaction (averaged over different reactions)[233] were considerably lower than for the electron neutrinos:

$$\sigma_{\mu,\tau's} \sim 5T\upsilon_{\mu,\tau's} x 10^{-45}\ cm^2, \qquad \text{(B.15)}$$

whereas

$$\sigma_{\upsilon_{e's}} \sim 9x\left(\frac{T\upsilon_e}{MeV}\right]^2 x 10^{-43}\ cm^2. \qquad \text{(B.16)}$$

Detailed models expect $T\upsilon_{e's} =$ 3-7 MeV, and $T_{\upsilon_{\mu,\tau's}} =$ 8-11 MeV.

B.5 Detector efficiencies

The graphs below represent the probability that Cerenkov radiation of a given energy was detected as such.

Figure 30. Kamiokande efficiency[104]

Figure 30 has been removed because of the unavailability of copyright

From Schramm, D.N., 1987, *Comments in Nuc. Part. Phys.*, 17, 5, 239

Figure 31. IMB efficiency[104]

Figure 31 has been removed because of the unavailability of copyright

From Schramm, D.N., 1987, *Comments in Nuc. Part. Phys.*, 17, 5, 239

Figure 32. Mont Blanc efficiency[89]

Figure 32 has been removed because of the unavailability of copyright

From Aglietta, M., (and 19 coauthors), 1987, *SN 1987A in the Large Magellanic Cloud*, ed. Kafatos, M., Michalitsianos, A., 207

Figure 33. Baskan efficiency[233]

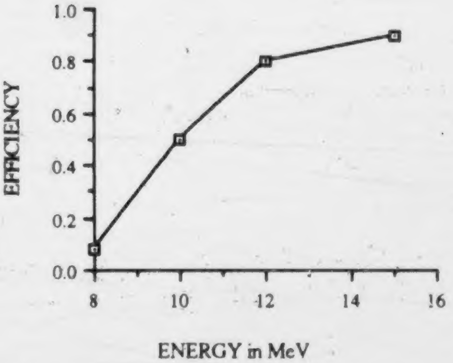

APPENDIX C - Radioactivity

C.1 Cobalt 56 decay?

From the bolometric light curve (Fig 25), the slope of the linear phase may be inferred from,

$$t = 0 \text{ days}, \qquad L = 10^{42.04} \text{ ergs/s};$$

$$t = 250 \text{ days}, \quad L = 10^{41.04} \text{ ergs/s}. \tag{C.1}$$

If the linear phase is given by radioactive decay then,

$$L(t) = L(o)\, e^{-\lambda\tau}, \tag{C.2}$$

where $\lambda = \frac{\ln 2}{\tau}$.

Rearranging yields,

$$\tau = \frac{(\ln\ 2)\ t}{\ln\left(\frac{L(0)}{L(t)}\right)}\ ; \tag{C.3}$$

substituting from (C.1),

$$\tau = 76.8 \text{ days}. \tag{C.4}$$

This is in good agreement with the laboratory value for ^{56}Co, that is 78.76 days [159]. Spline fits to the early light curve have shown the linear phase to have a half life of 71-80 days [49]

C.2 Mass of Cobalt 56

The initial mass of ^{56}Co is given as,

$$M \sim \frac{A m_p \dot{E}(t)}{Q_{Co} \lambda_{Co} (e^{-t/\tau_{Co}})} \quad g. \tag{V.17}$$

When A=56,

$$\dot{E}(t) = \frac{10^{41.04} x 3600 x 24 x 250}{250} \text{ ergs/day},$$

$$Q_{Co} = 3.695 x 1.602 x 10^{-6},$$

substitution into (V.16) gives,

$$M = 0.076\ M_{\odot}\ . \tag{C.5}$$

The accepted value is 0.075 $M_{\odot}$.